Metal Clusters, Metalloporphyrins and Gas Phase Redox Chemistry: Applications of FTMS

- Introduction to FTMS
- Two peptide problems
  - Distinguishing isomers: primary structure problem
  - Secondary structure of HPTH
- Dynamics and mechanism of transition metal redox reactions
  - A useful gas phase dehydrogenation reaction
  - A selective oxidation of CO by O_2
- Equilibrium in charge transfer reactions: Theory and Experiment
  - Flavin semiquinones
  - Halogenated iron porphyrins
- IR spectra of gas phase anionic metal clusters

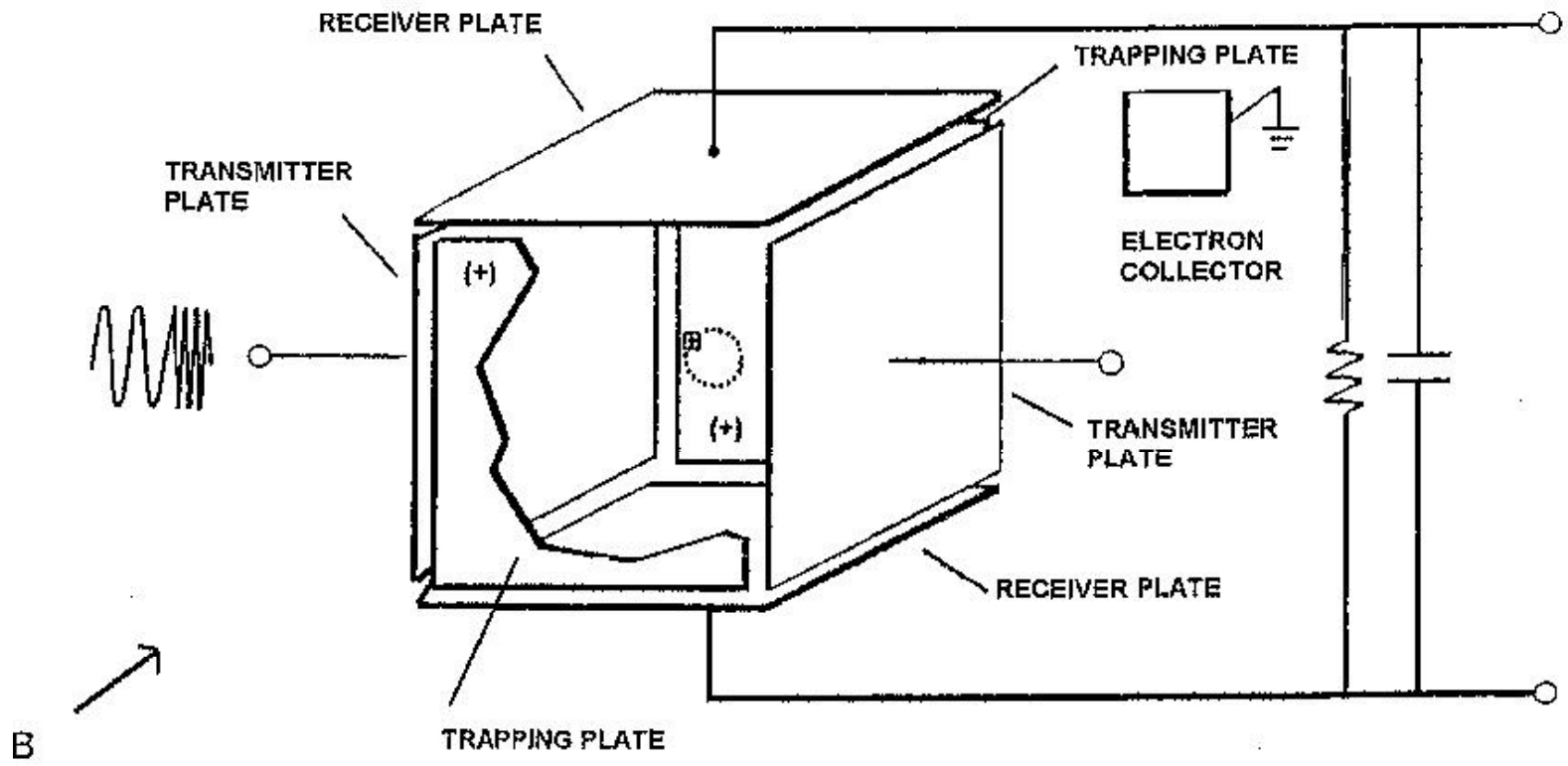
RECEIVER PLATE
TRAPPING PLATE
TRANSMITTER PLATE
ELECTRON COLLECTOR
(+)
(+)
TRANSMITTER PLATE
RECEIVER PLATE
TRAPPING PLATE
B

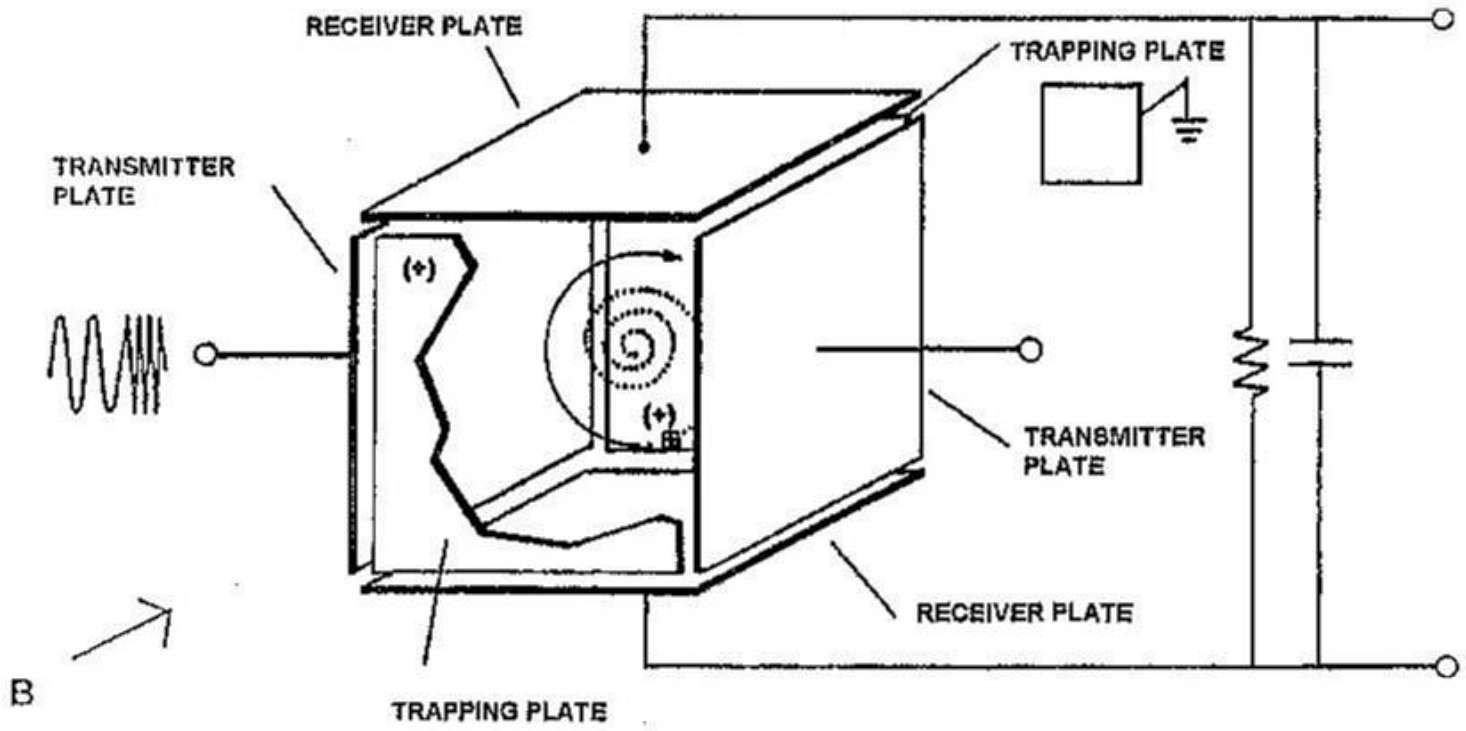
RECEIVER PLATE
TRAPPING PLATE
TRANSMITTER PLATE
(+)
(+)
TRANSMITTER PLATE
RECEIVER PLATE
B
TRAPPING PLATE

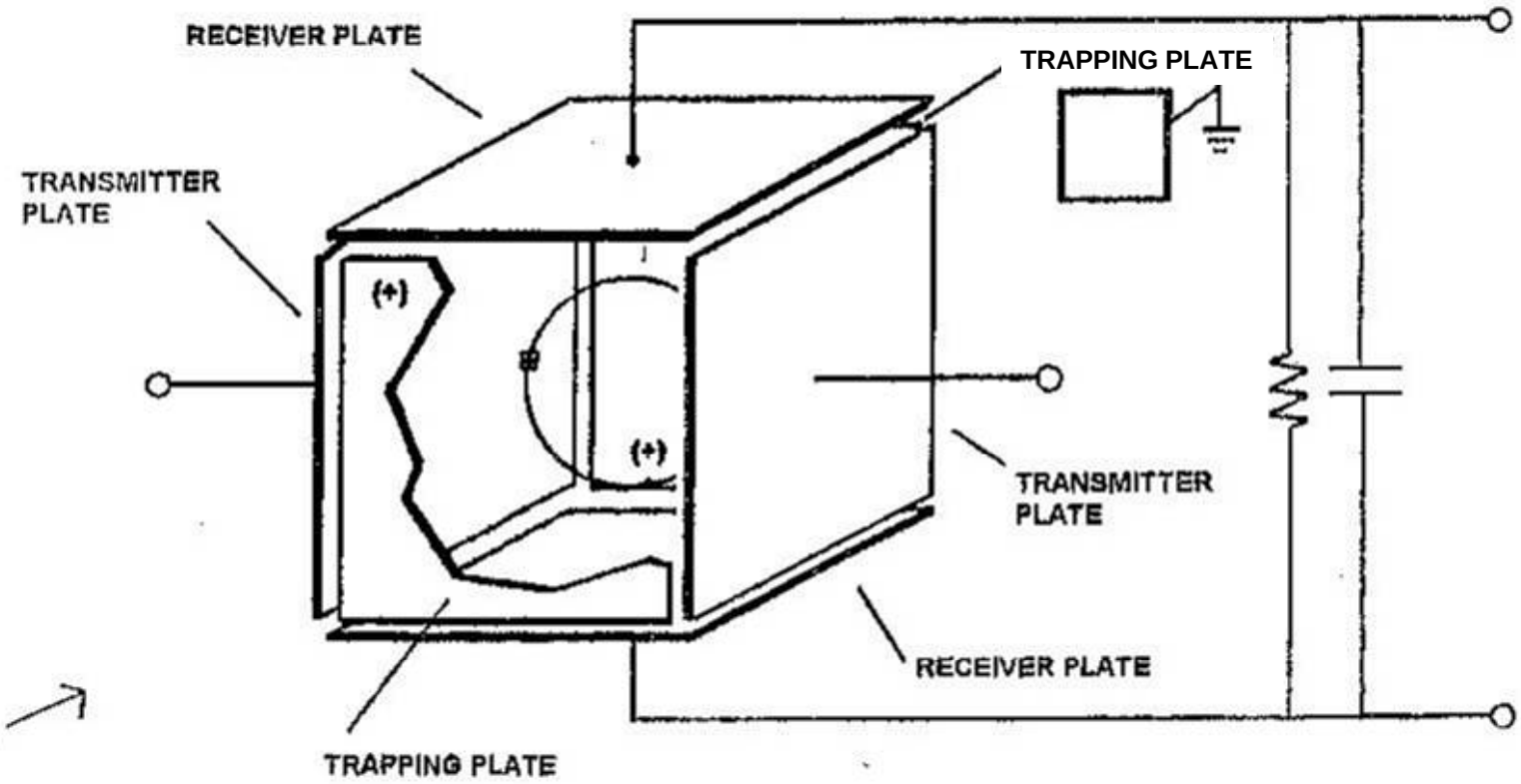
RECEIVER PLATE
TRAPPING PLATE
TRANSMITTER PLATE
(+)
(+)
TRANSMITTER PLATE
RECEIVER PLATE
TRAPPING PLATE

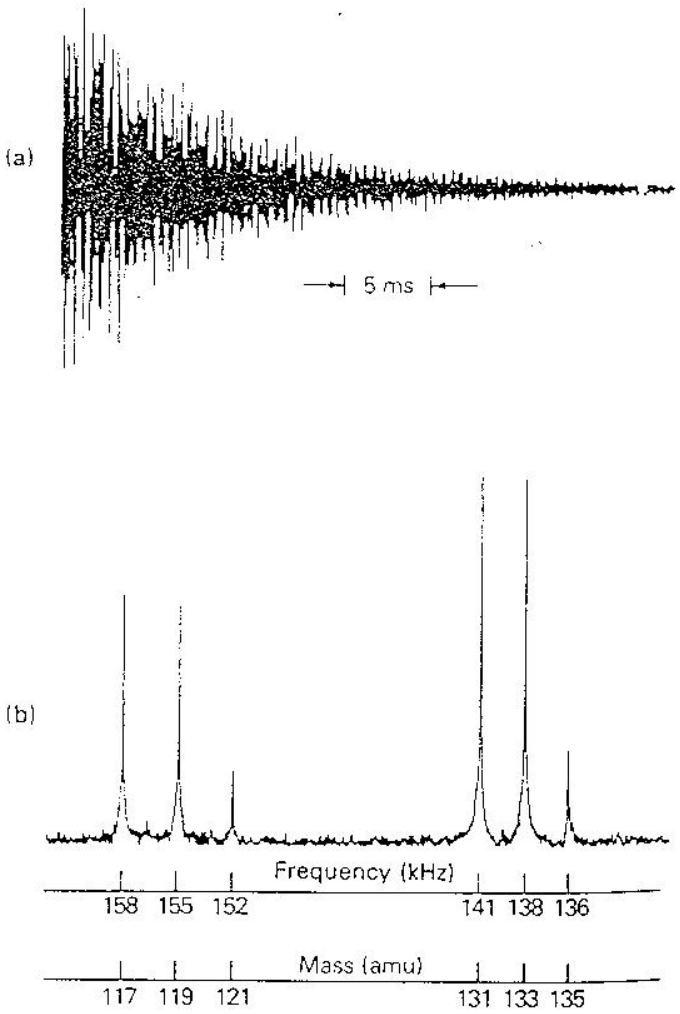

Figure 2.4 Time domain (a) and (b) frequency or mass domain spectrum for 1,1,1,2-tetrachloroethane. (Ref: Ledford Jr., E. B. et al., *Anal. Chem.*, **1980**, 52, 466)

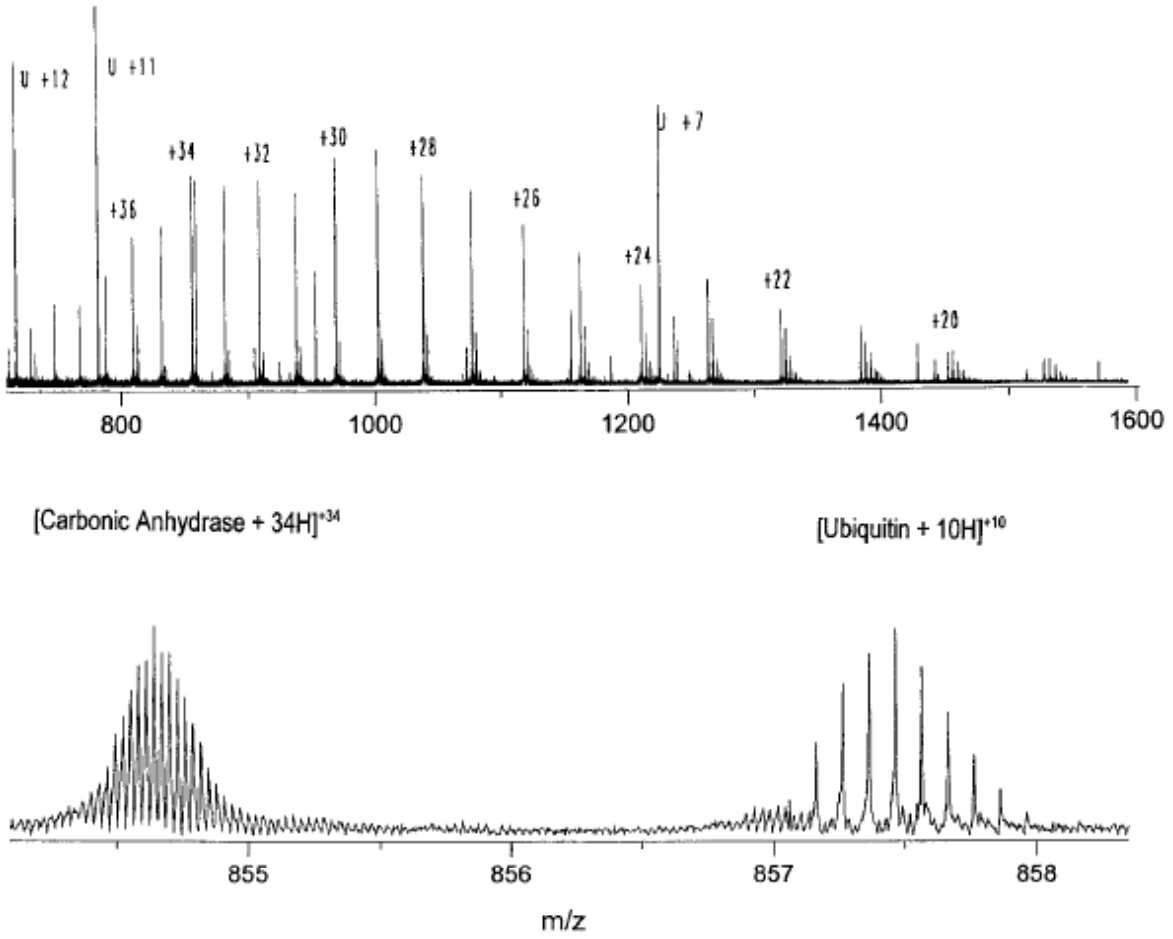

FIG. 4. ESI–FTICR spectrum of bovine carbonic anhydrase II (BCA II) with ubiquitin as internal calibrant, and an expansion of the region around *m/z* 856. While the tallest peak of ubiquitin is readily apparent, selection of the tallest BCA II peak is less certain.

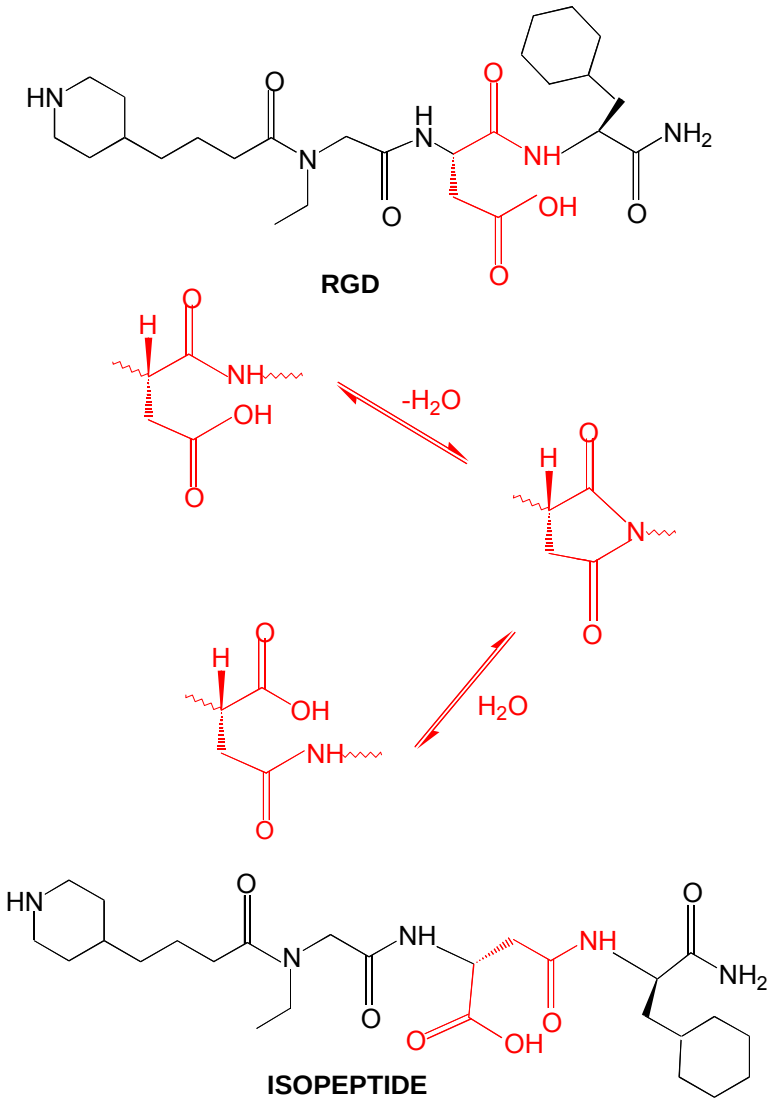

Scheme 1

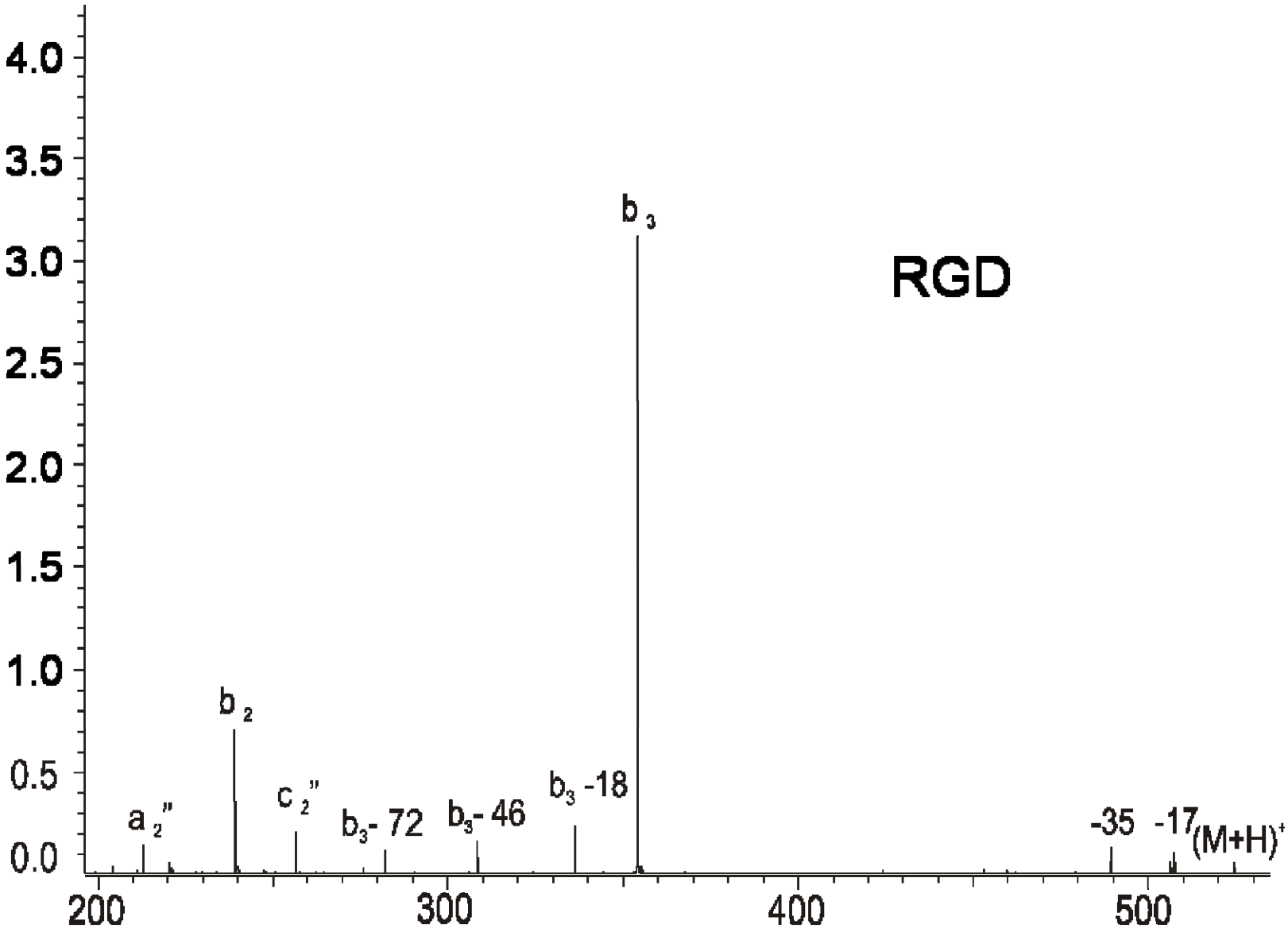
RGD
4.0
3.5
3.0
2.5
2.0
1.5
1.0
0.5
0.0
200
300
400
500
b 3
b 2
a 2"
c 2"
b3 - 72
b3 - 46
b3 -18
-35
-17
(M+H)+

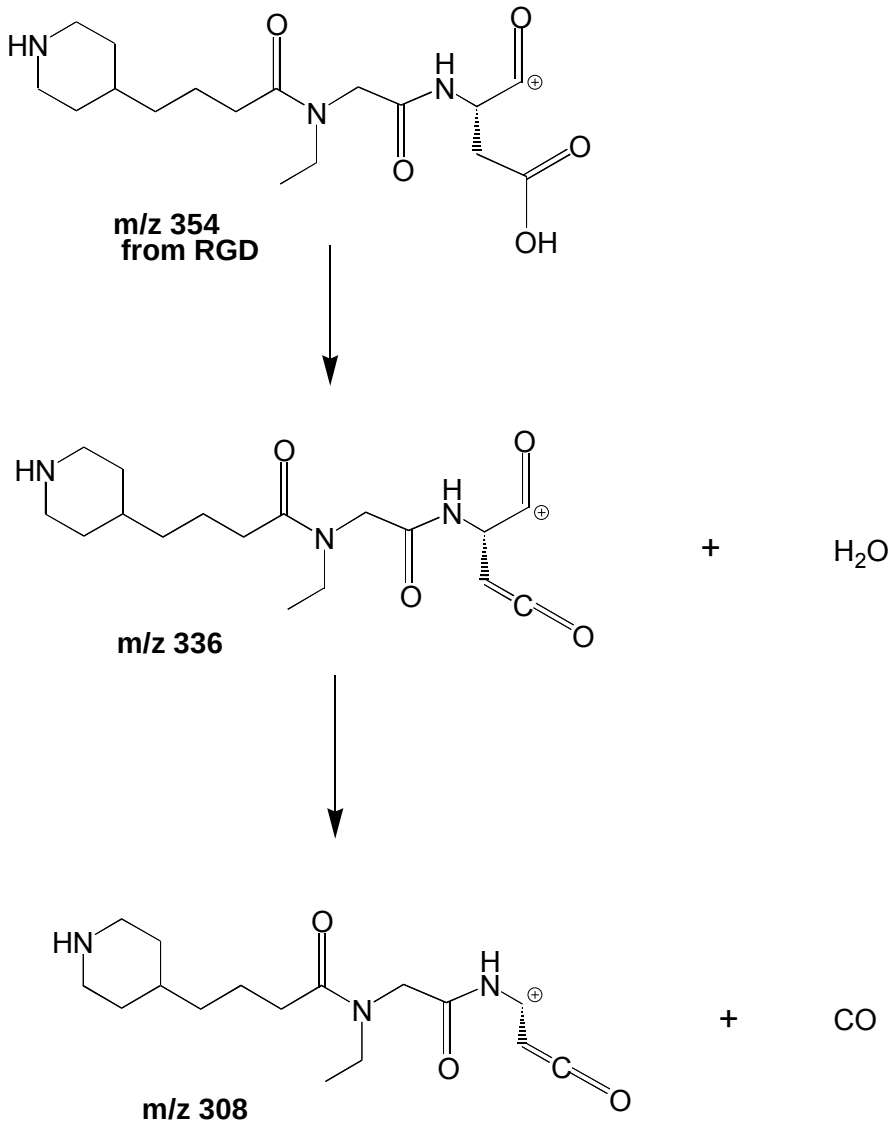

Scheme 5

Total Δm = 46.0032 (measured) vs. 46.0036 calculated)

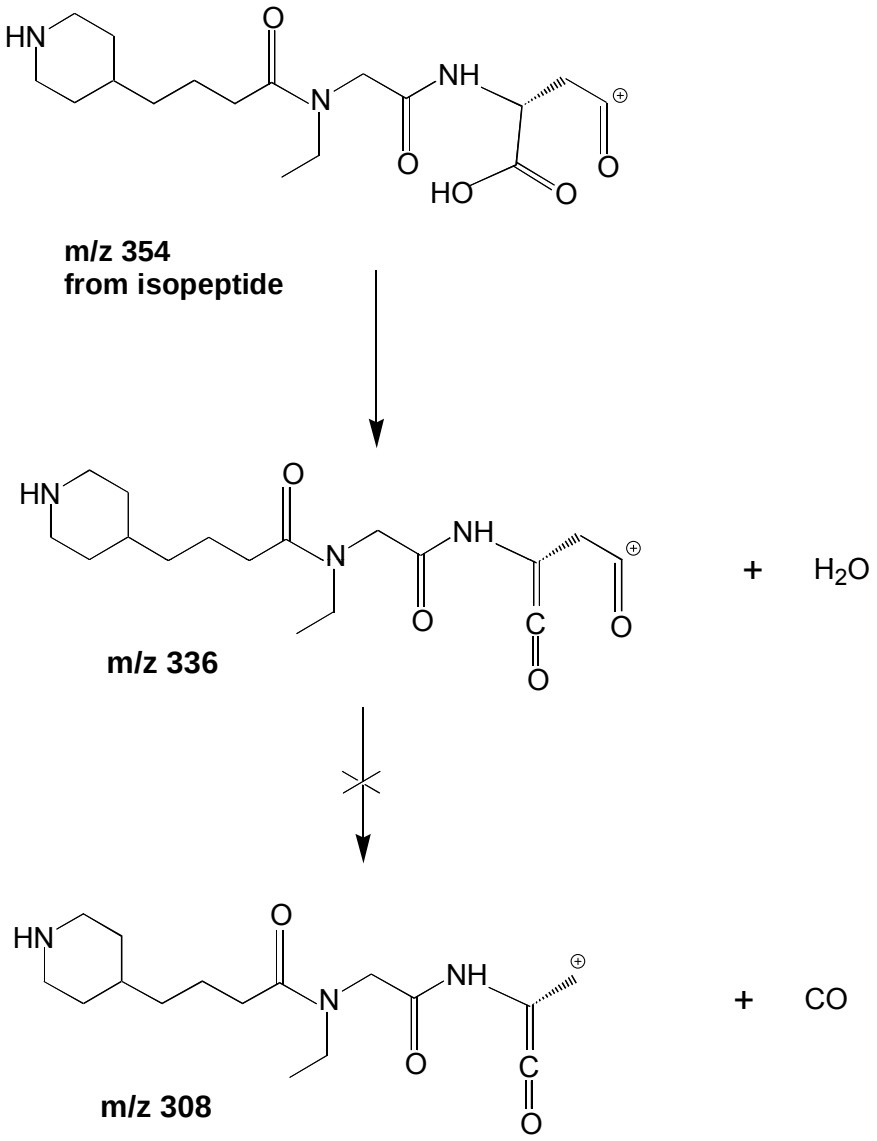
HN
O
N
NH
O
HO
O
O
m/z 354
from isopeptide
HN
O
N
NH
O
C
O
O
+ H2O
m/z 336
HN
O
N
NH
O
C
O
+ CO
m/z 308

Scheme 6

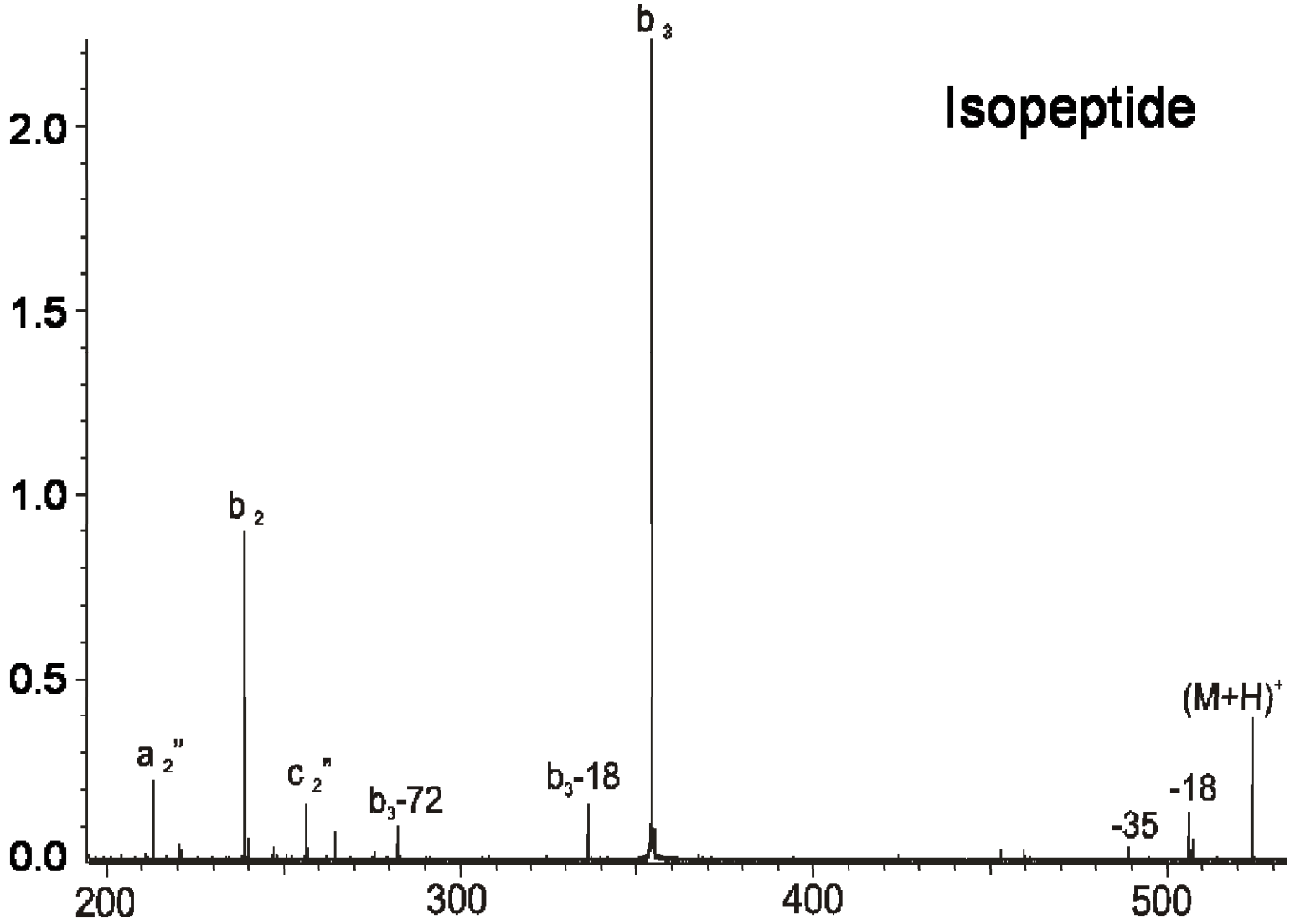
Isopeptide
b 3
b 2
a 2"
c 2"
b3-72
b3-18
-35
-18
(M+H)+
2.0
1.5
1.0
0.5
0.0
200
300
400
500

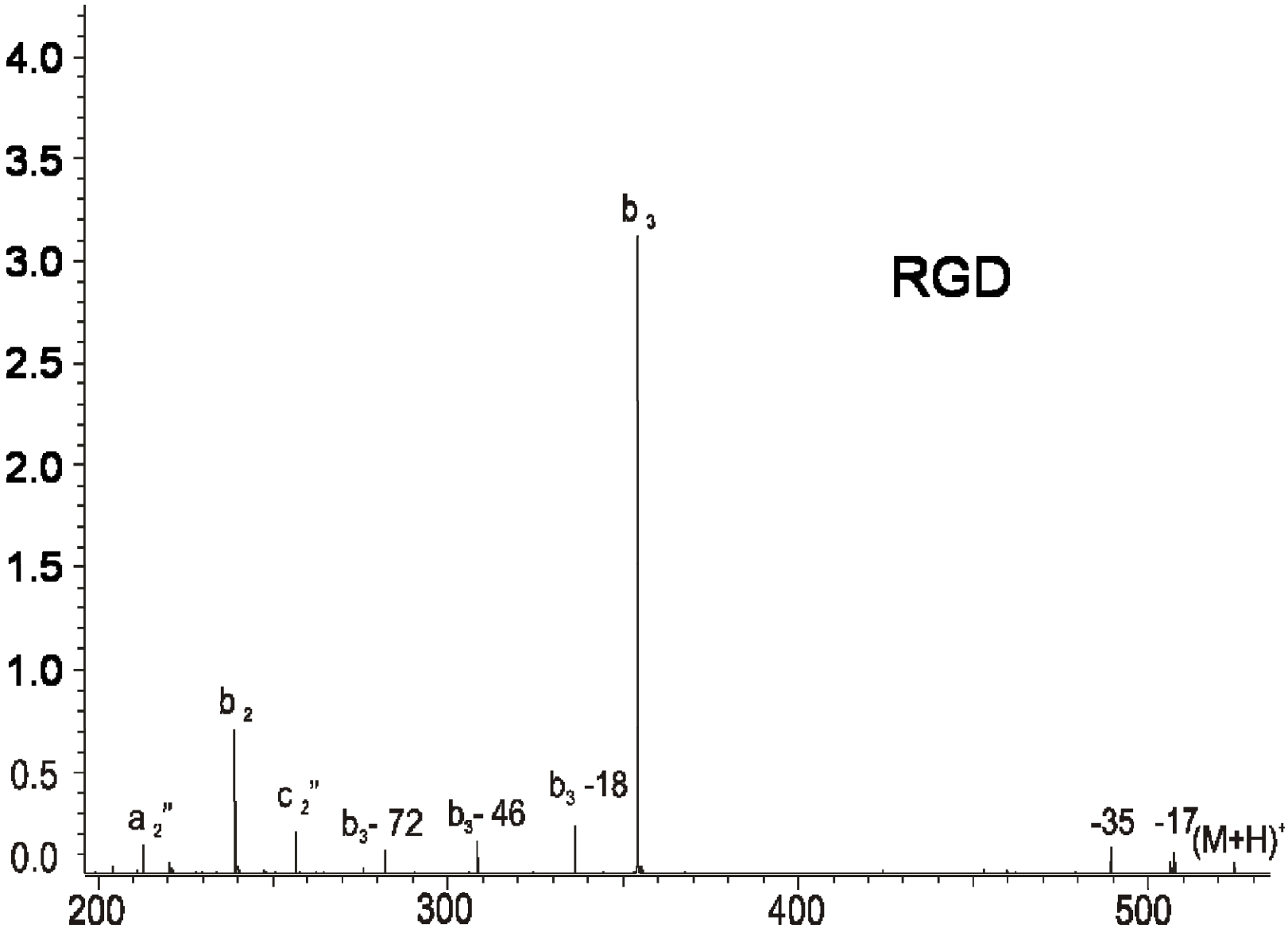
RGD
4.0
3.5
3.0
2.5
2.0
1.5
1.0
0.5
0.0
200
300
400
500
b 3
b 2
a 2"
c 2"
b3 - 72
b3 - 46
b3 -18
-35
-17
(M+H)+

European Journal of Mass Spectrometry

SPECIAL ISSUE DEDICATED TO:

JEAN FUTRELL

AND

BURNABY MUNSON

VOLUME 10 NUMBER 2

PAGES 135–317

ISSN 1469-0667

IMPublications

Synthetic hPTH (1-31)

1 2 3 4 5 6 7
H – ala – val – ser – glu – ile – gln – leu – nle
30 29 28 27 26 25 24

8 9 10 11 12 13 14 15
- his – asn – leu – gly – lys – lys – leu – asn
23 22 21 20 19 18 17 16

16 17 18 19 20 21 22 23
– ser – asp – glu – arg – val – glu - trp – leu
15 14 13 12 11 10 9 8

24 25 26 27 28 29 30
– arg – lys – leu - leu – gln – asp – val – NH_2
7 6 5 4 3 2 1

Conlon, et al., JACS **122**, 3007(2000)
Conlon, et al., Bioorg. Med Chem. **10**, 731(2002)

SORI-CID

- Charge state of interest was isolated (+4)
- SF_6 was introduced through a computer controlled pulsed valve (reservoir P ~ 13 mbar)
- Collision excitation was 500 Hz off-resonance

SORI-CID

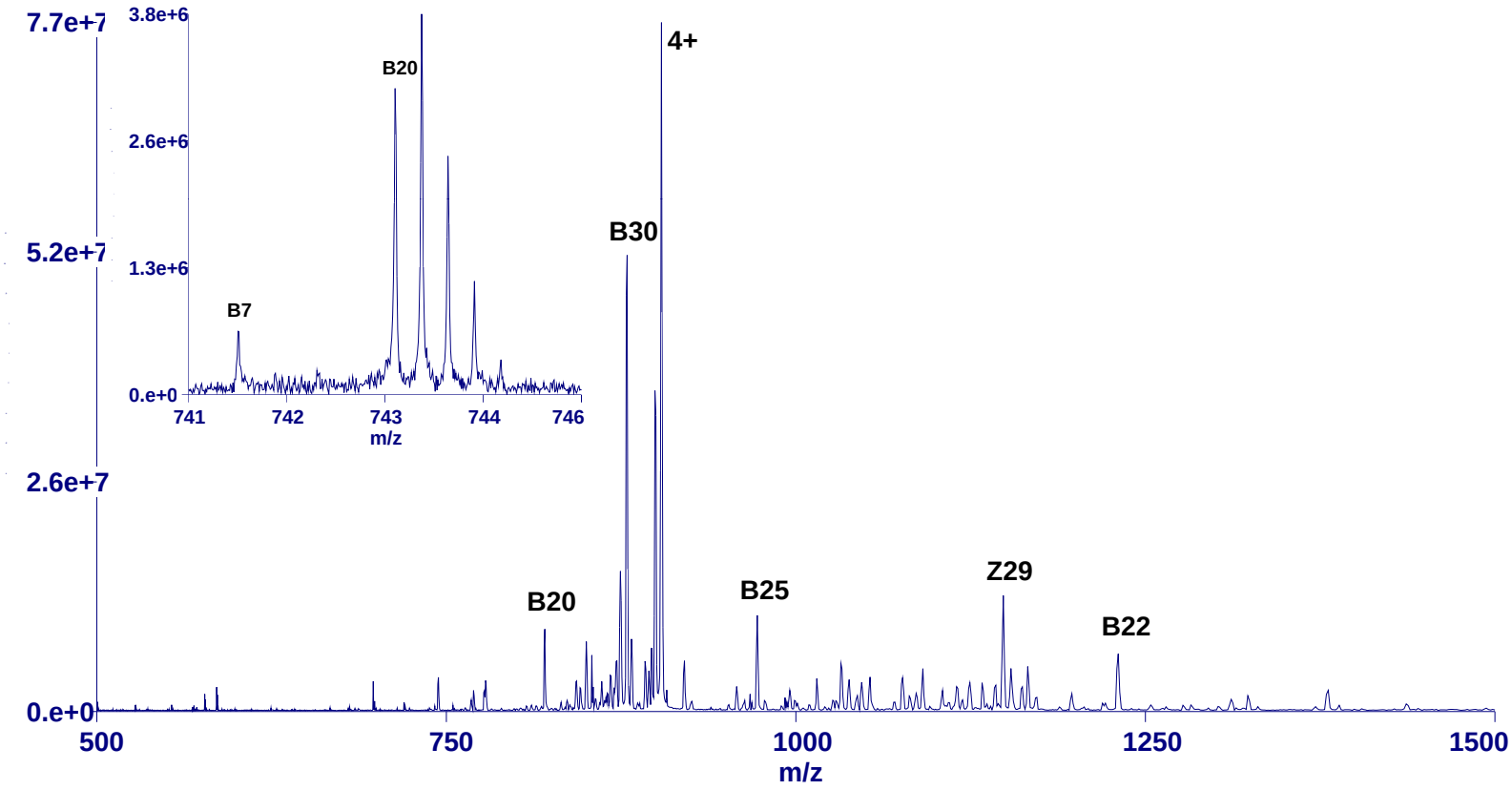
7.7e+7
5.2e+7
2.6e+7
0.e+0
500
750
1000
1250
1500
m/z
4+
B30
B20
B25
Z29
B22
3.8e+6
2.6e+6
1.3e+6
0.e+0
B7
B20
741
742
743
744
746
m/z

SORI-CID

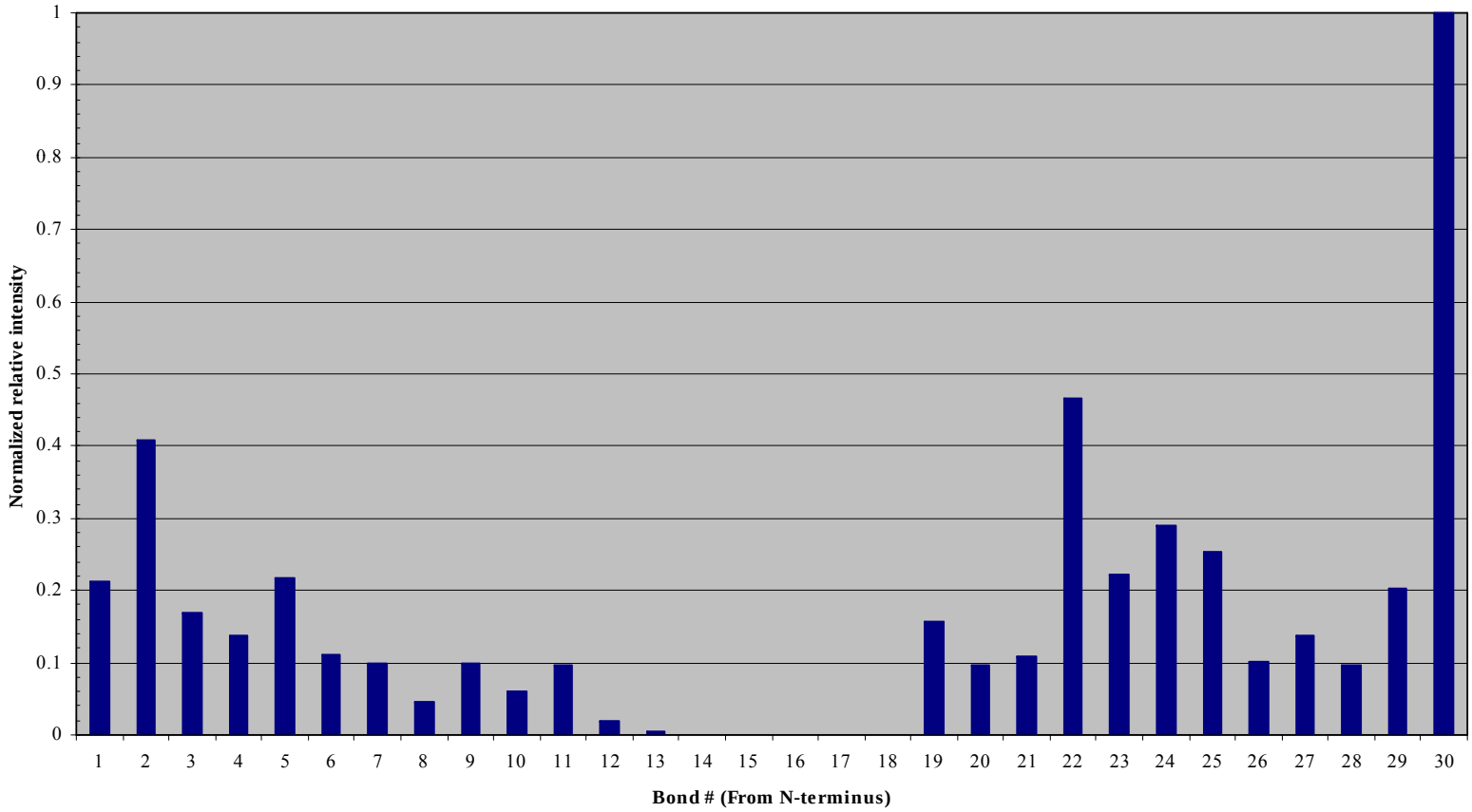
Normalized relative intensity
1
0.9
0.8
0.7
0.6
0.5
0.4
0.3
0.2
0.1
0
1 2 3 4 5 6 7 8 9 10 11 12 13 14 15 16 17 18 19 20 21 22 23 24 25 26 27 28 29 30
Bond # (From N-terminus)

Electron Capture Dissociation (ECD)

- Sample is irradiated with low energy, high current electrons (10 eV)
- A cooling gas (Ar or SF_6) is introduced through a computer controlled pulsed valve during the irradiation step
- ECD is a neutralization reaction

ECD Mechanism

Major Products

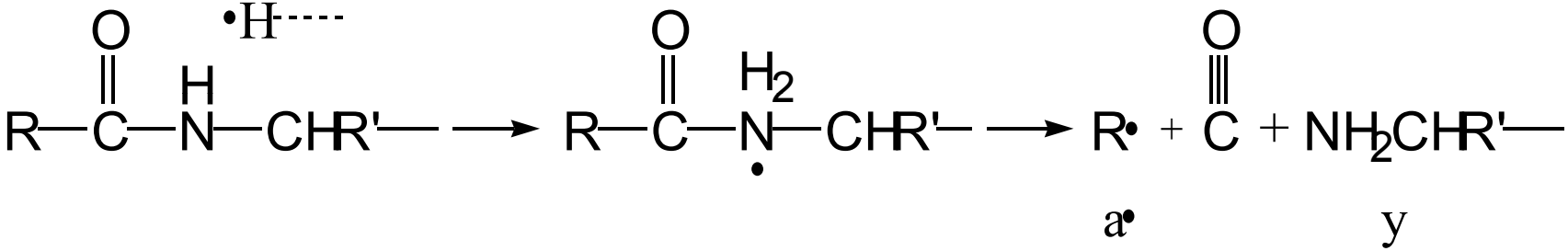

or

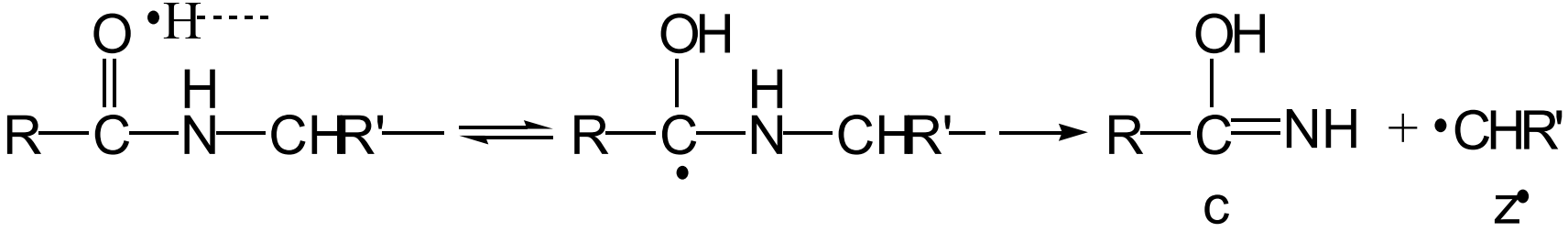

Why ECD?

- Neutral H radical is highly energetic and highly reactive
  - Can break higher energy bonds than SORI-CID
  - Can cleave disulfide bonds and post-translational modifications
  - Does not denature peptide. Cleavage local to protonation site.

ECD (SF_6 Cooling Gas)

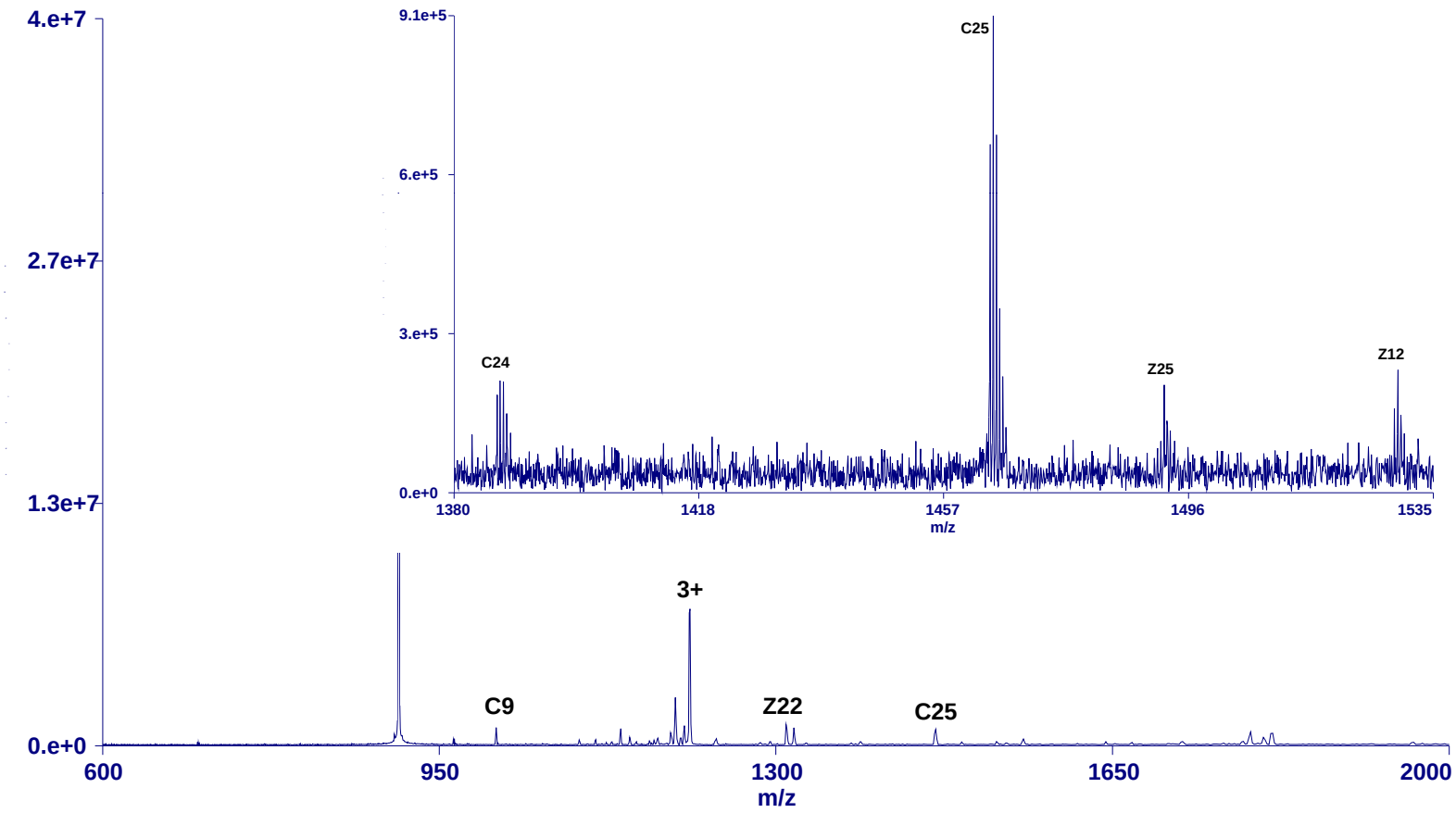

ECD (SF_6 Cooling Gas)

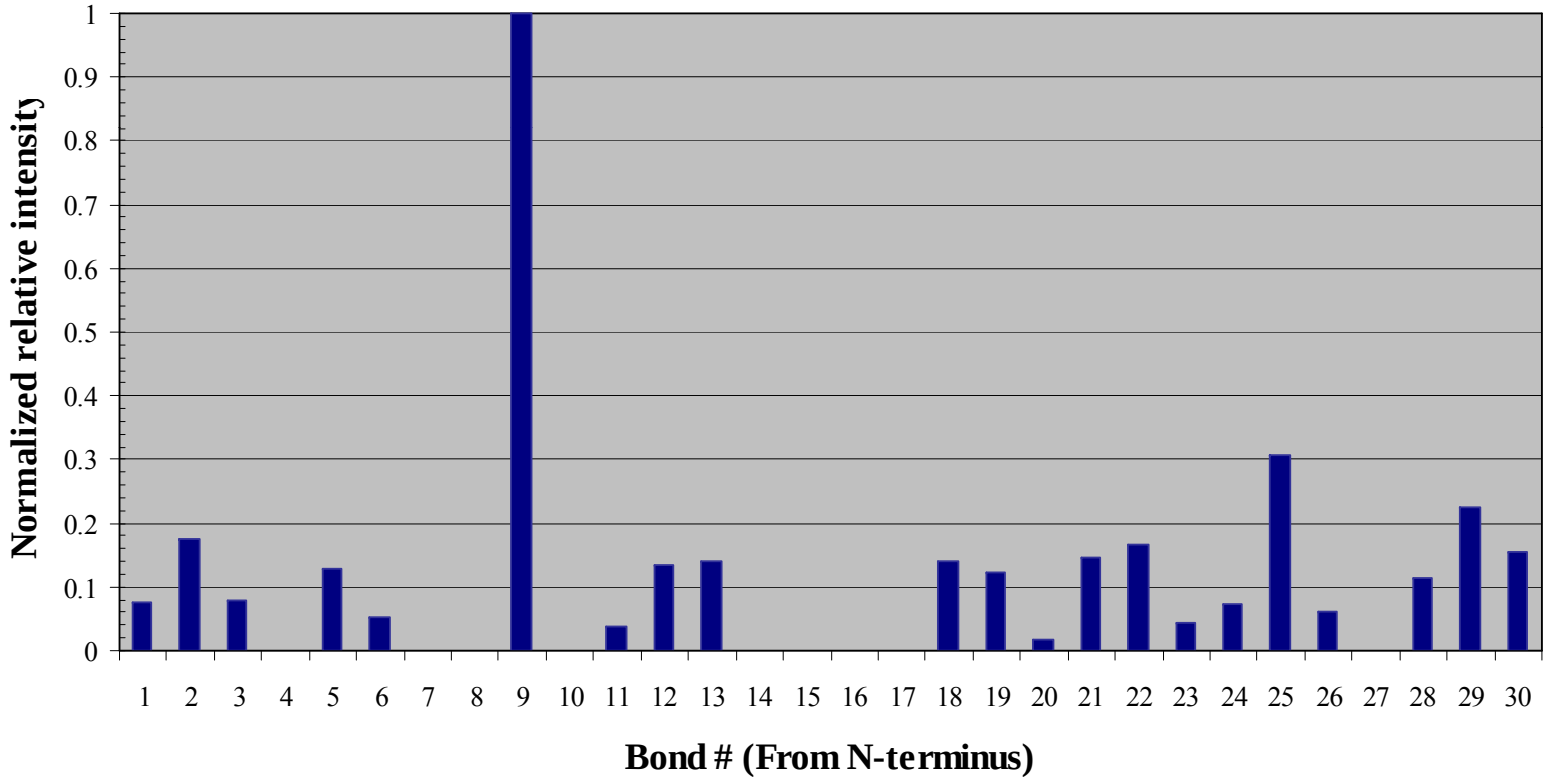

Synthetic hPTH (1-31)

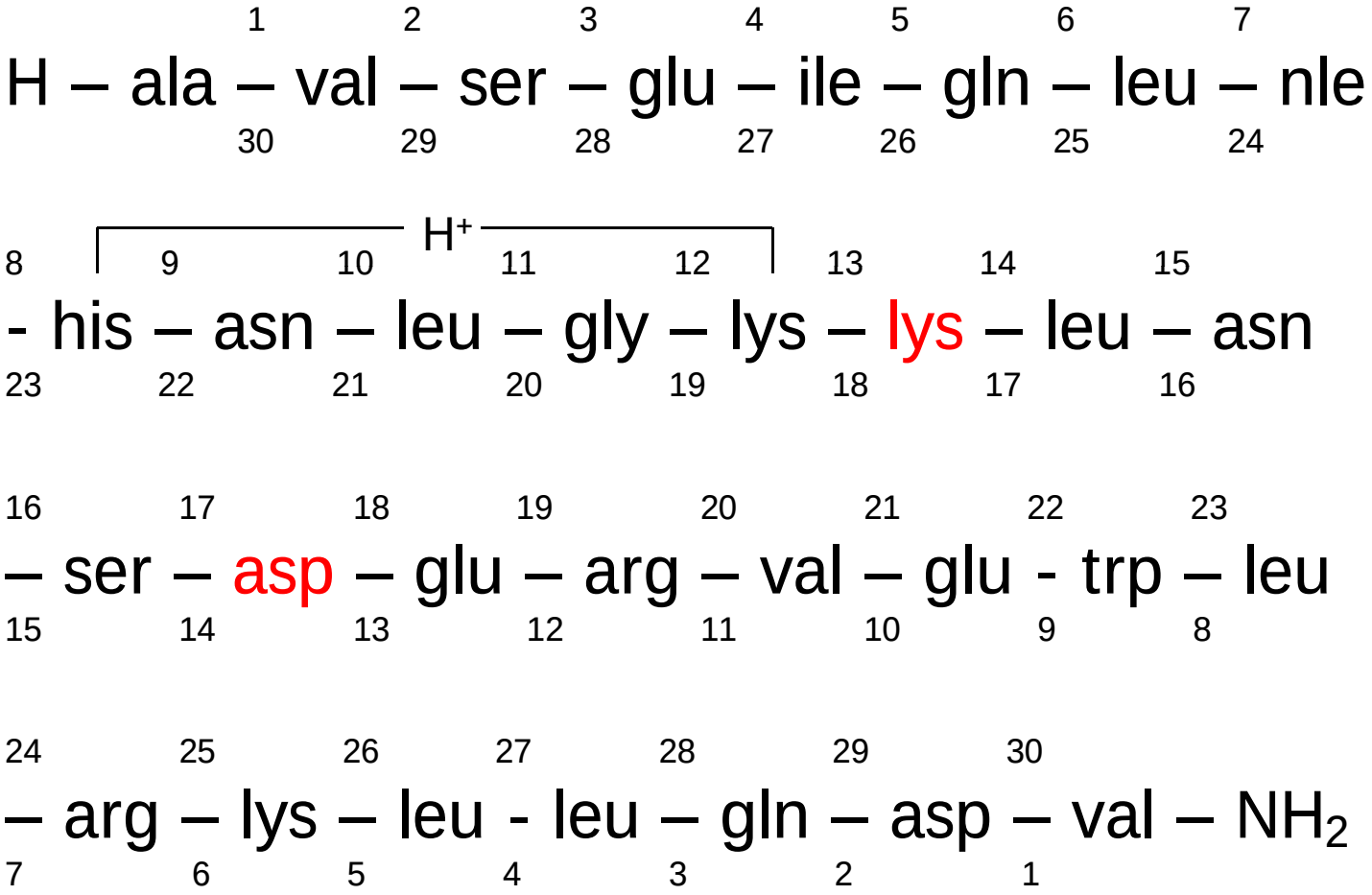

Peptide Bond #9

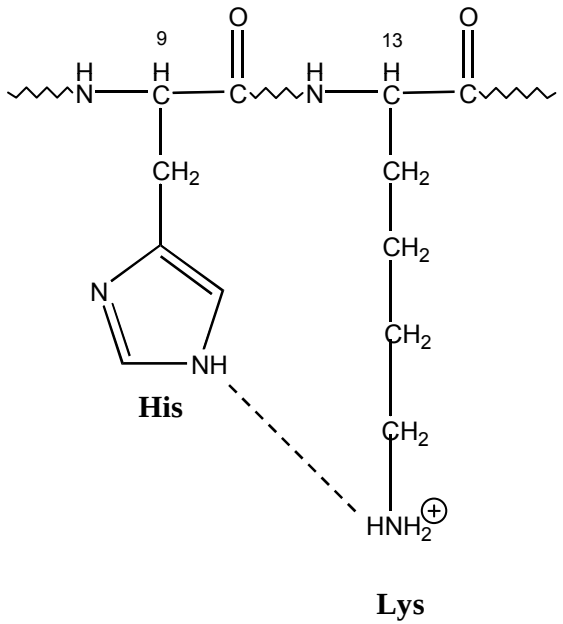

- Helical structure can di-solvate proton.
- His-9 may delocalize the radical.

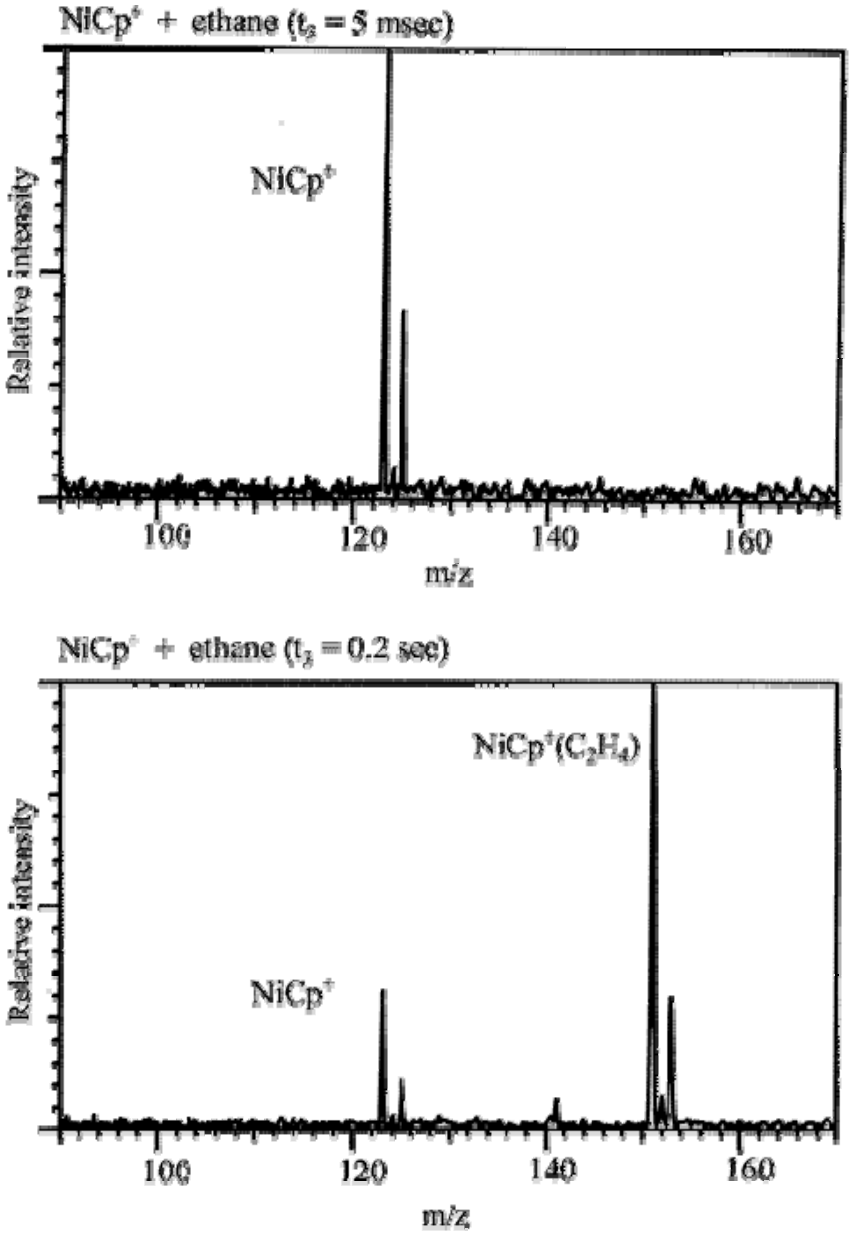
NiCp+ + ethane (t2 = 5 msec)
NiCp+
Relative intensity
100
120
140
160
m/z
NiCp+ + ethane (t2 = 0.2 sec)
NiCp+(C2H4)
NiCp+
Relative intensity
100
120
140
160
m/z

Scheme II

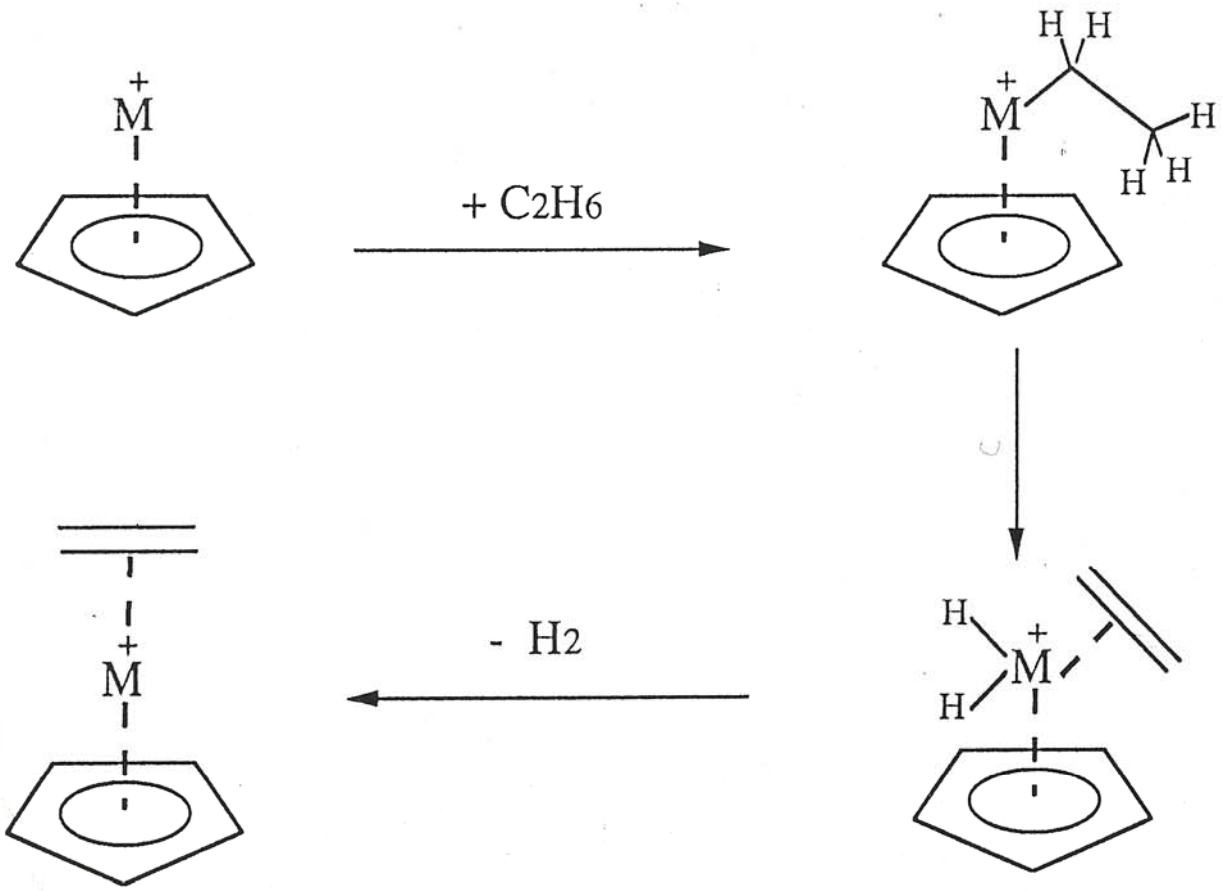

M=Co, Ni
N. R. for M=Fe

Ekeberg, Lin, Sohlberg, Chen, Ridge, et al., Organomet. 18, 40(1999)

Criteria for an Ideal Charging Agent for Polyolefins:

- Chemical modification inside the mass spectrometer
- Functionality in the hydrocarbon not required
- The predominant product characteristic of the original hydrocarbon (distribution)
- Minimal fragmentation

Charging Agent

Hydrocarbon

Adduct

Current Approach - Chain-end Derivatization

- Organic species (e.g. PR_3) covalently attached to the polymer forming an organic salt
- Labile endgroup necessary for derivatization
  - *e.g.* polyethylene – presence of vinyl group
- Aggressive reaction conditions necessary for saturated polyolefin derivatization
- Several days required for synthesis, sample work-up, and characterization

Current Approach - Atomic Transition Metal Ion (M^+) Chemistry

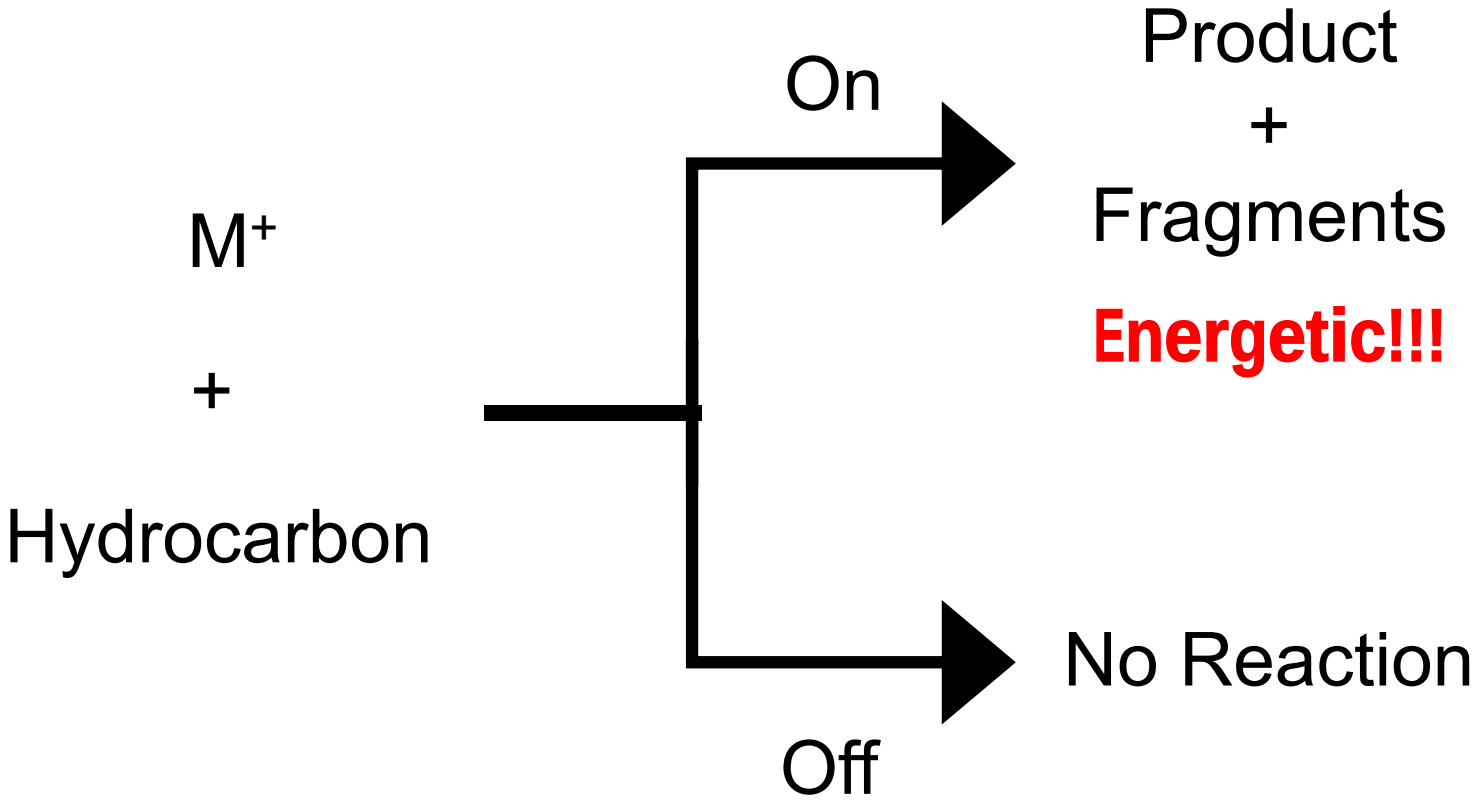

MS interpretation very complicated

Ligated TM chemistry allows better control of the ion-molecule reaction.

Higher MW Hydrocarbons Show Similar Double Dehydrogenation Reactivity

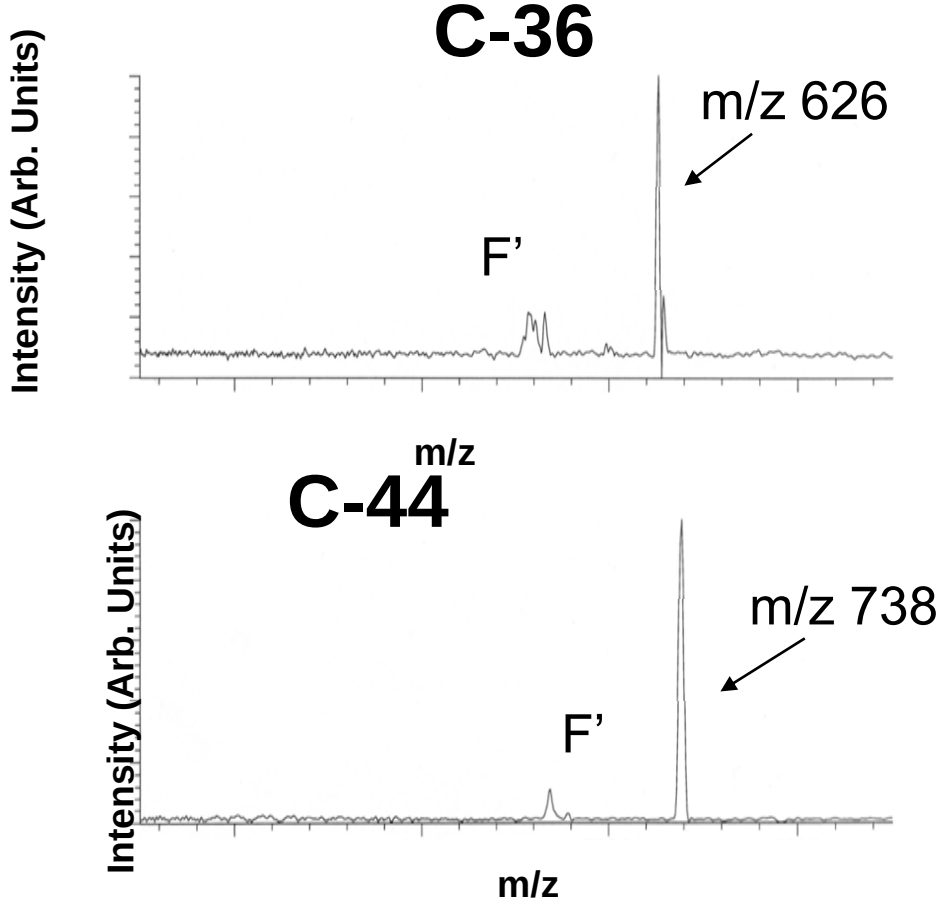

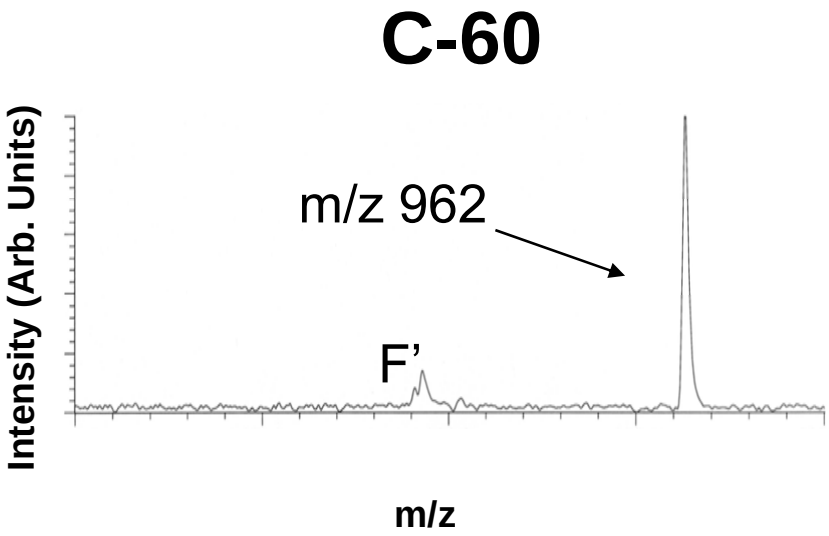

F′ - C_5H_6 loss from Adduct – $2H_2$

Comparison with Past Work

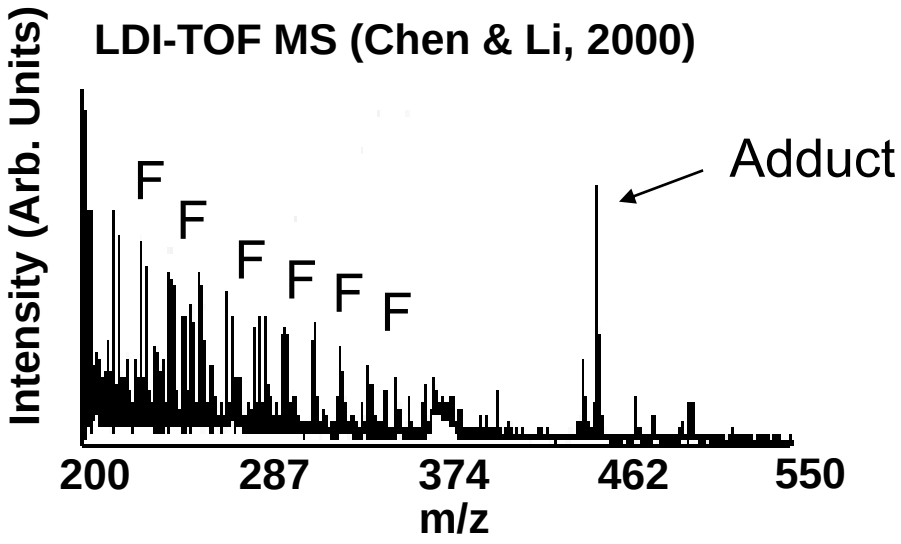

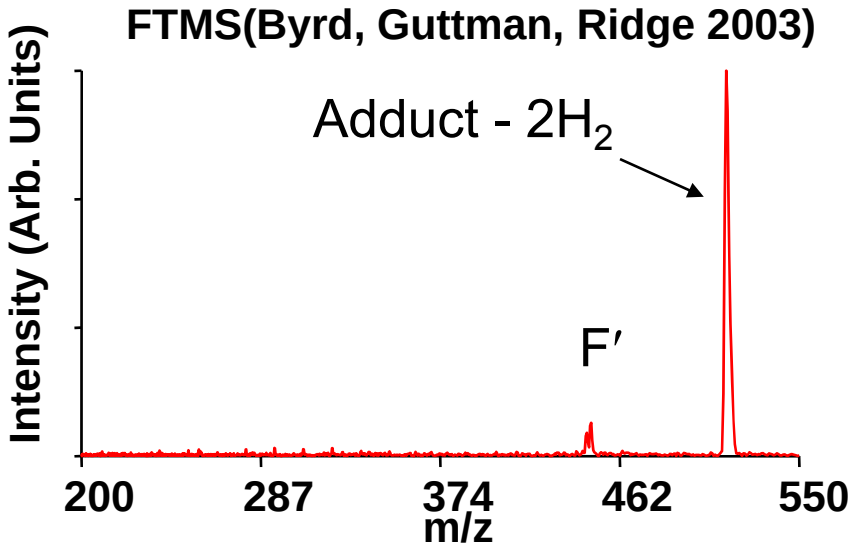

- reaction of C-28 with Co^+ produces adduct ion as well as extensive fragmentation
- reaction with $CpCo^{\bullet+}$ shows minimal fragmentation

F′ - C_5H_6 loss from Adduct –$2H_2$

Oxidation of Metal Monocarbonyl Cations

$M(CO)^+ + O_2 \rightarrow MO^+ + CO_2$ (1)

observed only for M = Fe

not observed for M = Cr, Mn, Co, Ni

Thermochemistry of O2 Oxidation of CO Ligand
(Kcal/mol)

M	$D(M^+\text{-}CO)$ [state]	$D(M^+\text{-}O)$ [state]	$\Delta H(1)$
Cr	21.4 [$^6\Sigma^+$]	85.8 [$^4\Sigma^-$]	-72.4
Mn	22.1 [$^5\Pi$]	68.0 [$^5\Pi$]	-52.3
Fe	31.3 [$^4\Sigma^-$]	80.0 [$^6\Sigma^+$]	-56.7
Co	41.5 [$^3\Delta$]	74.9 [$^5\Delta$]	-41.1
Ni	41.7 [$^2\Sigma^+$]	63.2 [$^4\Sigma^-$]	-29.6

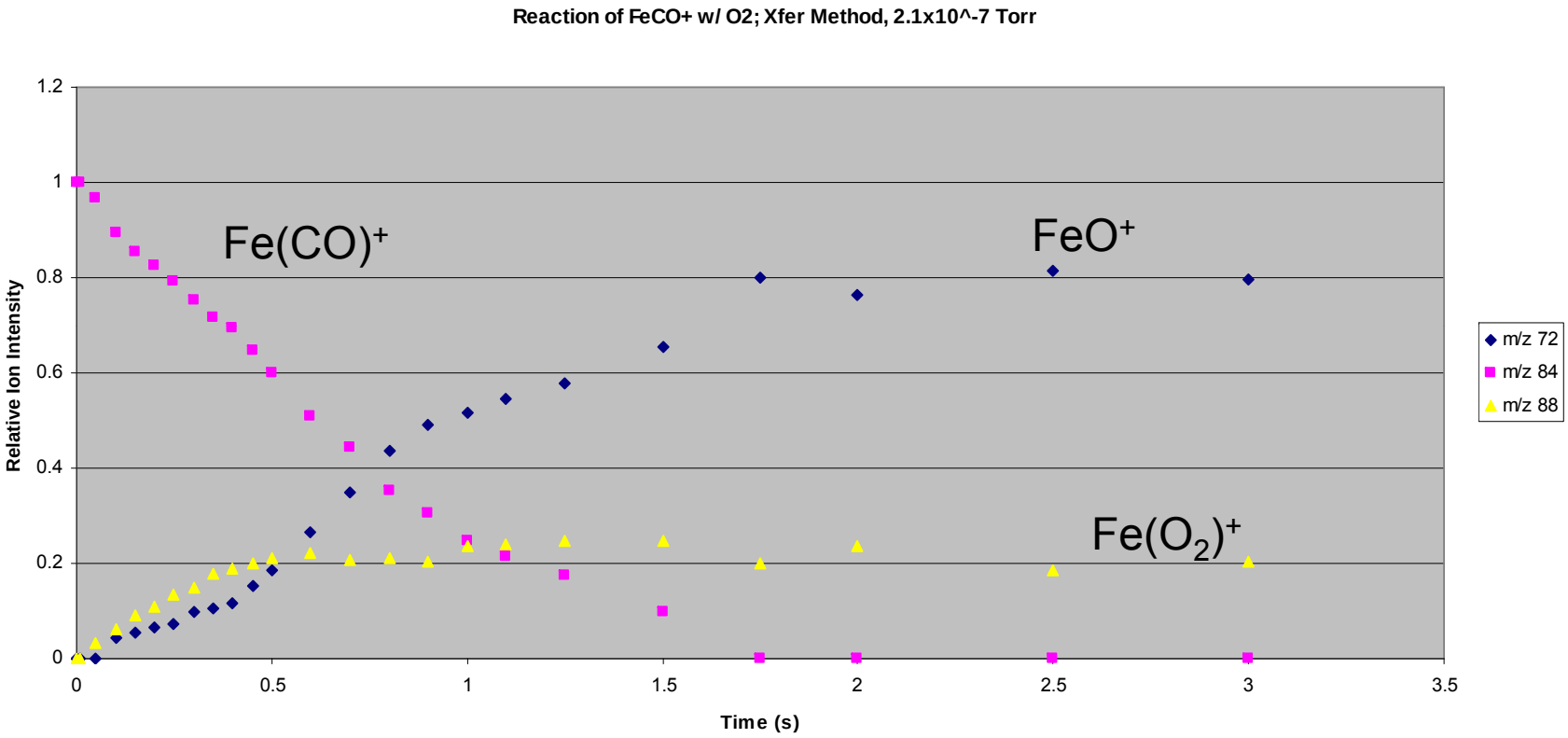
Reaction of FeCO+ w/ O2; Xfer Method, 2.1x10^-7 Torr
Relative Ion Intensity
Time (s)
Fe(CO)+
FeO+
Fe(O2)+
m/z 72
m/z 84
m/z 88
0
0.2
0.4
0.6
0.8
1
1.2
0.5
1.5
2
2.5
3
3.5

$Fe(CO)^+ + O_2 \rightarrow$ products

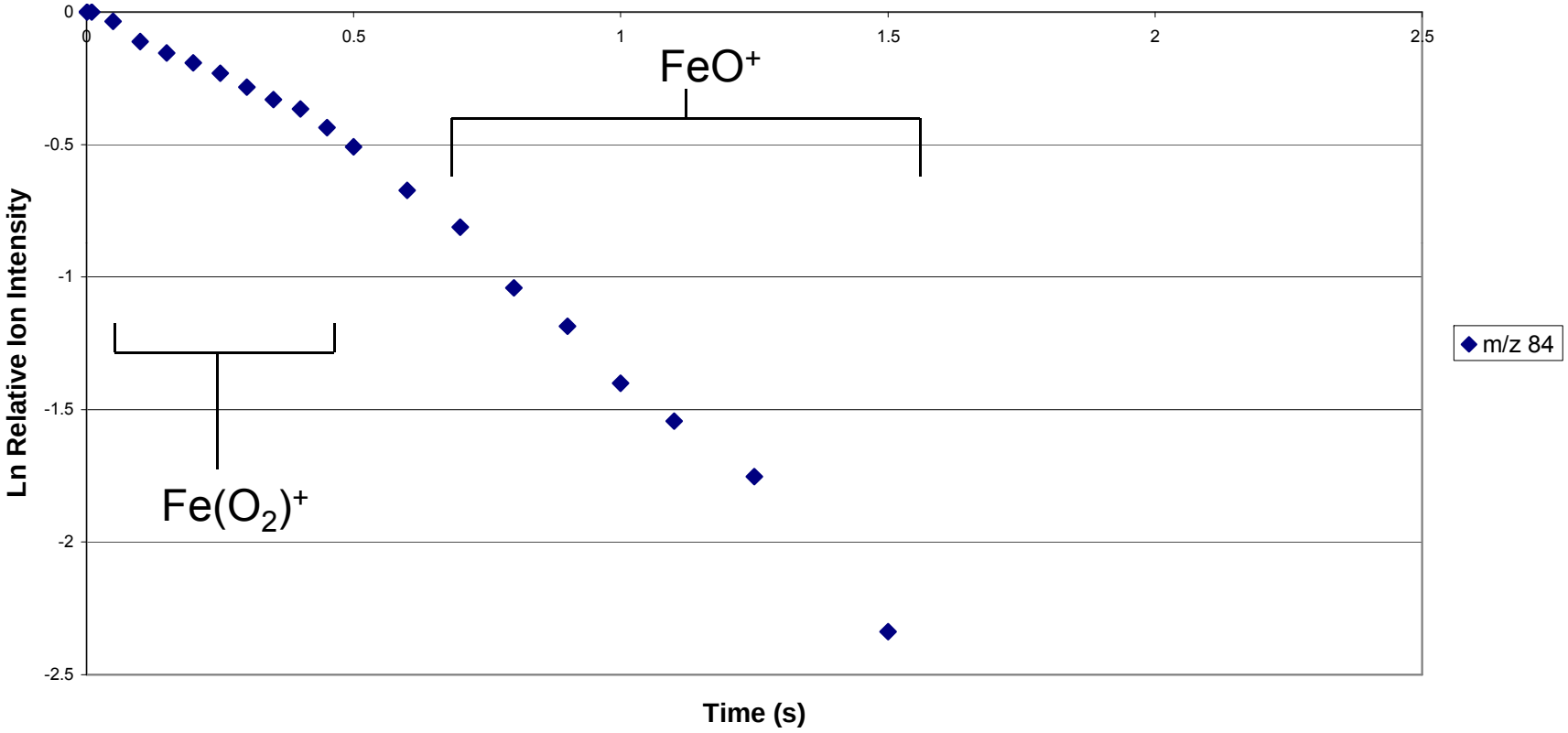

The Effect of Exciting $Fe(CO)^+$

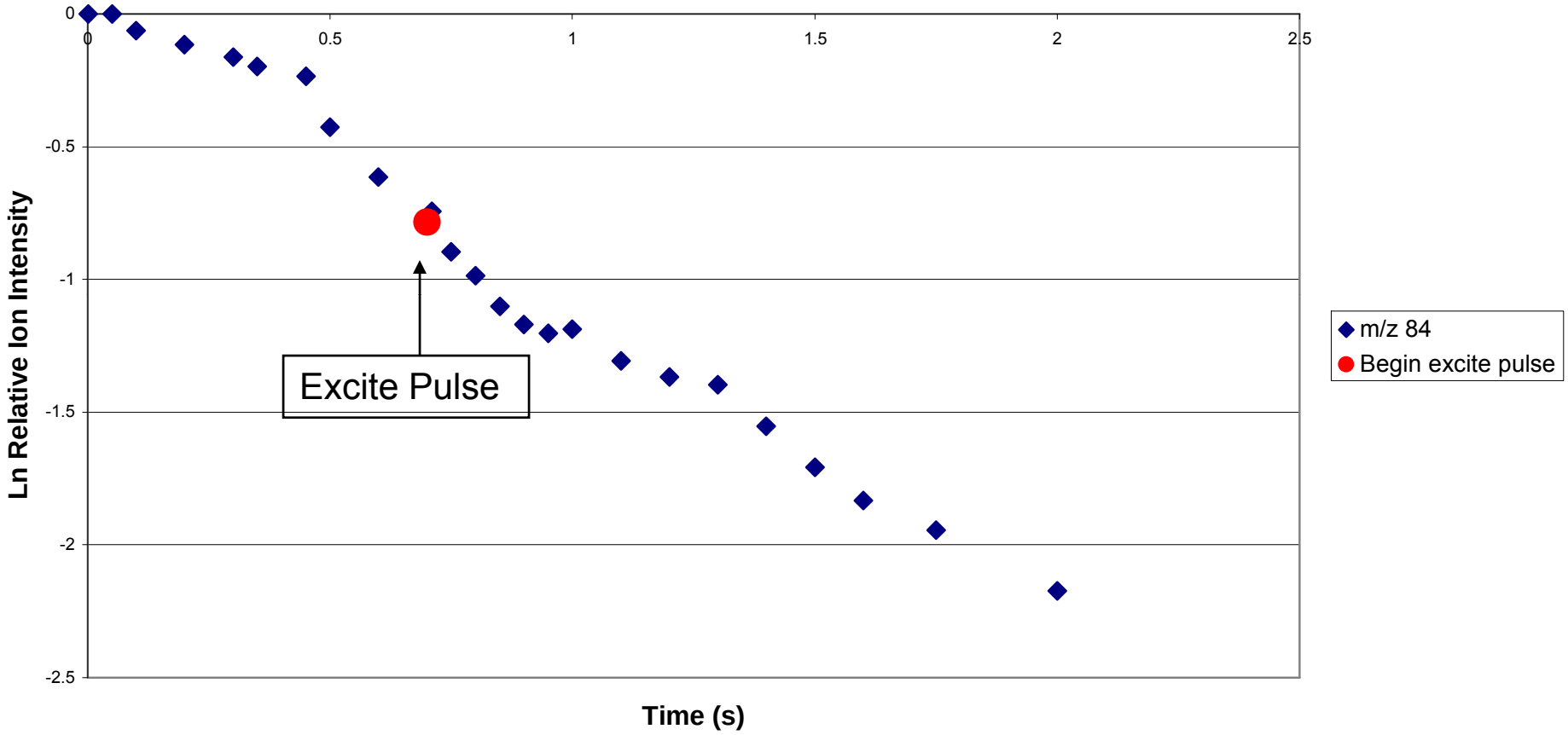

Potential Energy Surface
for $Fe(CO)^+ + O_2$

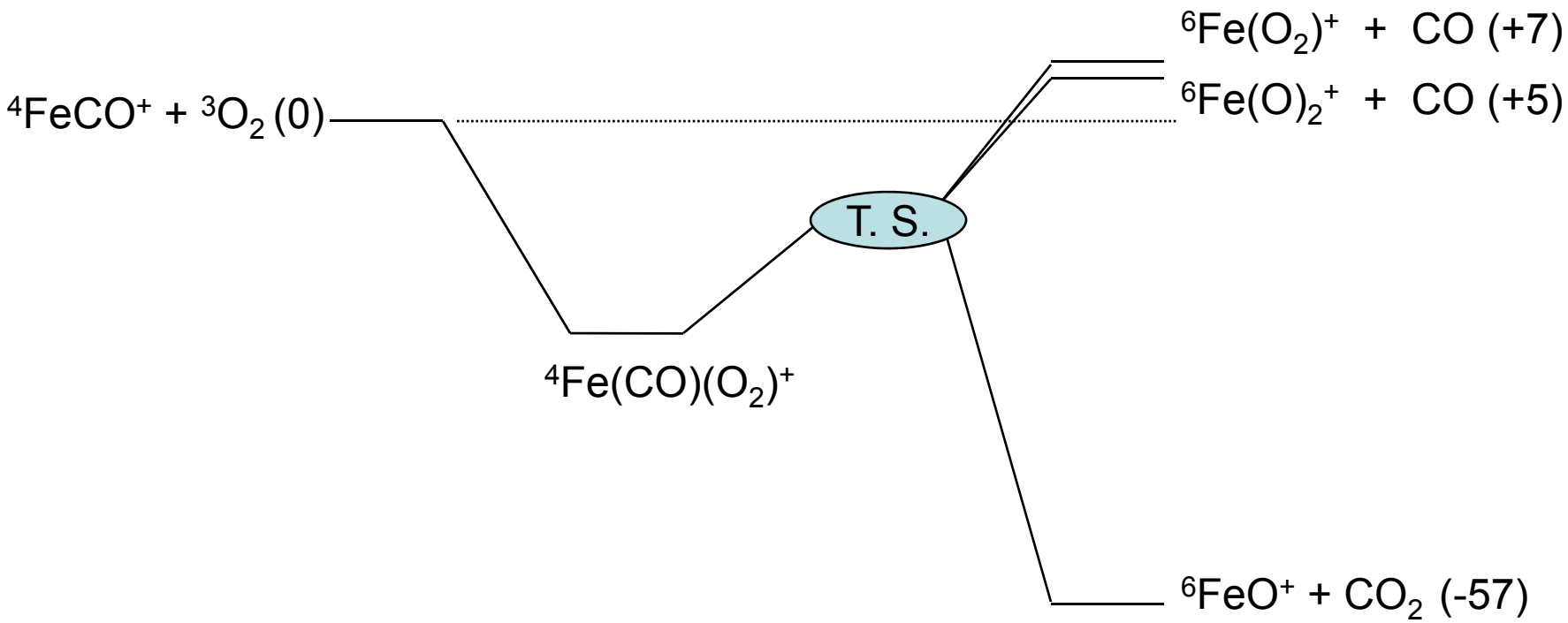

Potential Energy Surface
for $Cr(CO)^+ + O_2$

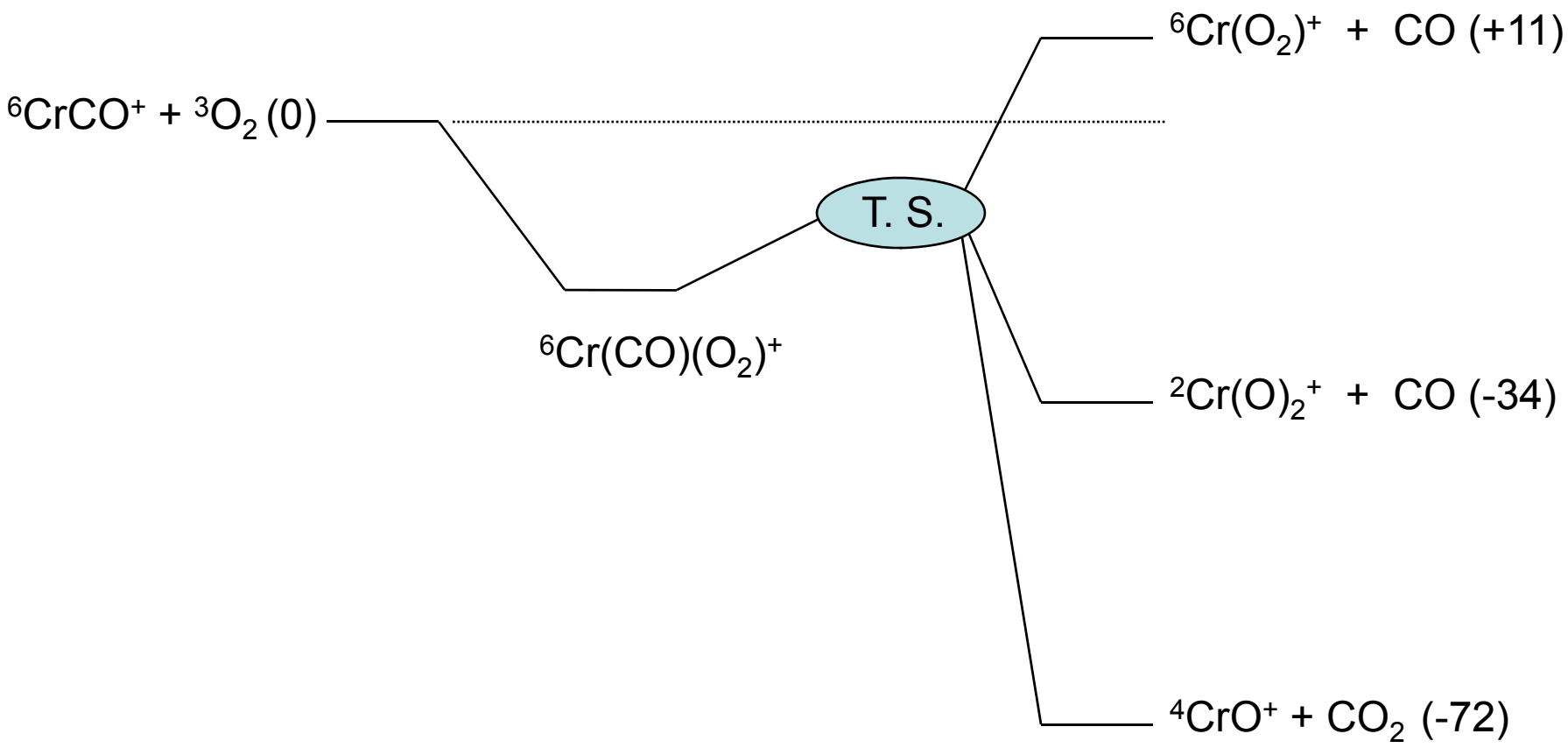

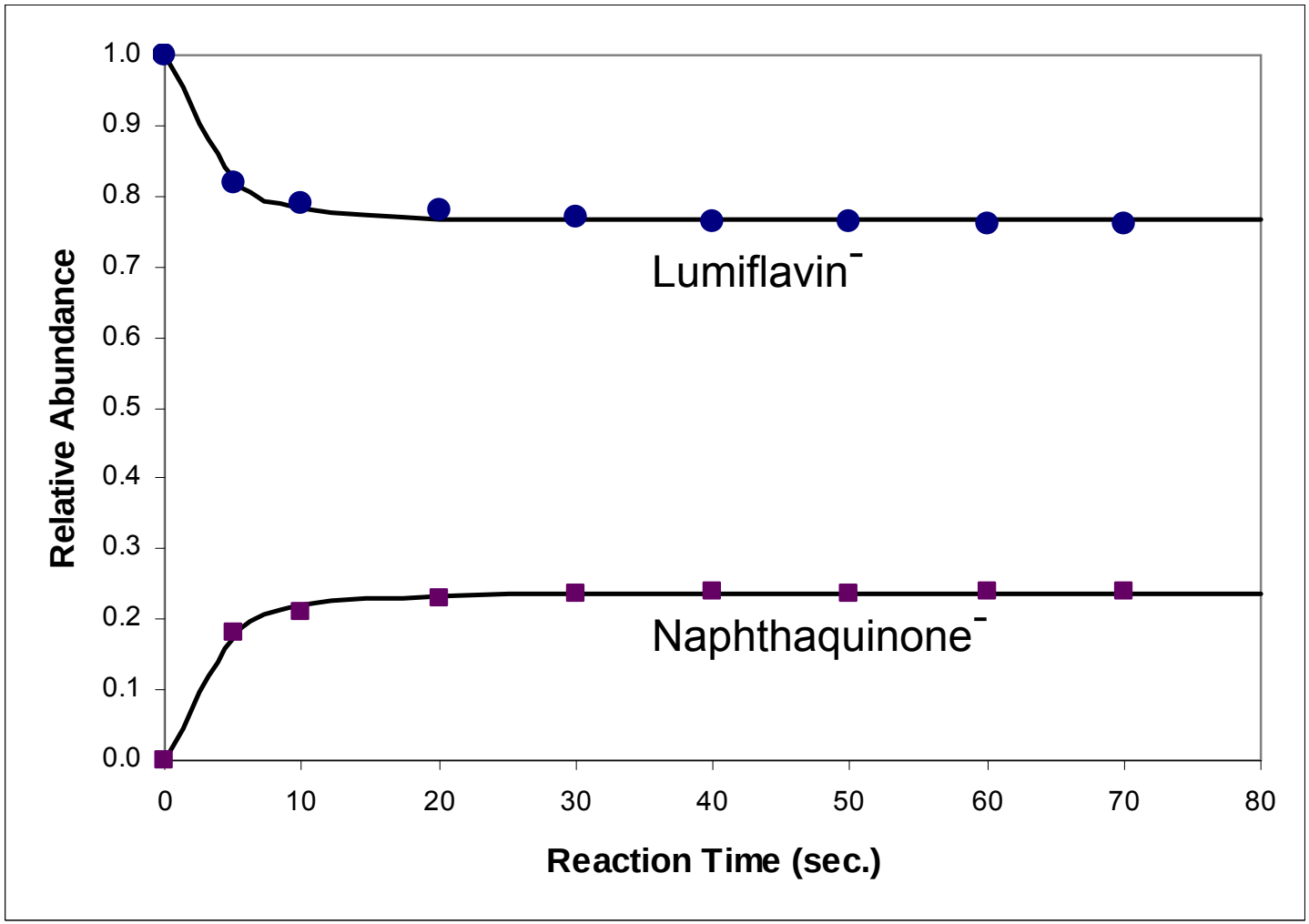

Variation with time of lumiflavin anion and 1,4 naphthoquinone anion in a mixture of the neutrals

Flavin in Various Oxidation States

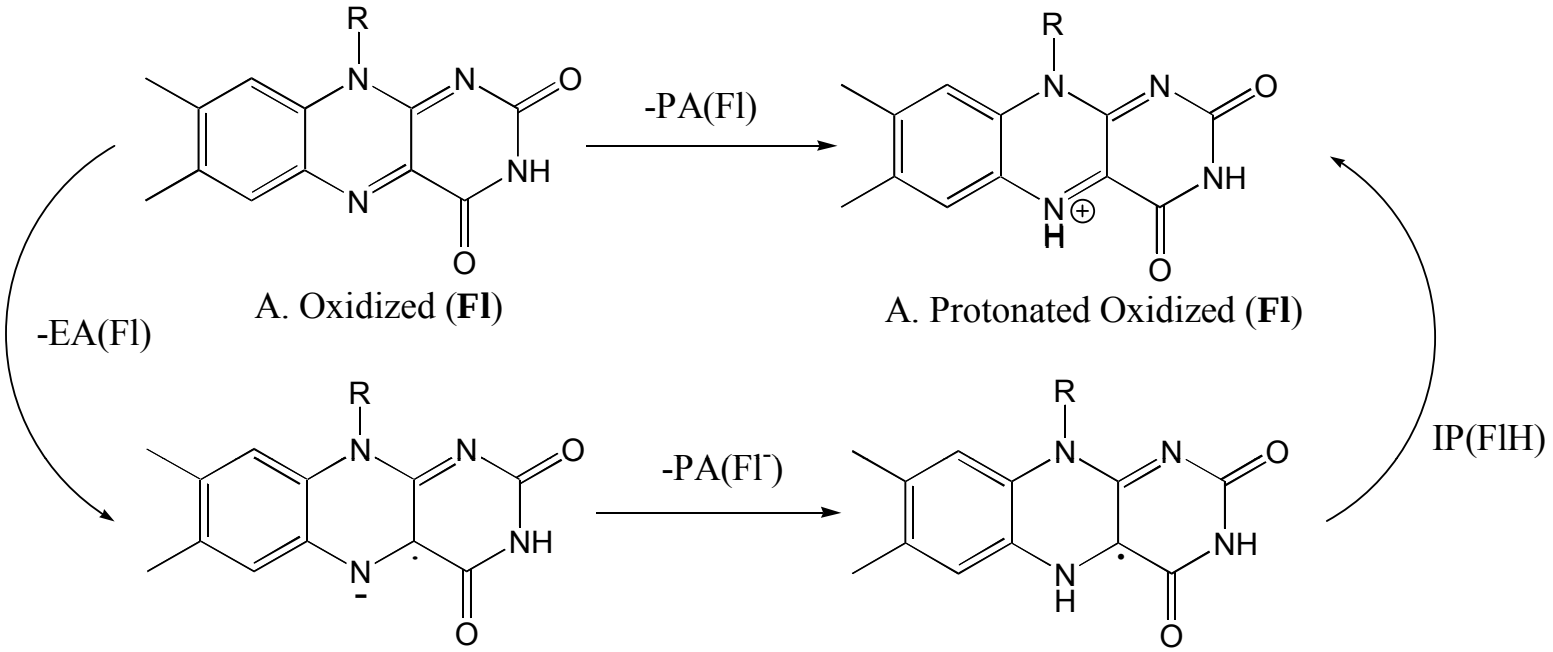

A. Oxidized (**Fl**)

A. Protonated Oxidized (**Fl**)

B. Red Semiquinone
(Radical Anion, **Fl**$^{-}$)

C. Blue Semiquinone
(Radical, **FlH**)

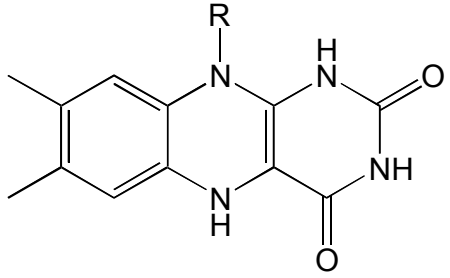

D. Fully Reduced (**FlH_2**)

Measured and Computed Properties of Redox Forms of Lumiflavin

Property	B3-LYP/6-31G(d)[a,b]	B3-LYP/6-31+G**[a,c]	Experimental FTMS (Electrochemistry)
EA(Fl)	1.54 eV (B3-LYP/6-311++G(d) 2.00 eV)	1.96 eV	1.86 ± 0.06 eV
PA(Fl)	221 kcal mol^{-1} (B3-LYP/6-311++G(d) 215kcal mol^{-1})		225.5 ± 2.2 kcal mol^{-1}
PA(Fl^{-})	332 kcal mol^{-1}	322 kcal mol^{-1}	332 ± 3.2 kcal mol^{-1}
D(Fl-H)	54.8 kcal mol^{-1}	54.2 kcal mol^{-1}	59.7 ± 2.2 kcal mol^{-1} (60.6 ± 2.4 kcal mol^{-1})
IP(FlH)	6.38 eV		6.40 ± 0.10 eV

a) Theoretical numbers correspond to 0 K.
b) Present Results
c) Hadad, et al. JACS **124**, 7226(2002)
d) Experimental measurements at 298 K.
e) Anderson, Biochem. Biophys. Acta **722**, 158(1983).

Iron Tetraphenyl-porphyrin Series

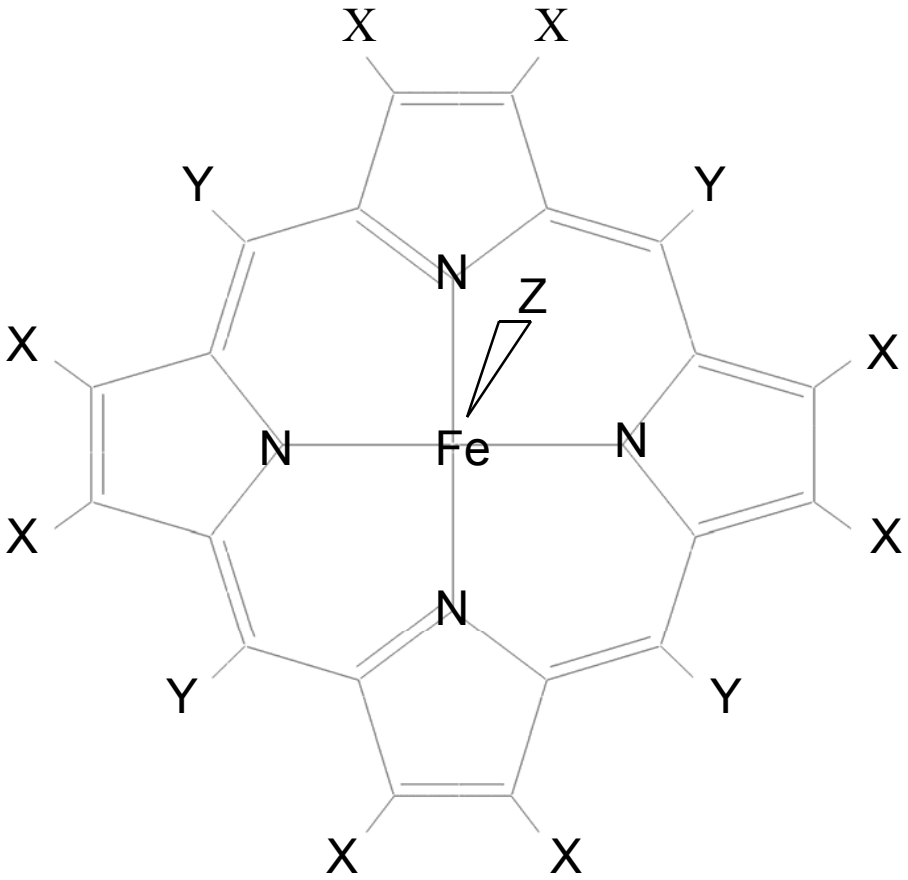

X, Y, Z	Symbol used in this work
X = H, Y = C_6H_5, No Z	FeTPP
X = H, Y = C_6H_5, Z = Cl	FeTPPCl
X = H, Y = C_6F_5, No Z	$FeTPPF_{20}$
X = H, Y = C_6F_5, Z = Cl	$FeTPPF_{20}Cl$
X = Cl, Y = C_6F_5, No Z	$FeTPPF_{20}Cl_8$
X = Cl, Y = C_6F_5, Z = Cl	$FeTPPF_{20}Cl_9$

Fluoroalkyl Series

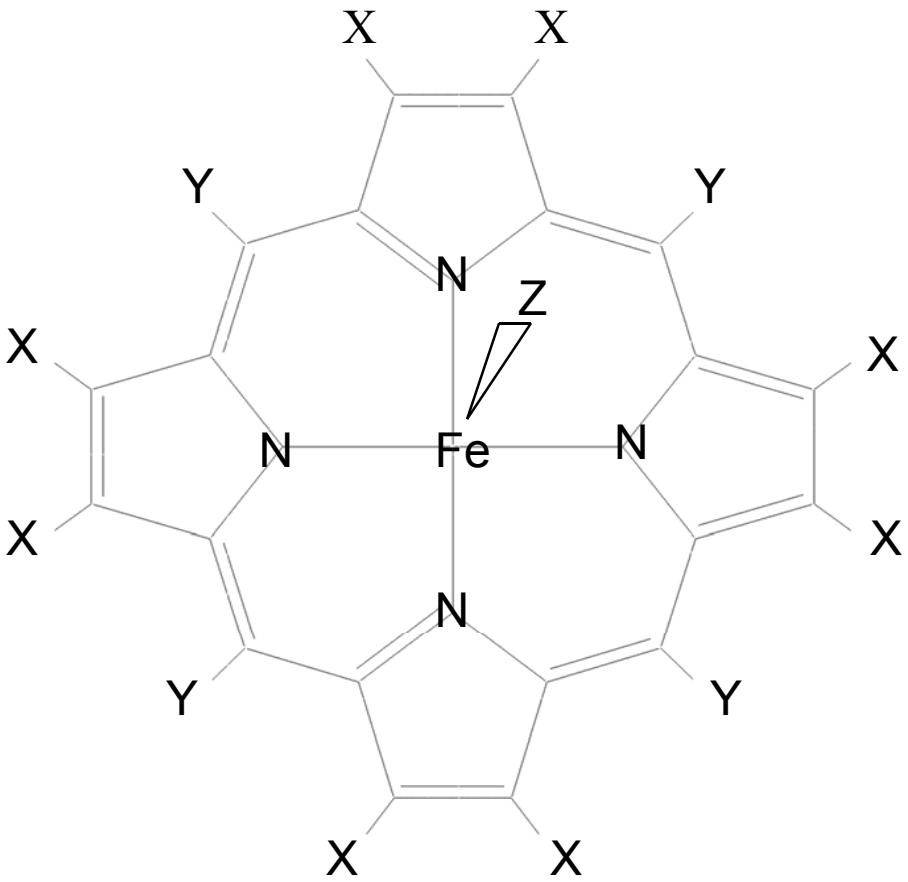

X, Y, Z	Symbol used in this work
X = Y = H, No Z	FeP
X = Y = H, Z=Cl	FePCl
X = H, Y = CF_3, Z = Cl	$FeP(CF_3)_4Cl$
X = H, Y = C_3F_7, Z = Cl	$FeP(C_3F_7)_4Cl$

Octaethyl Series

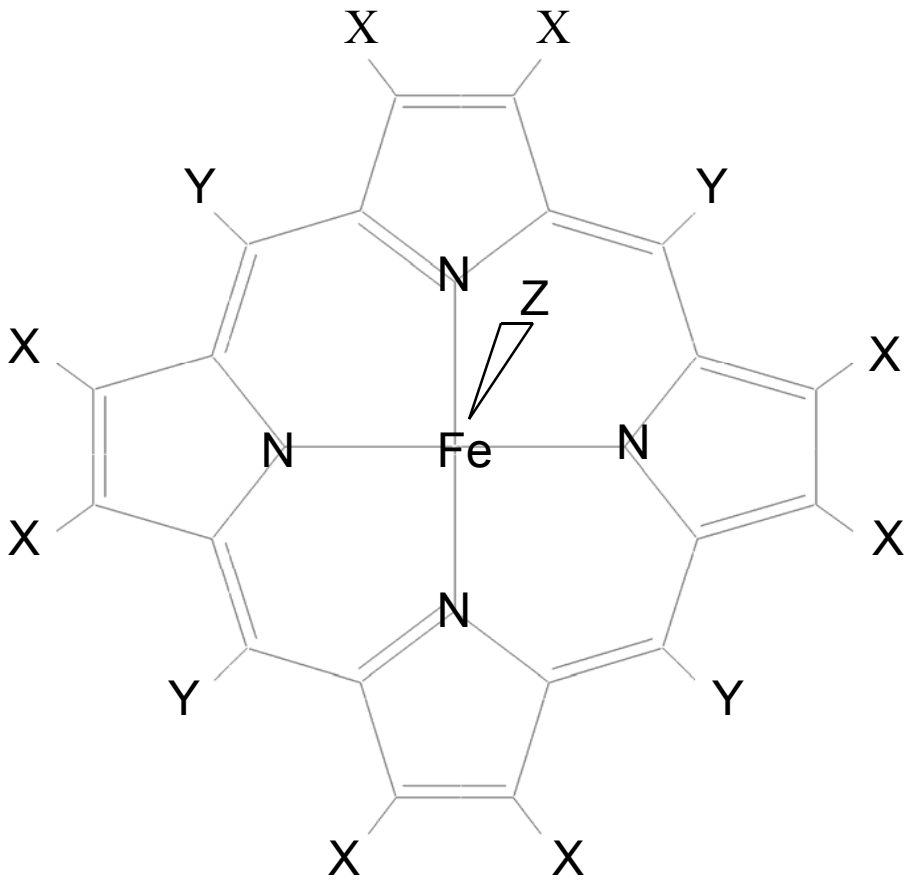

X, Y, Z	Symbol used in this work
$X = C_2H_5$, Y = H, No Z	FeOEP
$X = C_2H_5$, Y = H, Z = Cl	FeOEPCl
$X = C_2H_5$, $Y = NO_2$, Z = Cl	$FeOEP(NO_2)_4Cl$

Electron Affinity Ladder

Compound	EA (eV)
TCNE	[3.17]
$Fe(OEP)(NO_2)_4Cl$	2.93
F_4-BQ	[2.70]
$Fe(OEP)(NO_2)_2Cl$	2.54
Fe(OEP)(O)Cl	2.53
2,6-Cl_2BQ	[2.48]
NO_2	[2.29]
Fe(OEP)Cl	2.07
4-NO_2NB	[2.00]
BQ	[1.91]
NPQ	[1.81]
Fe(OEP)	1.68
3-NO_2NB	[1.65]

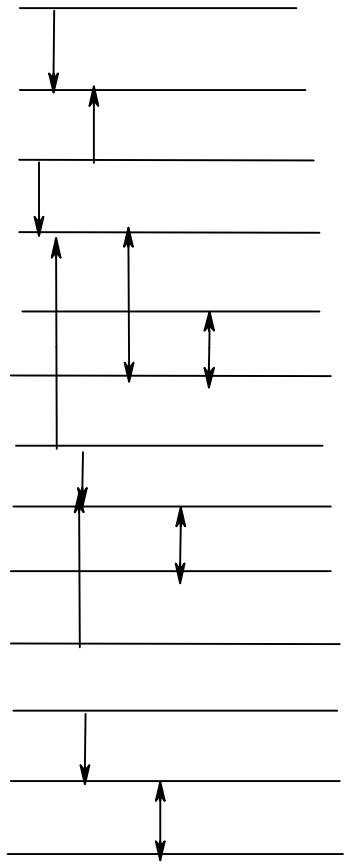

An Iron (II) Porphyrin (FeTPPF20) with C4v Symmetry

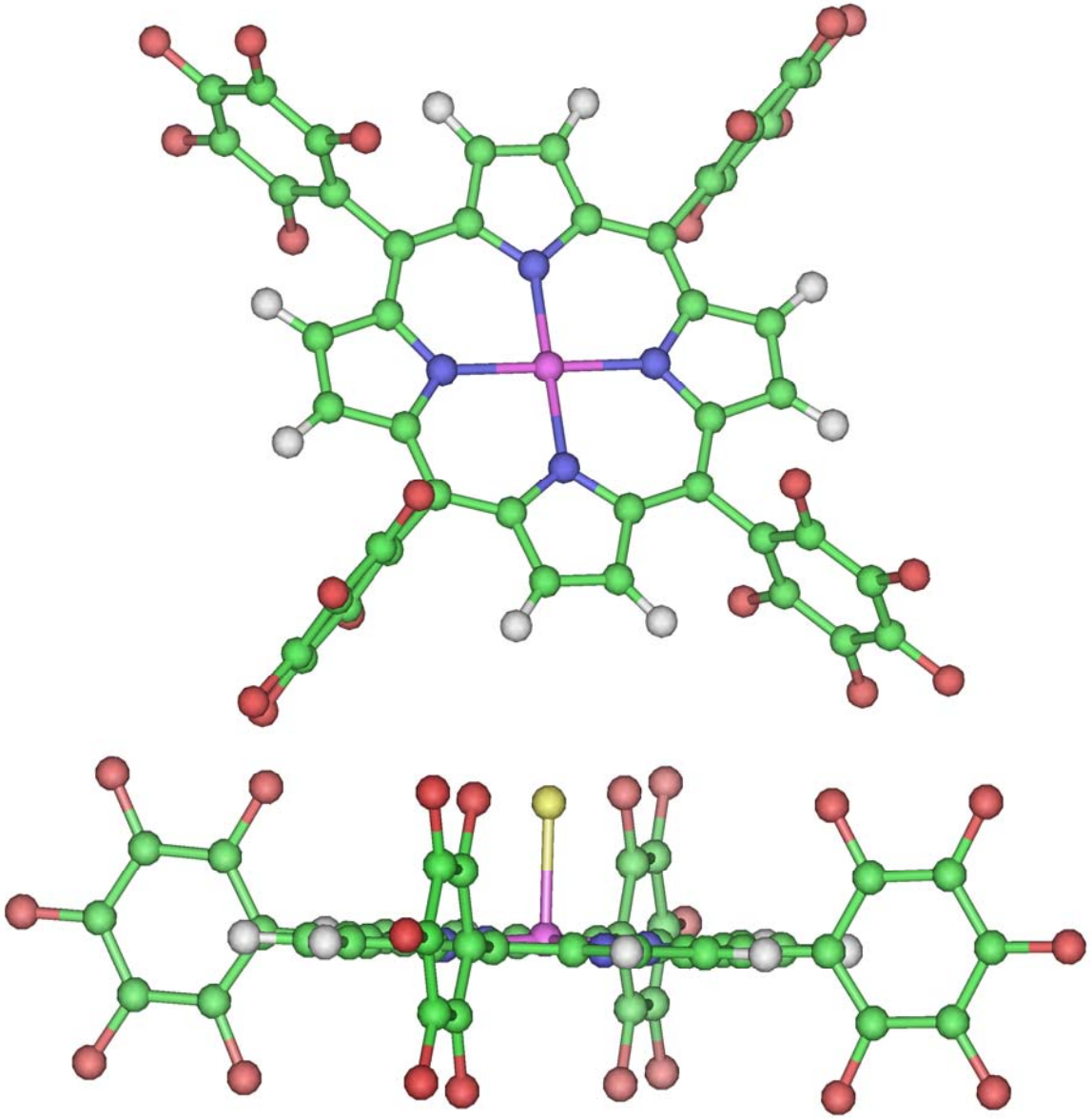

Figure 6.3 Addition of an Electron to the d_{π} Orbitals of FeTPP

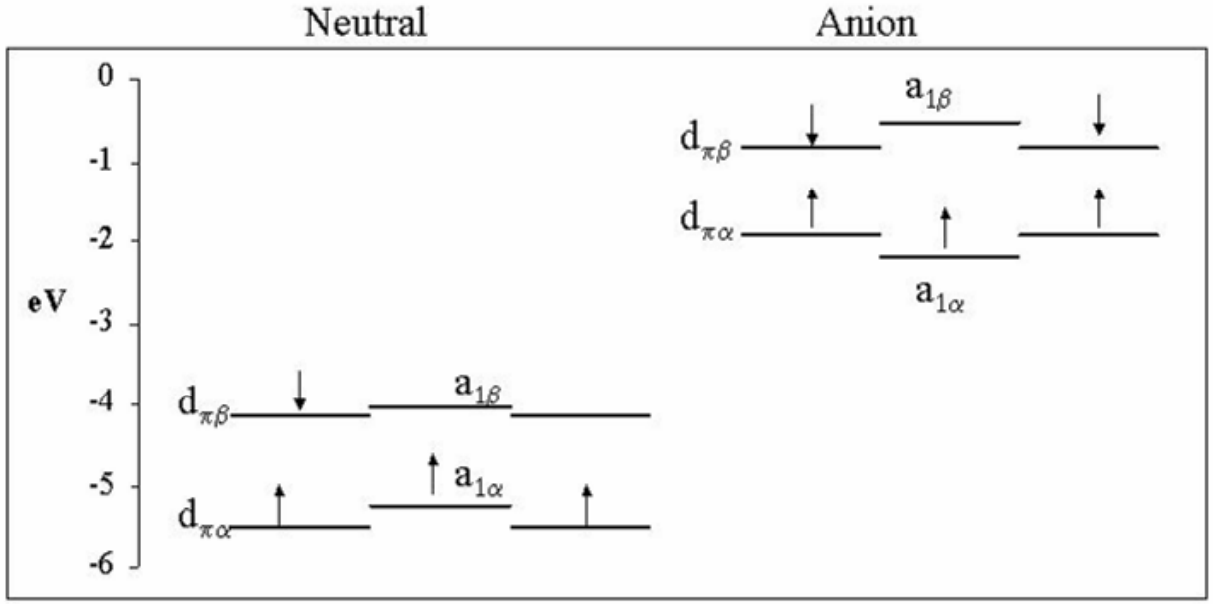

Dmol program, geometry optimized, BPW functionals, DNP basis set with “frozen” core potentials

Figure 6.1 Addition of an Electron to the d_{π} Orbitals of $FeP(CF_3)_4Cl$

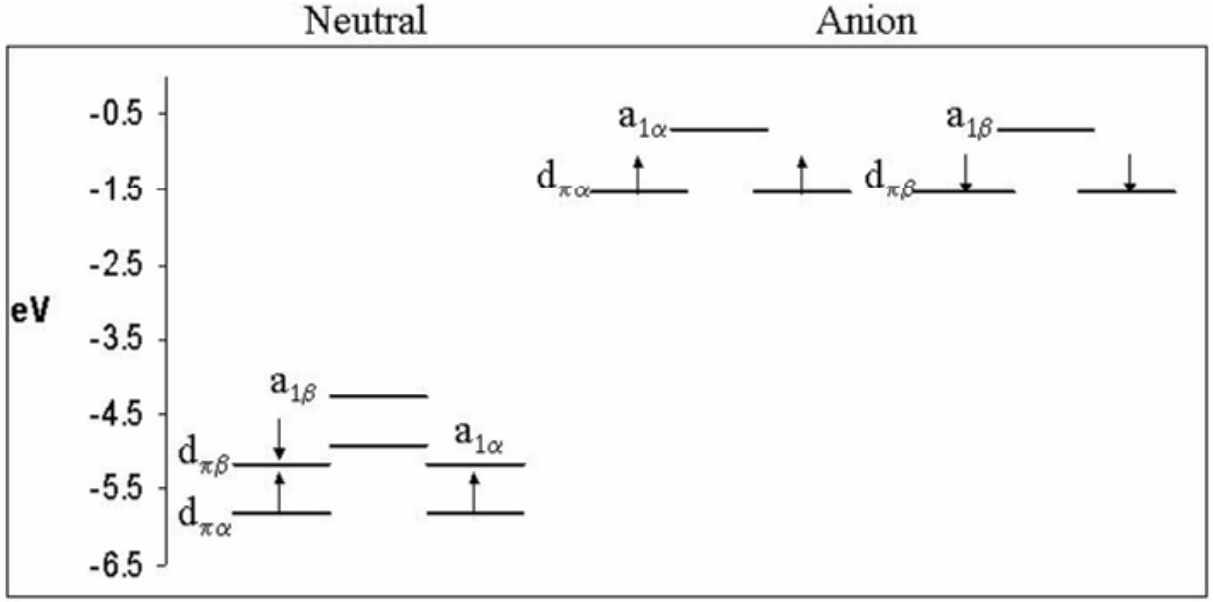

Dmol program, geometry optimized, BPW functionals, DNP basis set with "frozen" core potentials

Distances for Spin Unrestricted C_{4v} Fluoroalkyl Series

Molecule	Charge	Fe-N (Å)	Fe-Cl (Å)	Fe-N_4 plane (Å)
$FeP(CF_3)_4Cl$	Neutral	2.0064	2.1727	0.1333
	Anion	2.0022	2.2538	0.0685
$FeP(C_2F_5)_4Cl$	Neutral	2.0121	2.1714	0.1603
	Anion	2.0088	2.2447	0.0978
$FeP(C_3F_7)_4Cl$	Neutral	2.0121	2.1672	0.1823
	Anion	2.0102	2.2376	0.1163

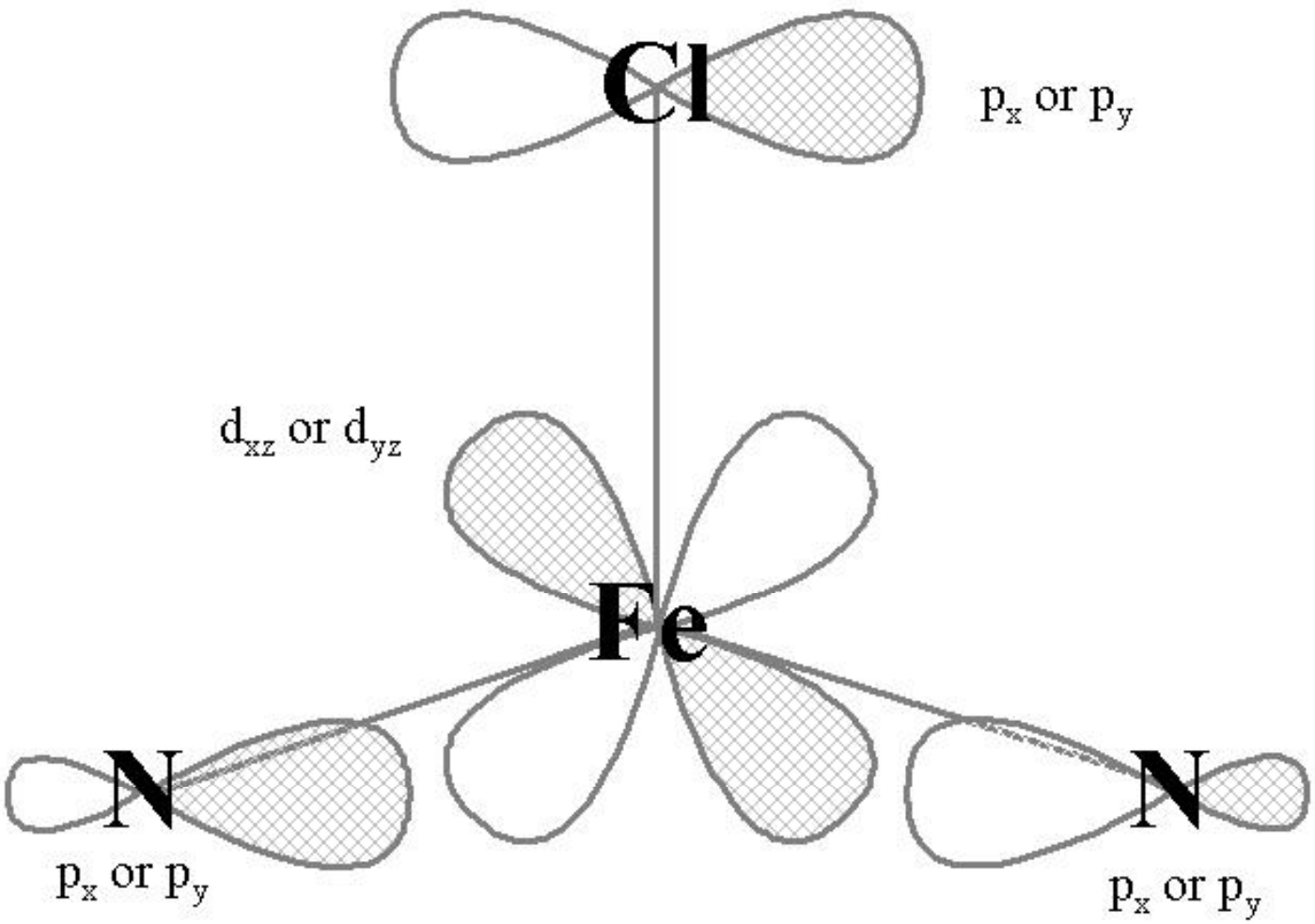
Cl
p_x or p_y
d_{xz} or d_{yz}
Fe
N
p_x or p_y
N
p_x or p_y

Bond Lengths from X-ray Diffraction for Tetraphenyl Series [*Present Results*]

[Molecule	Fe-N (Å)	Fe-Cl (Å)	Fe-N4plane (Å)
FeTPP	**1.972(4)**[i], [*1.9846*[a]]	N/A	
FeTPPCl	**2.049(9)**[ii], [*1.9902*[a]]	**2.192(12)**[ii][, [*2.1812*[a]]	**0.383(5)**[ii], [*0.2200*[a]]
$FeTPPF_{20}Cl$	**2.062(8)**[iii], [*1.9962*[a]]	**2.199(2)**[iii], [*2.1675*[a]]	**0.449(3)**[iii], [*0.1906*[a]]

a: Present spin unrestricted results for C_{4v} structures.

---

[i]. J.P. Collman, J. L. Hoard, N. Kim, G. Lang, C. A. Reed, *J. Am. Chem. Soc.*, **1975**, *97*, 2676.
[ii]. J. L. Hoard, G. H. Cohen, M. D. Glick, *J. Am. Chem. Soc.*, **1967**, *89*, 1992.
[iii]. B. Song, D. C. Swenson, H. M. Goff, *Acta Crys. Sect C.*, Volume 54, Part 11 (November 1998), cif-access (metal-organic compounds). IUC9800058.

Electron Affinities(eV)

Molecule	Electron Affinity (DFT)	Electron Affinity (Exp)
FeOEP	1.7557	1.68±0.03
FeTPP	2.134	1.87±0.03
FeOEPCl	2.2724	2.07±0.03
FeTPPCl	2.4704	2.15±0.15
$FeTPPF_{20}$	2.9887	2.15±0.15
$FeTPPF_{20}Cl$	3.3162	3.14±0.03
$FeP(CF_3)_4Cl$	3.363	3.16±0.03
$FeP(C_3F_7)_4Cl$	3.5151	3.30±0.03

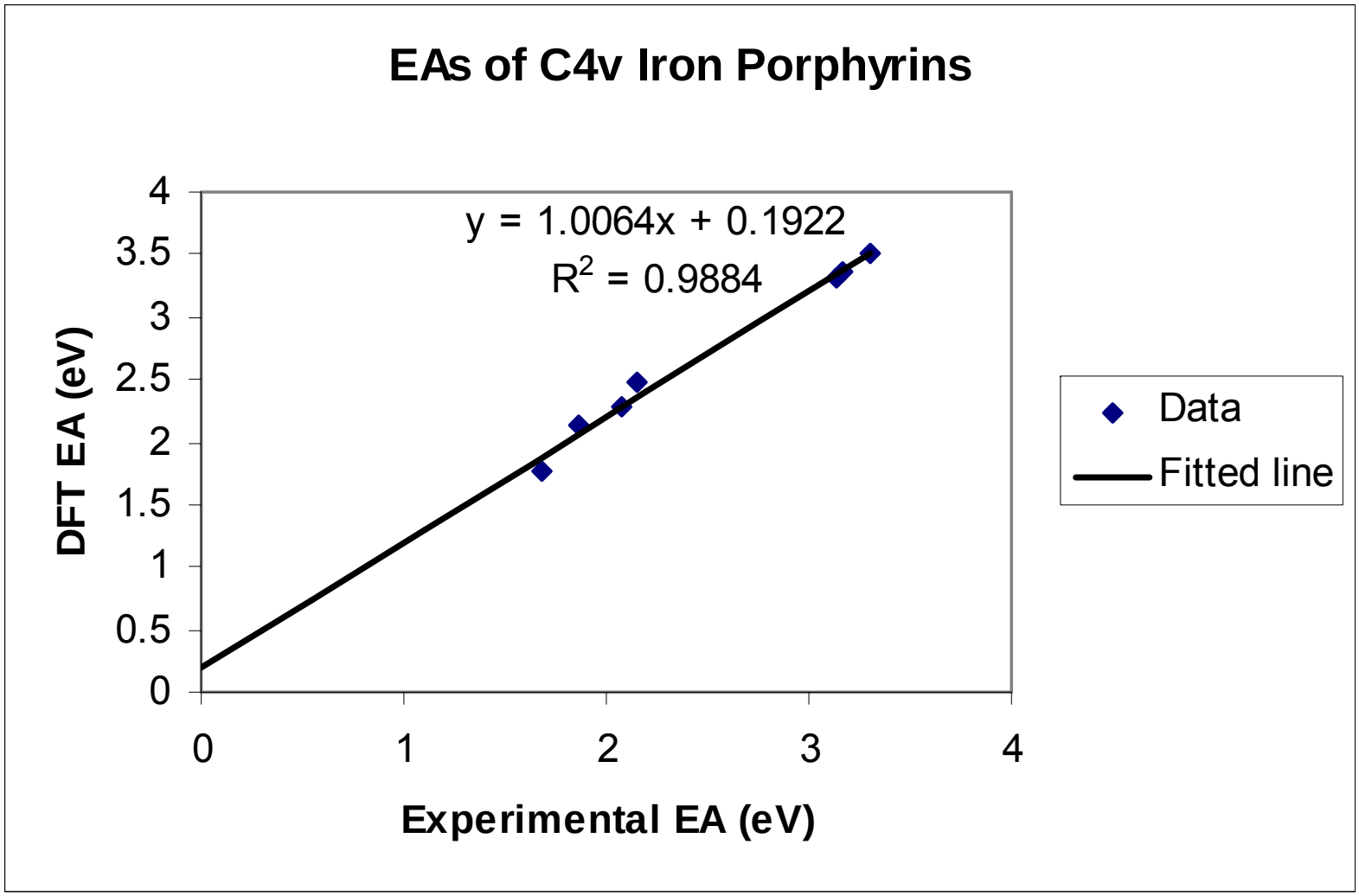
EAs of C4v Iron Porphyrins
y = 1.0064x + 0.1922
R2 = 0.9884
DFT EA (eV)
Experimental EA (eV)
0
0.5
1
1.5
2
2.5
3
3.5
4
0
1
2
3
4
Data
Fitted line

IR Spectra of Gas Phase Ions

- Absorption spectroscopy inaccessible
- Multiphoton IR photodissociation possible
- IRMPD spectrum reflects absorption spectrum
- Candidate ions: $Mn(CO)_m^{+/-}$, $M_n(CO)_m(alkane)^+$, $M_n(CO)_m(O_2)^{+/-}$, etc.
- Requires tunable IR laser

Free Electron Laser for Infrared eXperiments "FELIX"

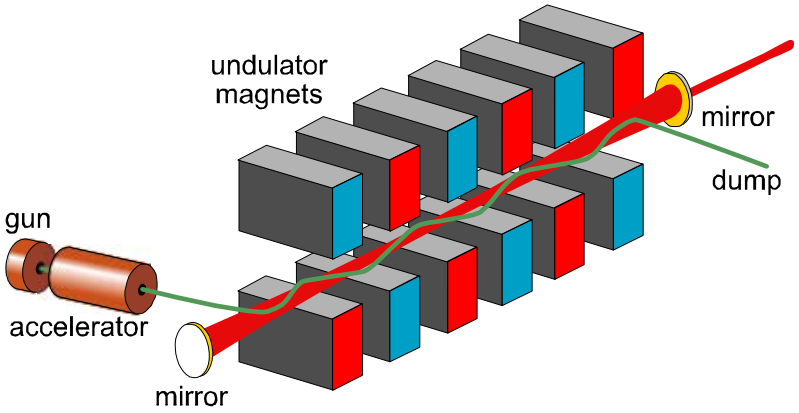

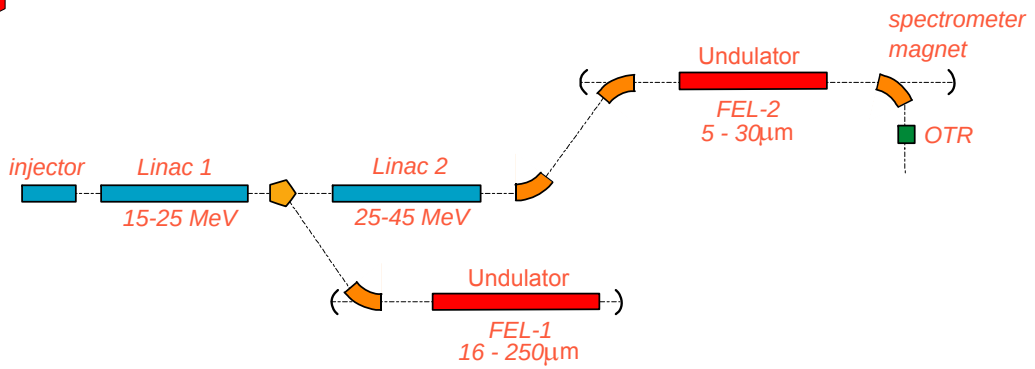

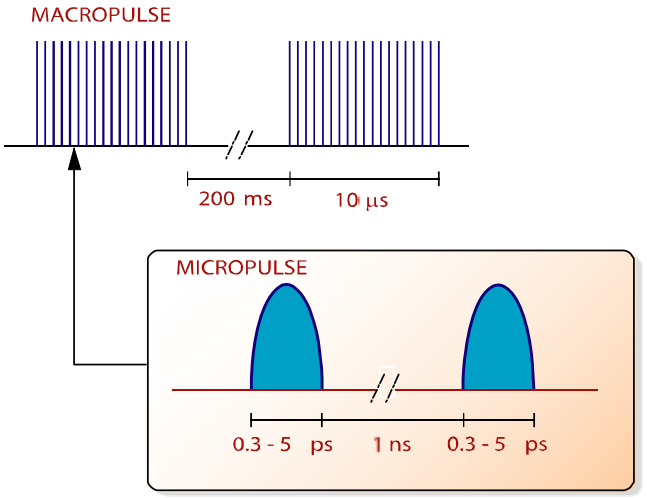

- Continuously tuneable between 40 - 2000 cm^{-1}
- Macropulse energy: 50 - 100 mJ @ 5 or 10 Hz
- Bandwidth: Transform limited - typically 0.2-0.5% of central λ
- Tuned by varying magnet spacing - increases tuning range and stability
- User facility - excellent support & straightforward operation

Principles of FTICR-MS

-charged particles trapped by strong, homogeneous magnetic field B (Lorentz force)

- particles orbit magnetic field with frequency dependent only on m/z (for fixed B)

- trapped particles are confined axially by small static voltage to trapping plates (T)

- applying RF to excite plates (E) at cyclotron frequency bunches ions and expands their orbital radii, improving dynamic range → also used to eject unwanted ions

- current induced by moving ions is detected (D) and amplified in time domain, then Fourier Transformed to obtain frequencies of trapped ions

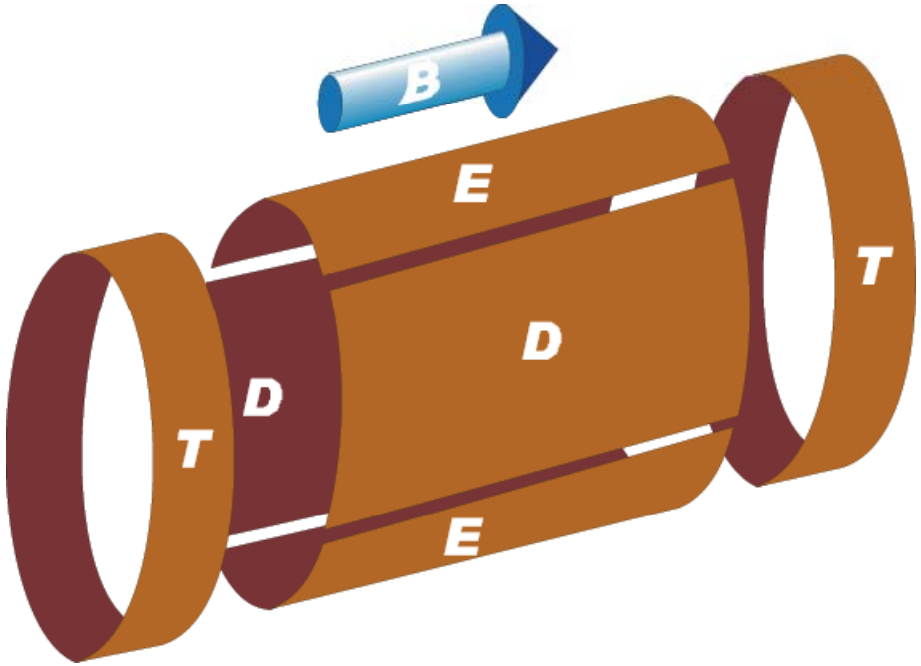

Cyclotron frequency

$f \sim Bz/m$

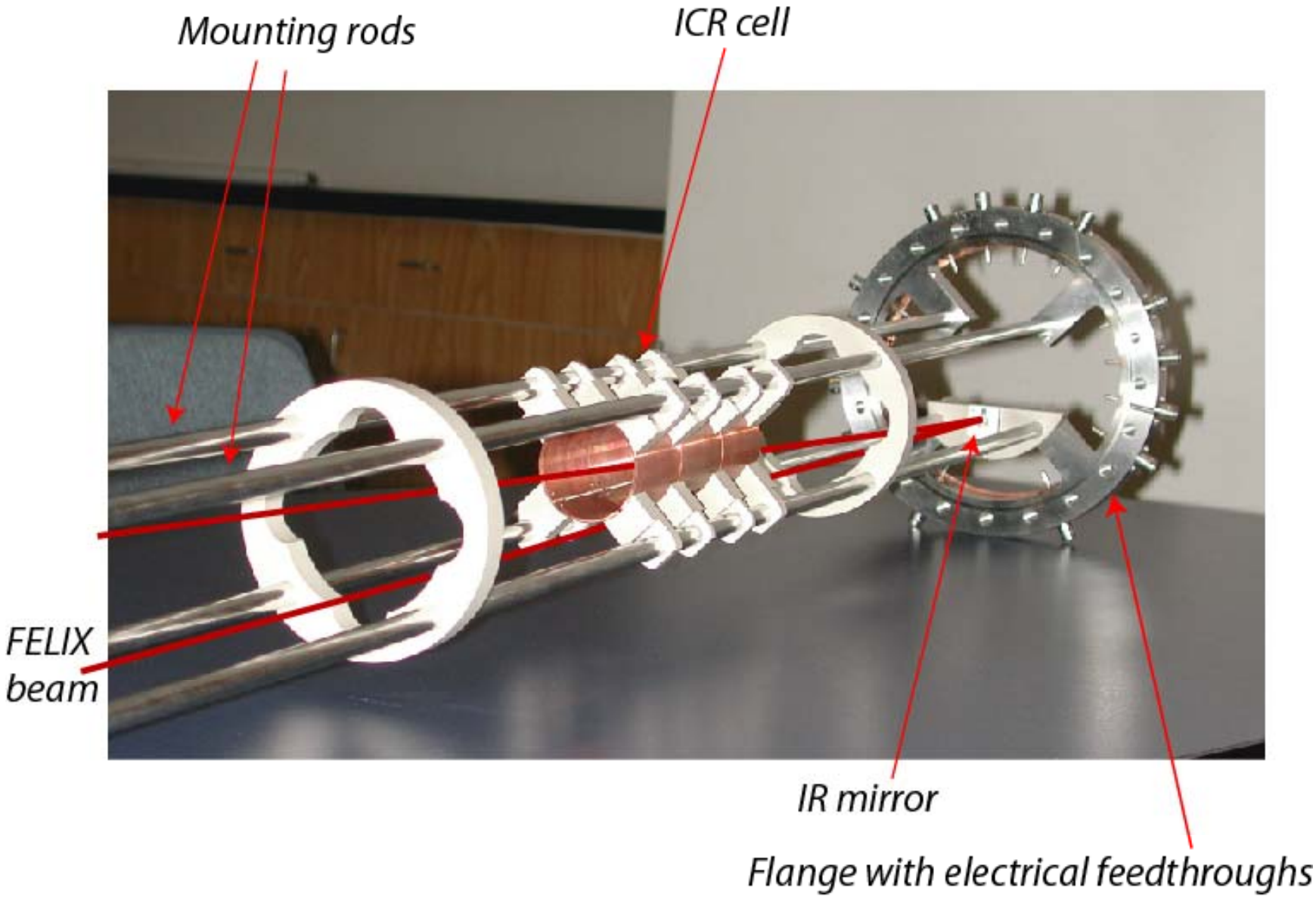
Mounting rods
ICR cell
FELIX
beam
IR mirror
Flange with electrical feedthroughs

Anionic Metal Carbonyl Clustering Reactions

Scheme II

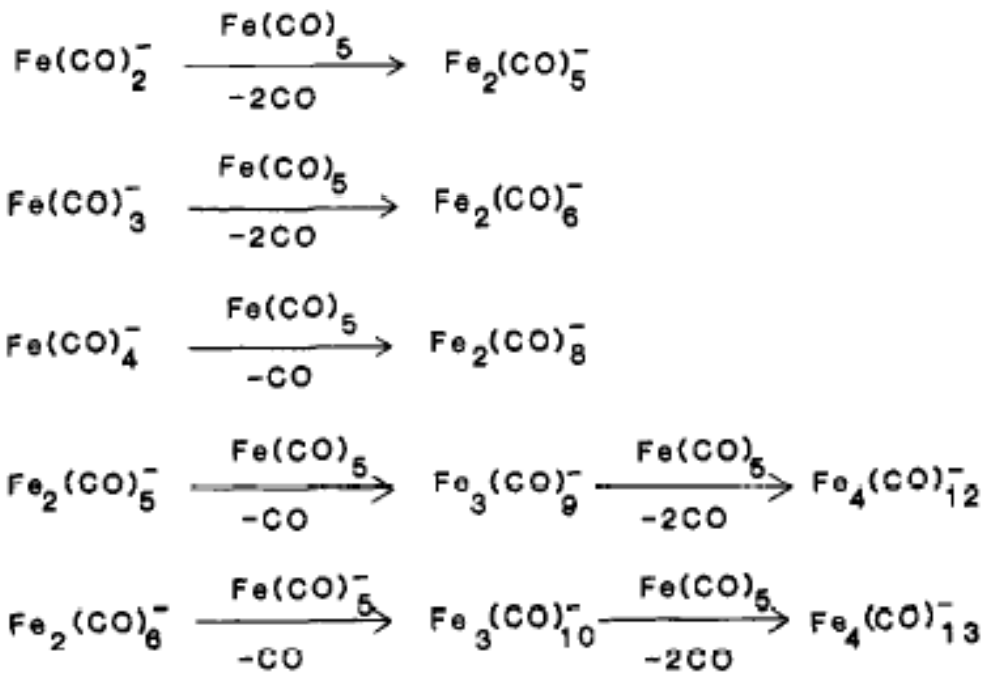

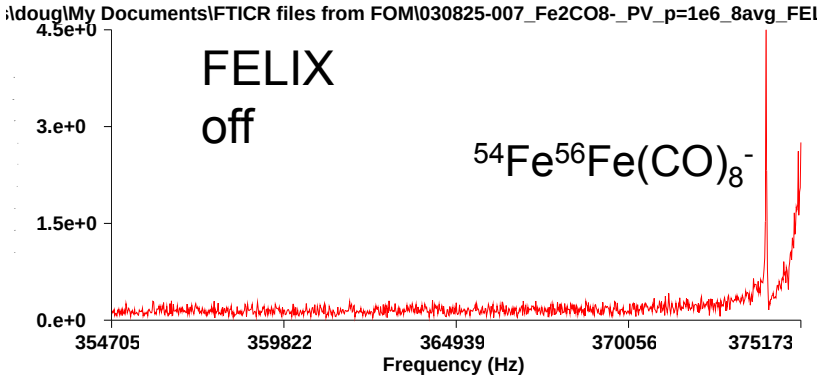
\doug\My Documents\FTICR files from FOM\030825-007_Fe2CO8-_PV_p=1e6_8avg_FEl
4.5e+0
3.e+0
1.5e+0
0.e+0
FELIX
off
$^{54}Fe^{56}Fe(CO)_8^-$
354705
359822
364939
370056
375173
Frequency (Hz)

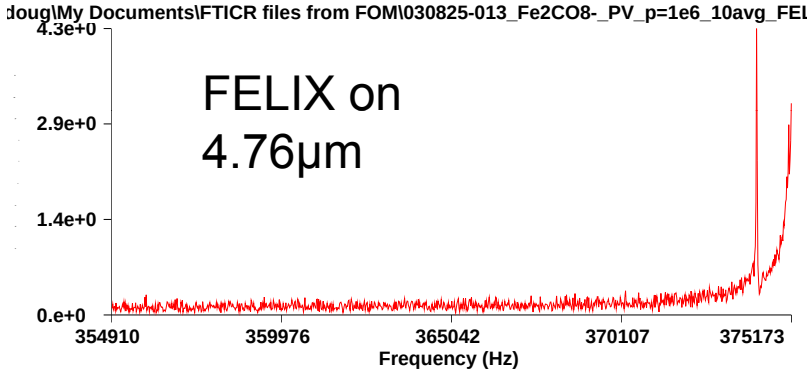
doug\My Documents\FTICR files from FOM\030825-013_Fe2CO8-_PV_p=1e6_10avg_FEl
4.3e+0
2.9e+0
1.4e+0
0.e+0
FELIX on
4.76µm
354910
359976
365042
370107
375173
Frequency (Hz)

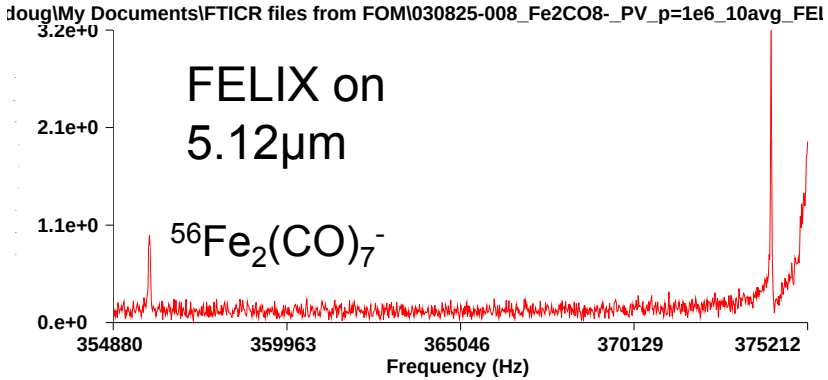
doug\My Documents\FTICR files from FOM\030825-008_Fe2CO8-_PV_p=1e6_10avg_FEl
3.2e+0
2.1e+0
1.1e+0
0.e+0
FELIX on
5.12µm
$^{56}Fe_2(CO)_7^-$
354880
359963
365046
370129
375212
Frequency (Hz)

SORI up to higher masses

- By adding additional frequencies to the SORI excitation pulse, larger and larger cluster can be synthesized
- In each case, a large percentage (40-100%) of the ion population is transferred into the target mass channel
- Spectra show a blue shift with increasing size, converging to a value around 2000 cm^{-1}
- Structure in spectrum also disappears with increasing size -- indication of transition from organometallic complexes to metal-cluster-adsorbate systems?

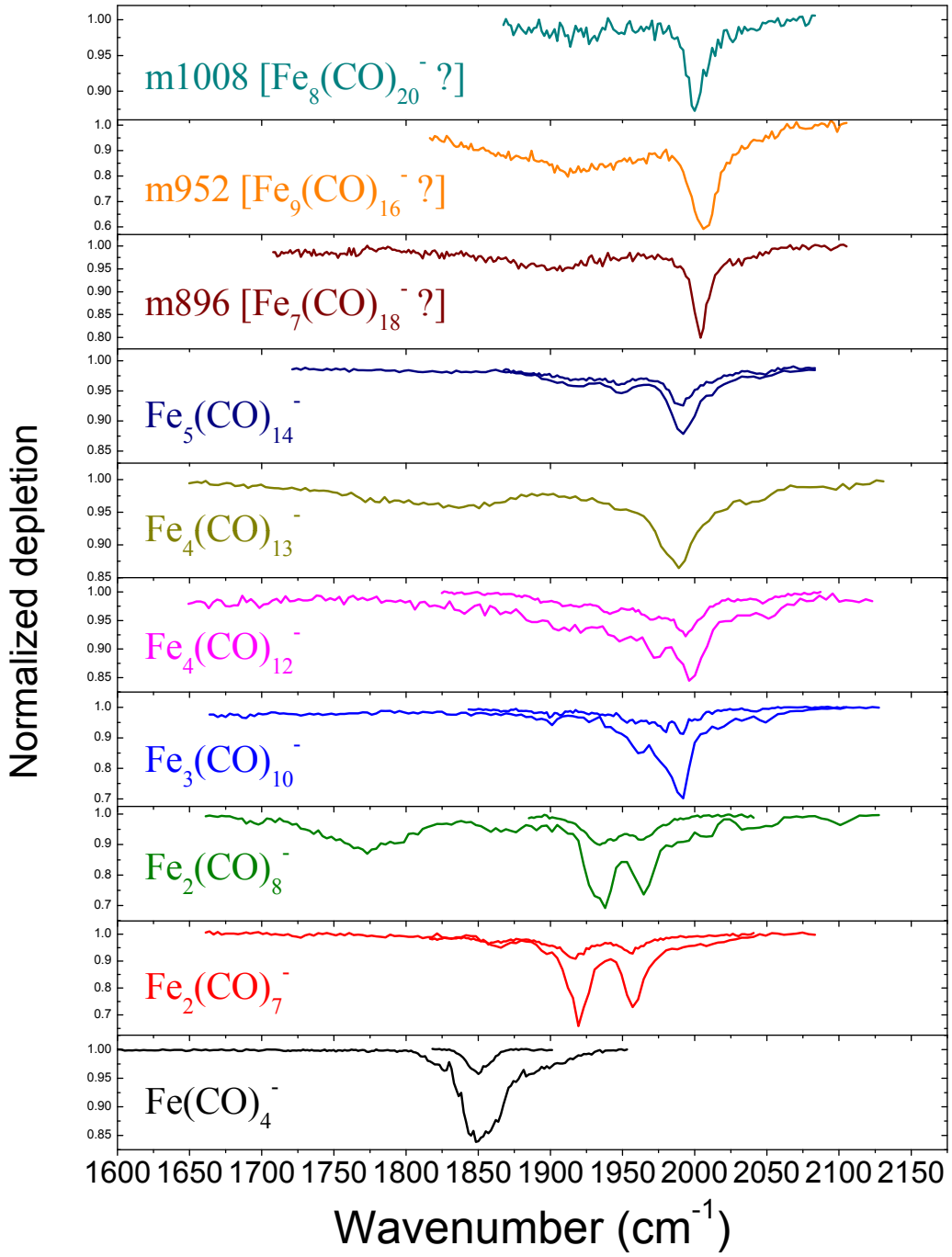

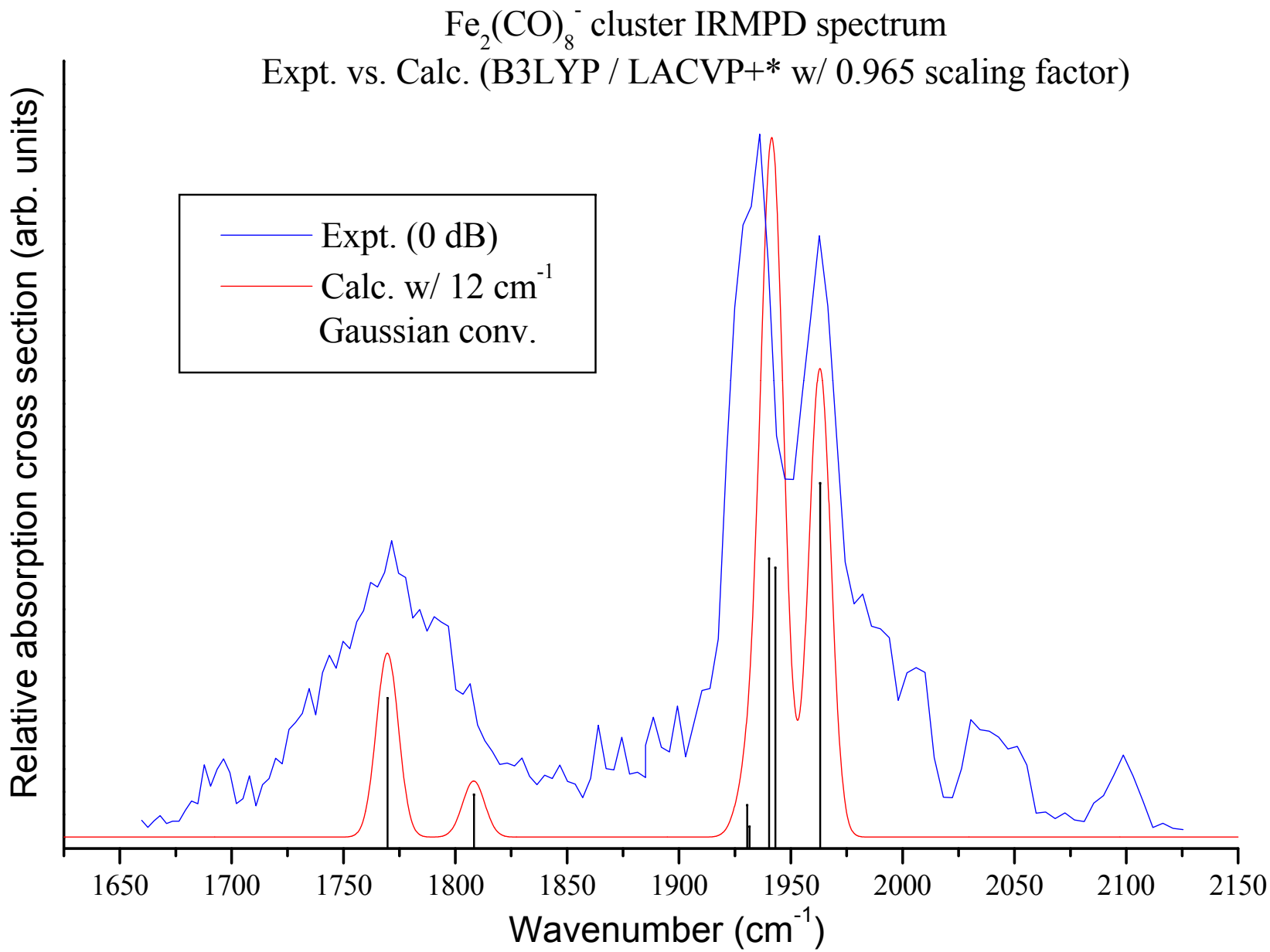
$Fe_2(CO)_8^-$ cluster IRMPD spectrum
Expt. vs. Calc. (B3LYP / LACVP+* w/ 0.965 scaling factor)
Expt. (0 dB)
Calc. w/ 12 cm-1
Gaussian conv.
Relative absorption cross section (arb. units)
1650
1700
1750
1800
1850
1900
1950
2000
2050
2100
2150
Wavenumber (cm-1)

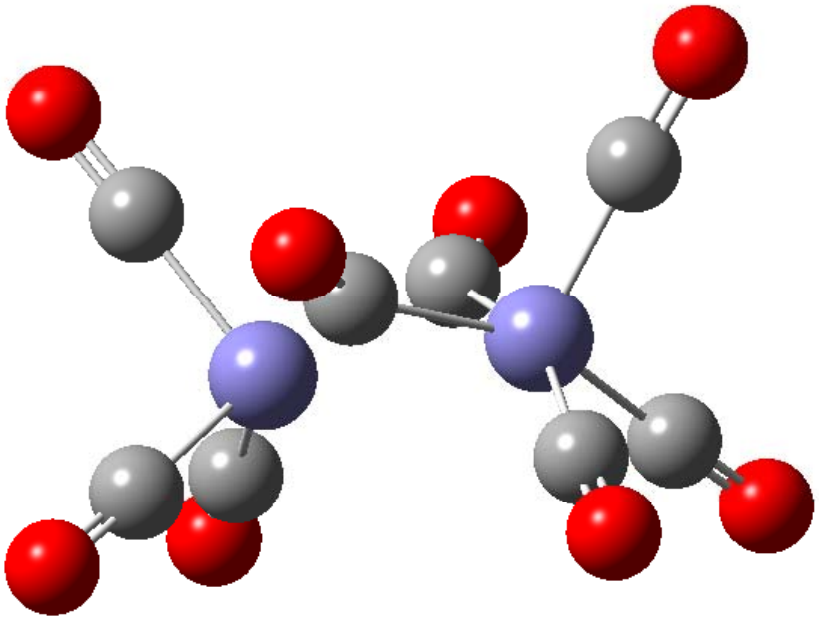

IR spectrum of anionic $Fe_2(CO)_7$ cluster

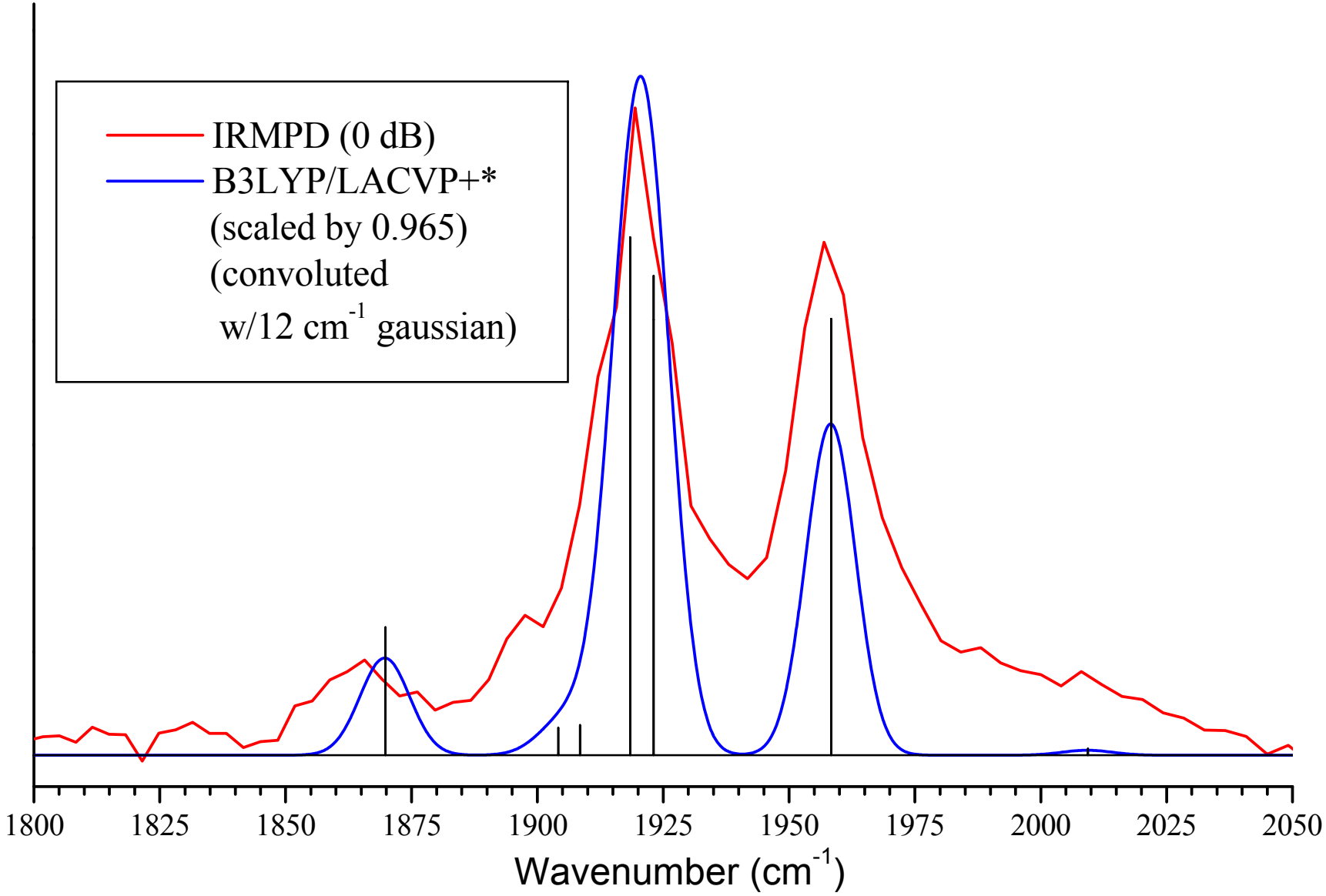

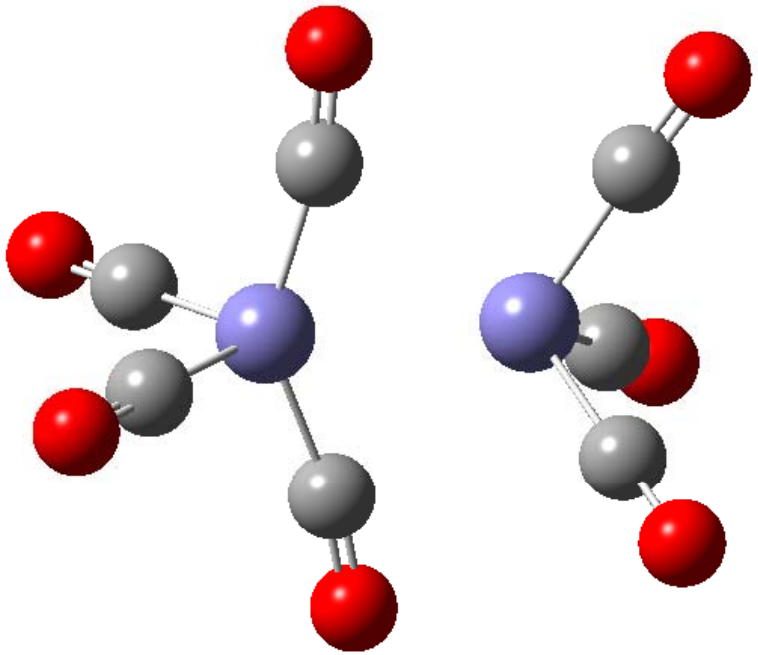

Acknowledgments

Delaware

Scott Robinson

David Finneran

Richard Ochran

Jim Witkoski

Nganha Luu

Ounan Chen

Jennifer Sterner

Steve Bennett

Lei Jin

Tianlan Zhang

Fred Arnold

Henglong Chen

Karl Sohlberg

Hung-Yu Lin

NHFML & FOM (Utrecht)

David Moore

John Eyler

NIST

Michelle Byrd

Charles Guttman

University of Oslo

Einaar Uggerud

Dag Ekeberg

Bruker Instruments

Gary Kruppa

Rhone-Poulenc Rorer

Runzhi Zhao

Robert McKean

Stephen Conlon

Sun Company

Jim Lyons

Paul Ellis

Tilak Wijesekera

Funds

NSF

Sun

RPR

NIST

Acknowledgements

Delaware

Scott Robinson

David Finneran

HeeYeon Park

Richard Ochran

Tom Bailey

Nganha Luu

Ounan Chen

Steve Bennett

Jennifer Sterner

Lei Jin

Fred Arnold

Tianlan Zhang

Henglong Chen

Delaware (contd)

Robin Kinser

Hung Yu Lin

Yi Lin

Ying Pan

Barbara Larsen

Fred Strobel

John Wronka

Gary Kruppa

Thuy Nguyen

Art Smith

Rob Freas

Gary Weddle

Dana Chattalier

Tom Dietz

John Allison

Rhone-Poulenc Rorer

Runzhi Zhao

Robert McKean

Steve Conlon

Sun Company

Jim Lyons

Paul Ellis

NHFML & FOM

John Eyler

David Moore

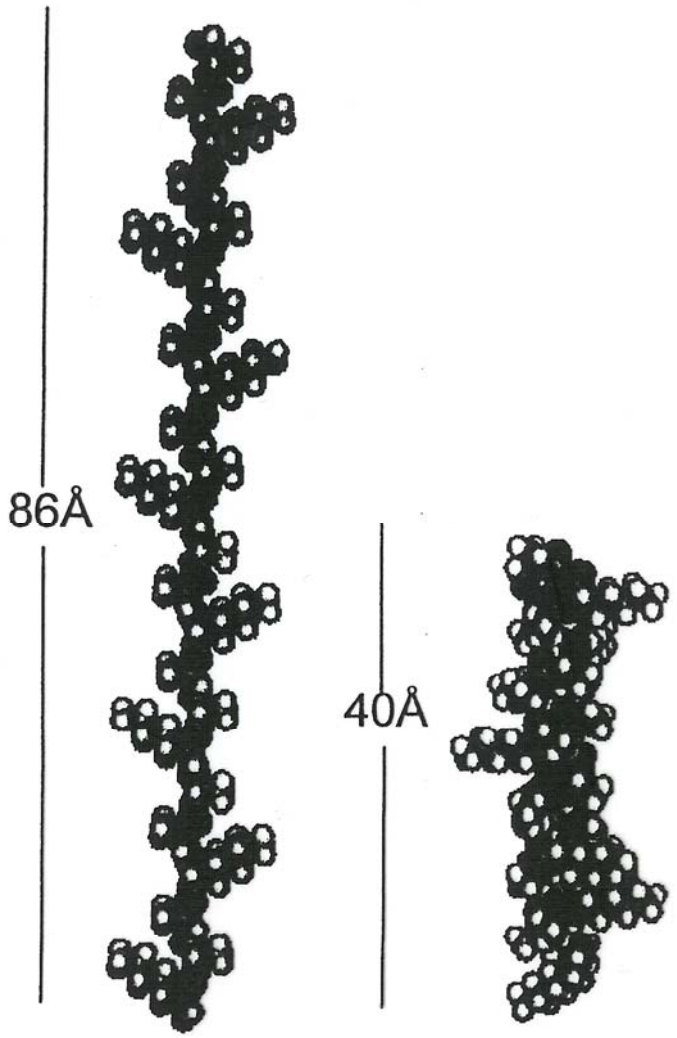
86Å
40Å
(KAA)8
β Structure
(KAA)8
α Structure

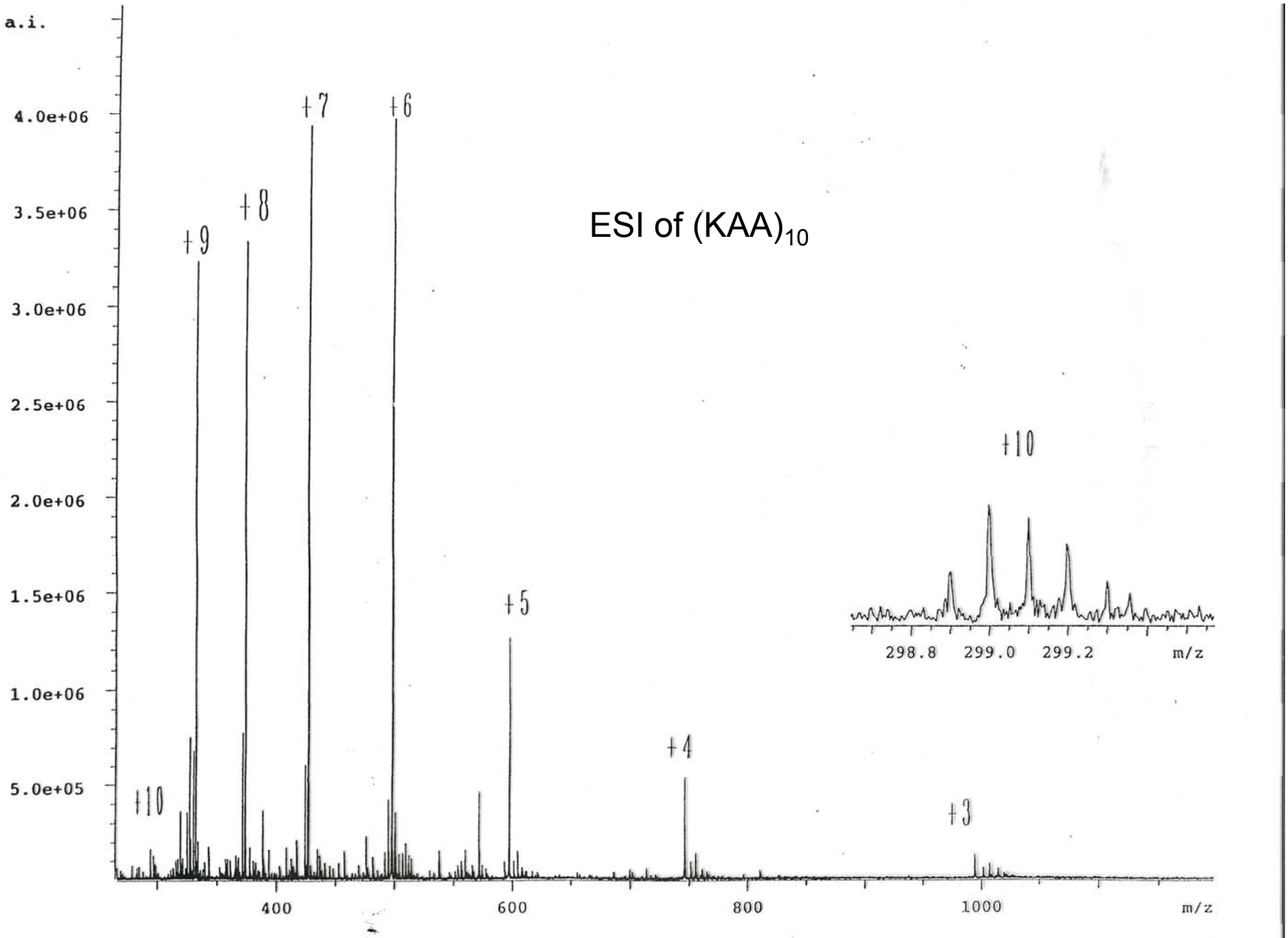
a.i.
4.0e+06
3.5e+06
3.0e+06
2.5e+06
2.0e+06
1.5e+06
1.0e+06
5.0e+05
+10
+9
+8
+7
+6
+5
+4
+3
400
600
800
1000
m/z
ESI of (KAA)10
+10
298.8
299.0
299.2
m/z

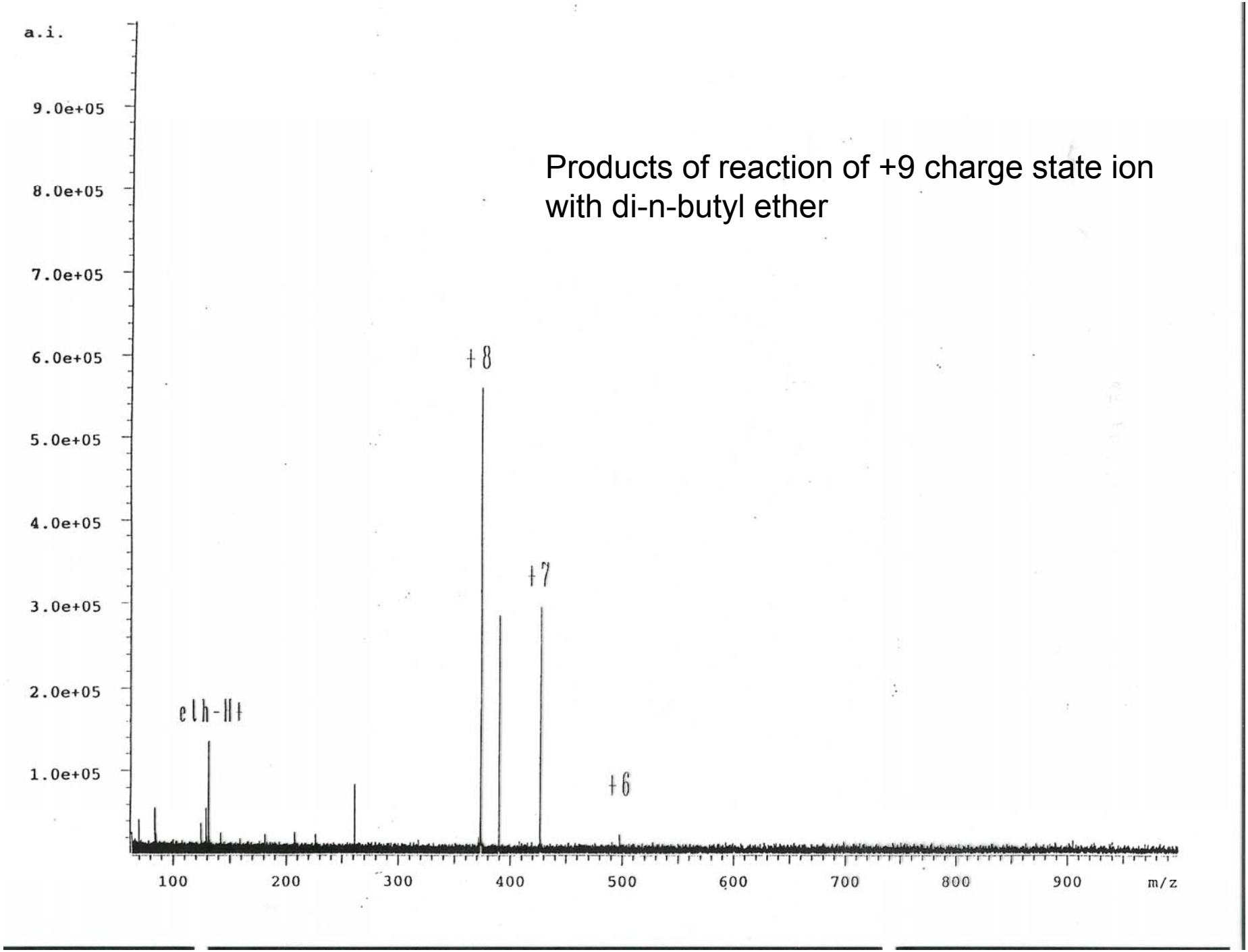
Products of reaction of +9 charge state ion with di-n-butyl ether
a.i.
9.0e+05
8.0e+05
7.0e+05
6.0e+05
5.0e+05
4.0e+05
3.0e+05
2.0e+05
1.0e+05
+8
+7
+6
elh-Ht
100
200
300
400
500
600
700
800
900
m/z

Ref Cmpd	Charge State +8	+7	+6	+5	+4	+3	+2	+1	PA (kcal/mol)
Benzene									180.9
Methanol									181.9
Ethanol									188.1
n-Butanol									191.0
1,4 Dioxane									193.8
Acetone									196.7
Ethyl Ether		N							200.2
n-Butyl Ether		Y							203.7
Isopropyl Ether			N						206.0
Pyrrole			Y	N					207.6
2-Fluoro-pyridine				Y					210.6
DMF					N				211.4
Pyridine					Y				220.8
2-Methoxy-pyridine									221.9
3,5 Lutidine						N			225.5
2,6 Lutidine						Y			228.2
Triethyl-amine									232.3
Tributyl-amine							N	N	235.4

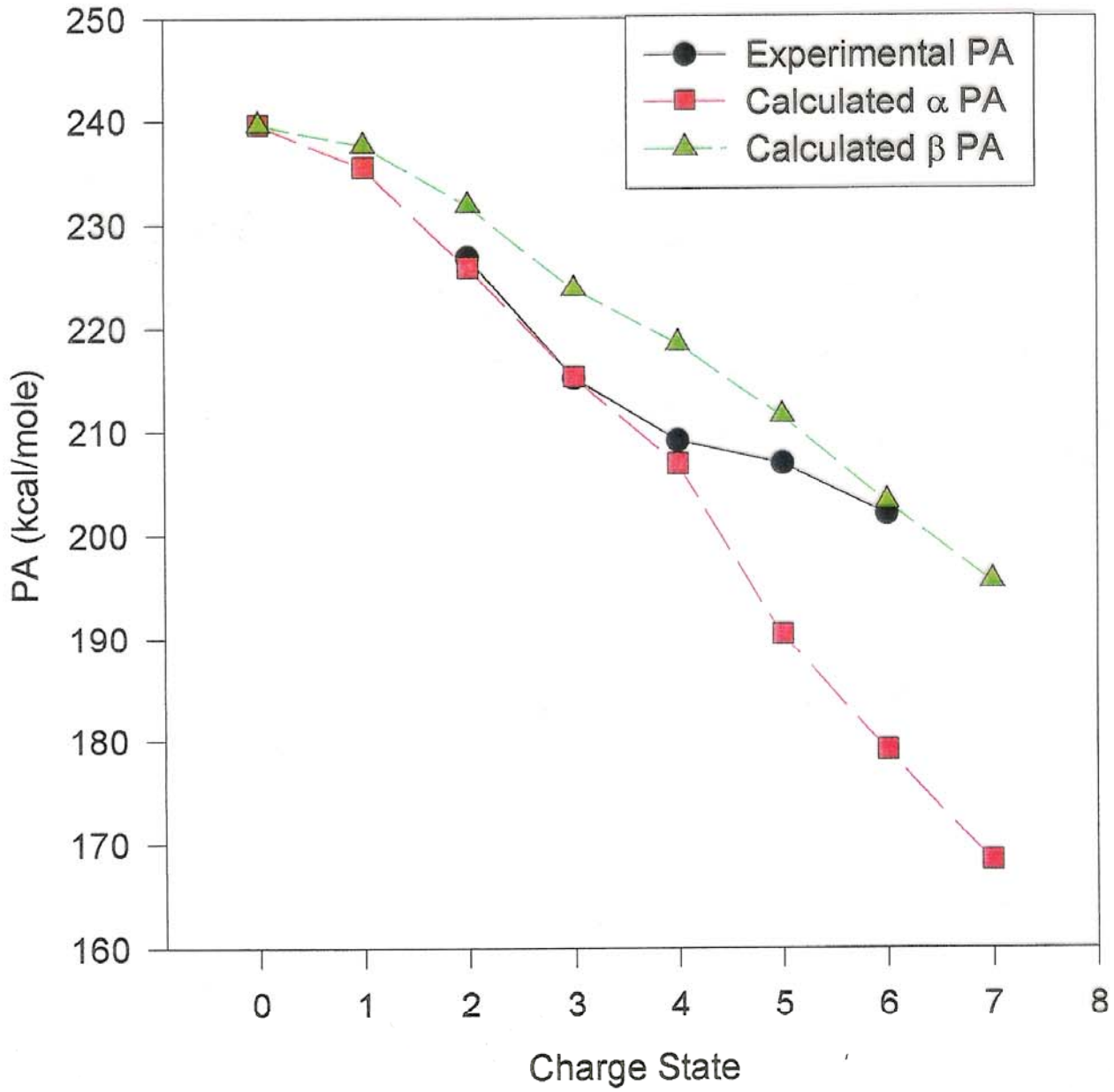
Experimental PA
Calculated α PA
Calculated β PA
PA (kcal/mole)
250
240
230
220
210
200
190
180
170
160
0
1
2
3
4
5
6
7
8
Charge State

Methods

- SORI-CID and ECD were performed on a All samples were dissolved to 5 μM in 50:50 MeOH:water, 1% acetic acid
- Bruker Apex 4.7T instrument
- IRMPD experiments were performed on a Bruker Apex 3T instrument

SORI-CID

- Cleavage observed at 25 of 30 backbone positions
- Produced 7 *a*, 19 *b*, 5 *c*, 2 *x*, 13 *y*, and 16 *z* ions
- No cleavage observed within the lactam bridge

ECD (Ar Cooling Gas)

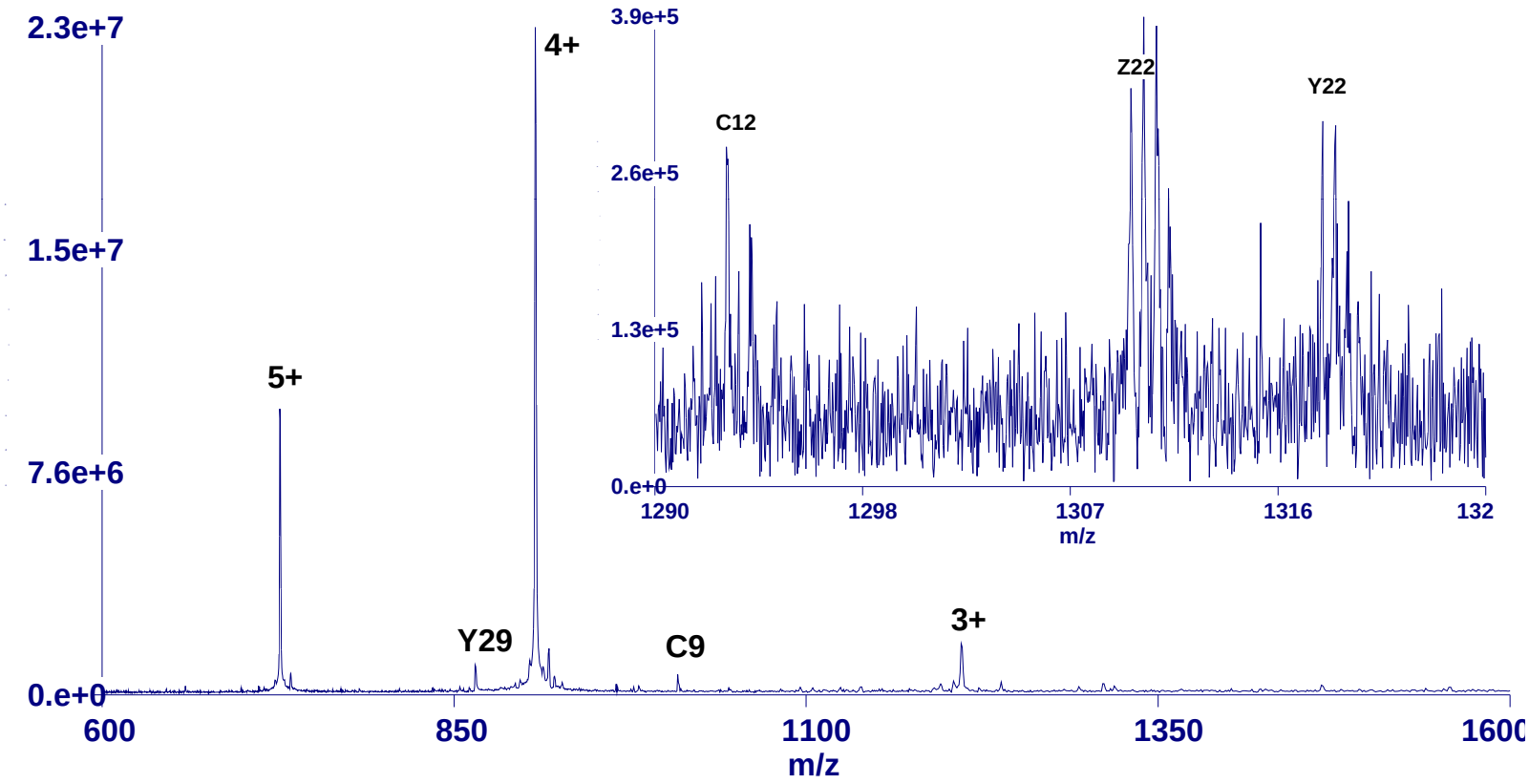

ECD (Ar Cooling Gas)

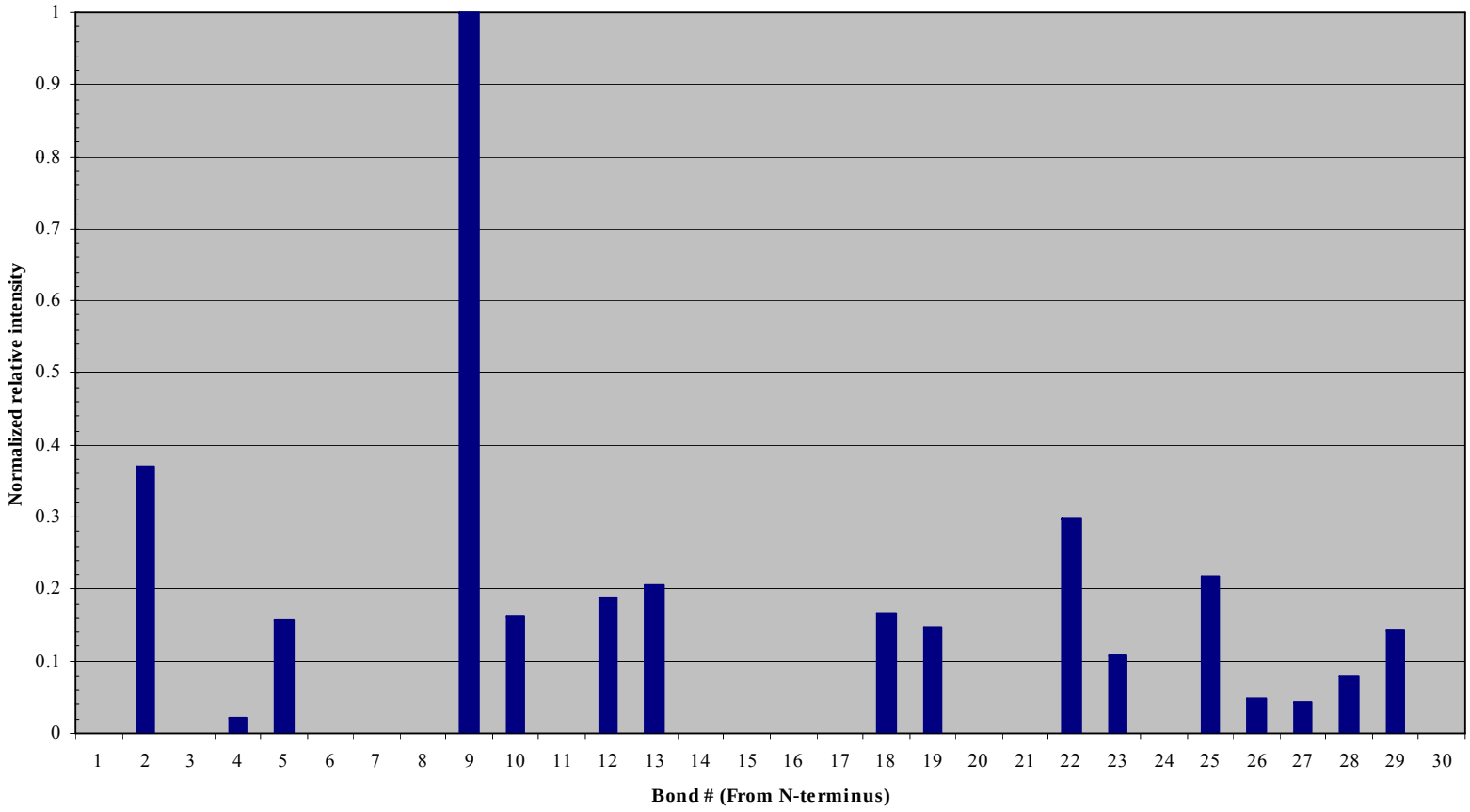

ECD (Ar Cooling Gas)

- Cleavage observed at 16 of 30 backbone positions
- Produced mostly *c* and *z* ions (1 *a*, 1 *b*, 13 *c*, 1 *x*, 7 *z*)
- No cleavage observed within the lactam bridge

ECD: A Non-selective Technique?

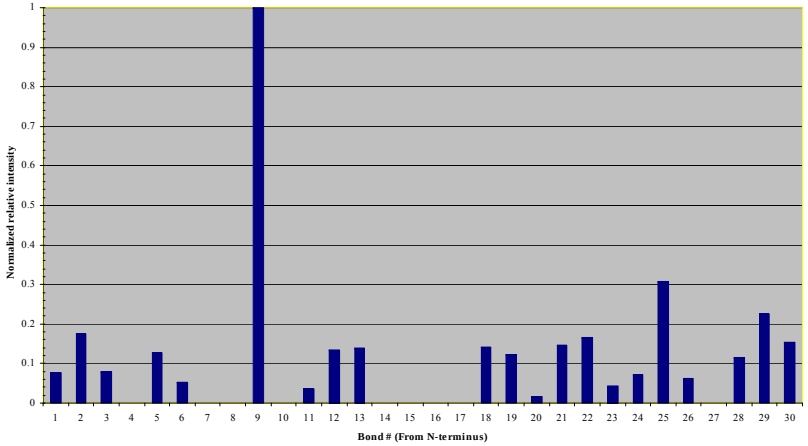

- ECD w/ Ar: Cleavage between **His**-9 and **Asn**-10 accounted for 29.8% of the total normalized ion abundance
- ECD w/ SF_6: Cleavage after **His**-9 = 29.4%

Major Products

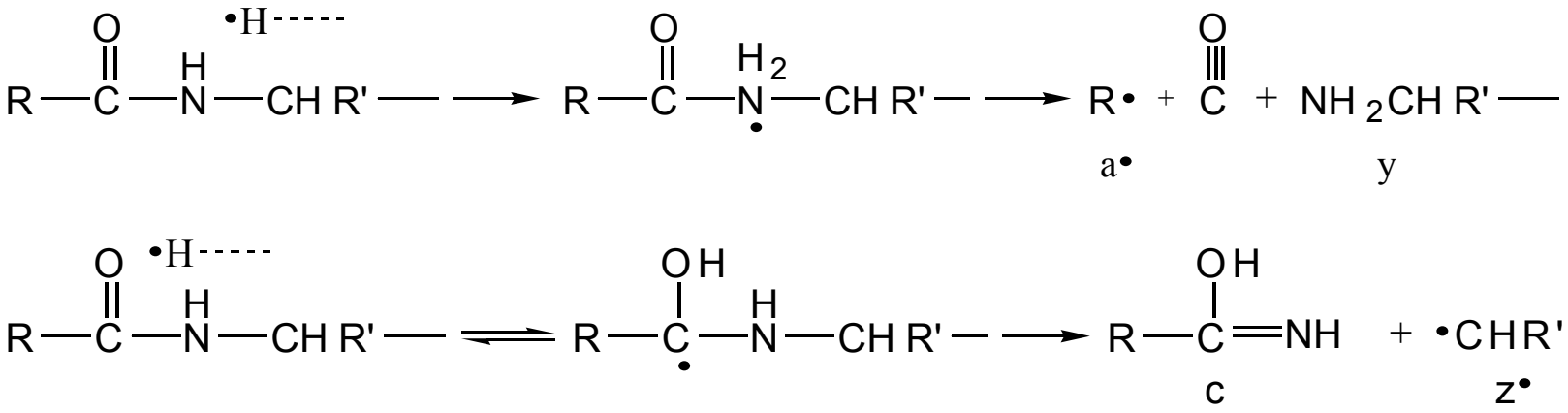

- Peptide Bond #9
  - Only site where reverse products (a, y•, c•, z) are observed
  - Is there an explanation in the structure?

ECD (SF_6) Cooling Gas

- Cleavage observed at 21 of 30 backbone positions
- Produced 2 *a*, 14 *c*, 1 *x*, 4 *y*, 13 *z*
- No cleavage observed within the lactam bridge

Polyolefin Mass Spectrometry - Importance

- Polyethylene (PE) & polypropylene (PP)
  - **Large production volume and fast growth**
  - **New metallocene catalysts produce new polyolefin types**
  - **NIST provides saturated polyolefin standards**
- Central Challenge in PE/PP mass spectrometry
  - **Polymer functionality for cationization absent**
  - **Masses over ~ 2000 u cannot be determined**
  - ➢ **Creating an intact, gas-phase macromolecular ion**

New Approach -η^5-Cyclopentadienylcobalt Ion ($CpCo^{\bullet+}$)

$CpCo^{\bullet+}$ ion shows favorable reactivity toward low mass alkanes.

$$CpCo^{\bullet+} + C_nH_{2n+2} \xrightarrow[-\ mH_2]{} CpCoC_nH_{2n-2m+2}{}^{\bullet+}$$

n = 2-6, m = 1, 2

- predominant dehydrogenation product
- little fragmentation in MS

Müller & Goll ’73, Jacobson & Freiser ’85, & Ekeberg, Ridge, *et al.* ‘99

Double Dehydrogenation Dominates All Three Reactions

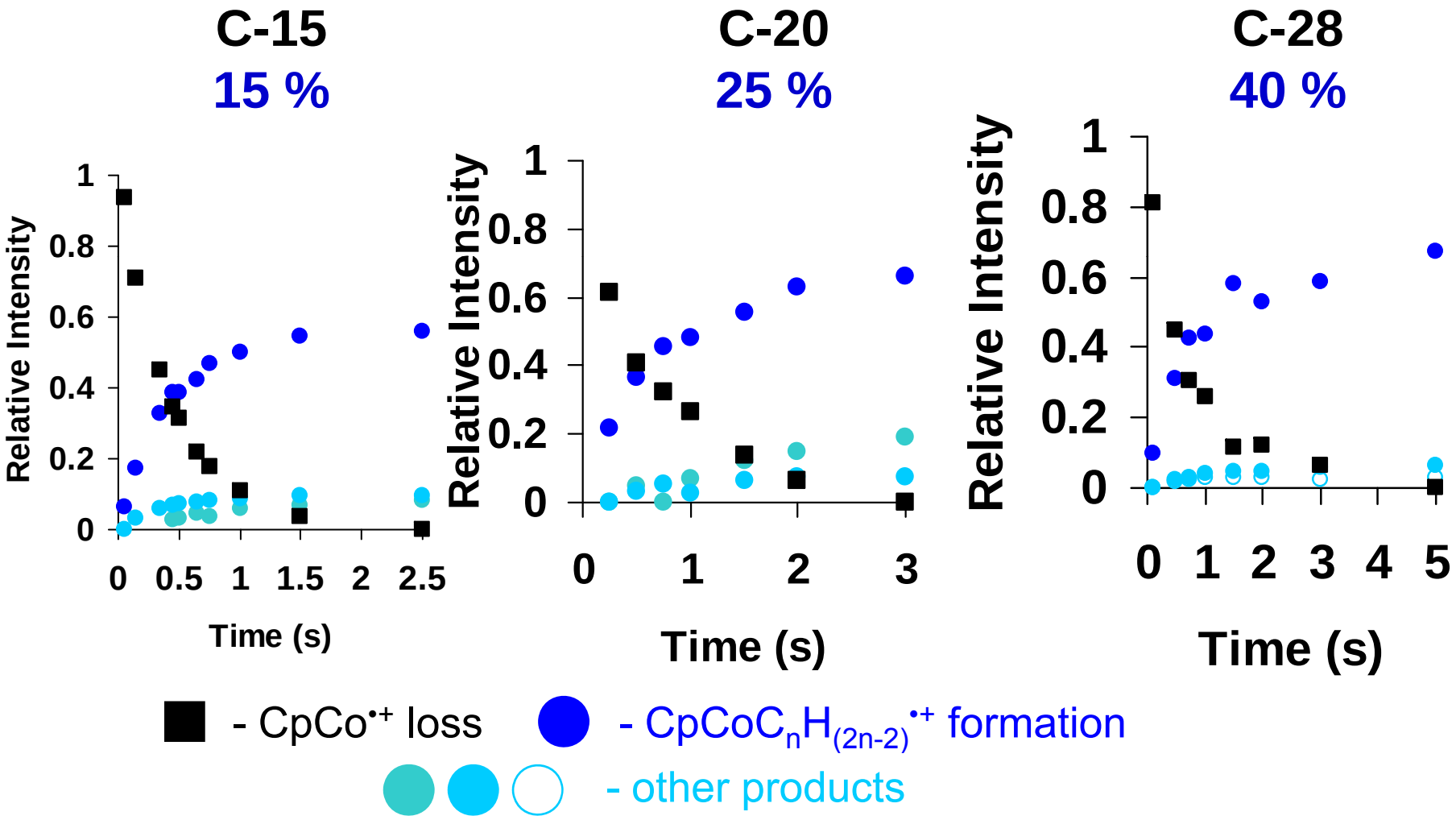

Byrd, Ridge & Guttman, *J. Am. Chem. Soc. Mass Spectrom.* 2003, 14, 51-57.

Structures of Flavins

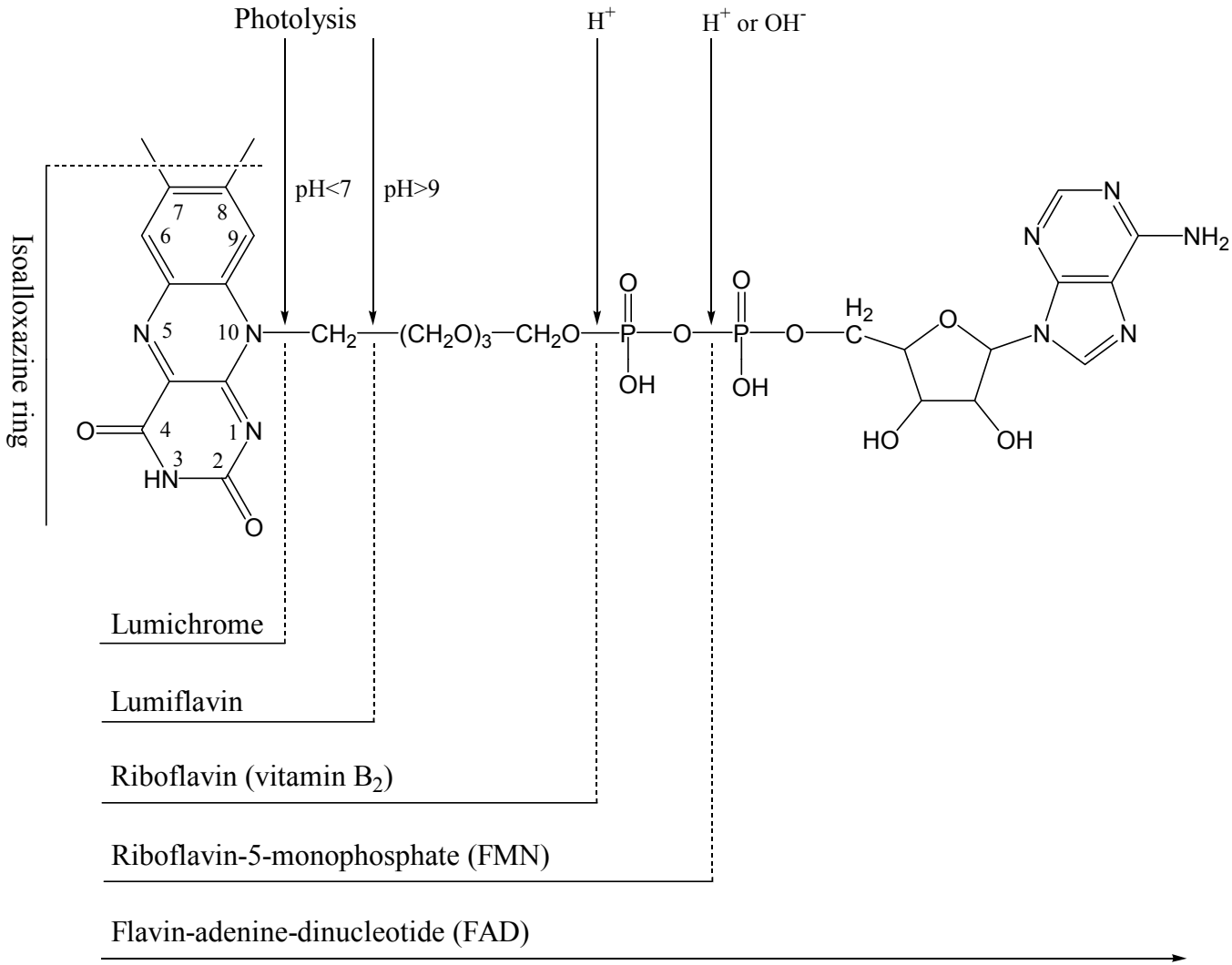

ESI of cyt. C, 5 pm/ul, flow rate of 68 ul/hr, bb 256k dataset, 3/1/96

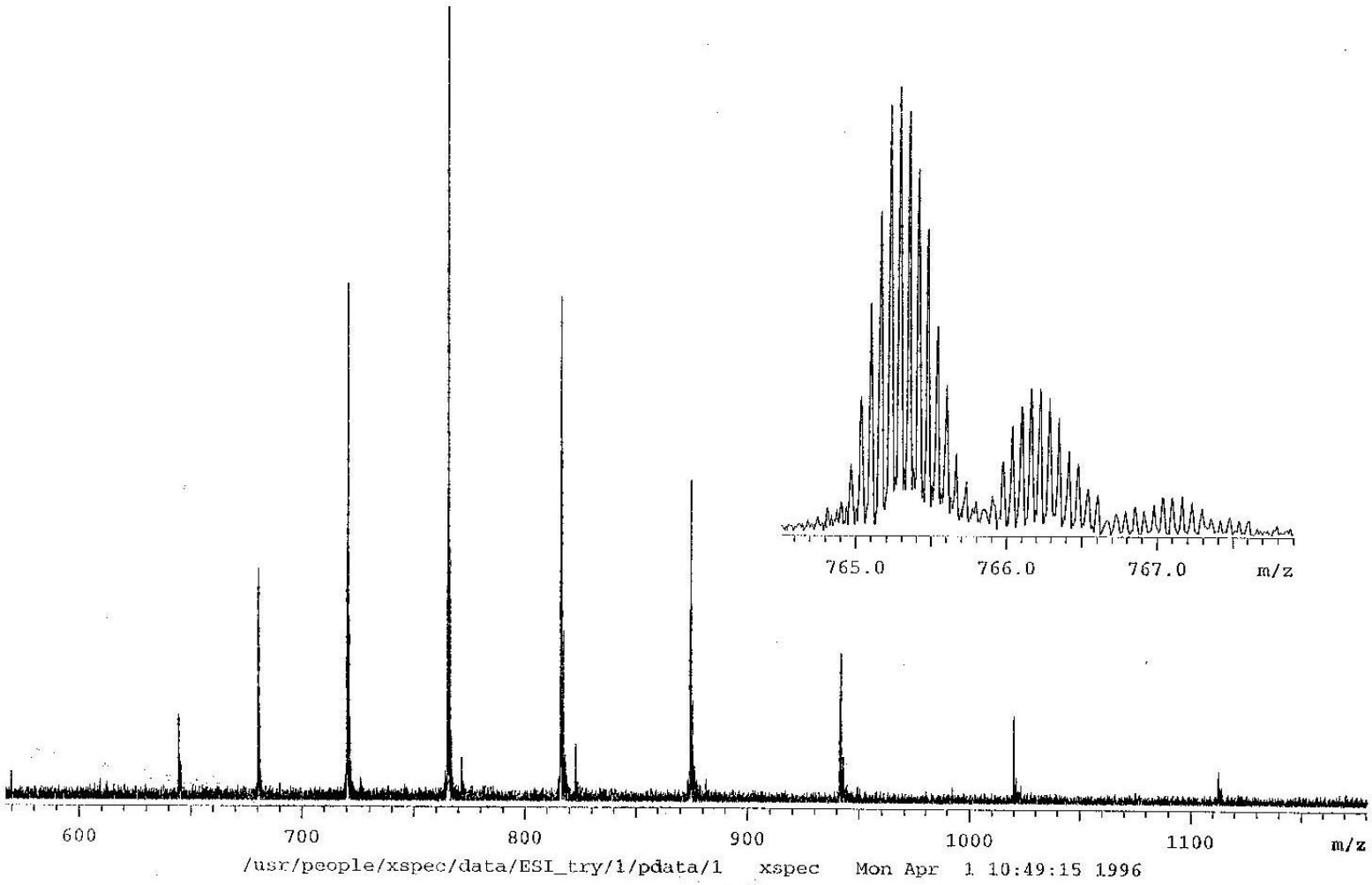

Distances for Spin Unrestricted C4v Tetraphenyl Series

Molecule	Charge	Fe-N (Å)	Fe-Cl (Å)	Fe-N_4 plane (Å)
FeTPP	Neutral	1.9846	N/A	0.0093
	Anion	1.9856	N/A	0.0040
FeTPPCl	Neutral	1.9902	2.1816	0.2200
	Anion	1.9868	2.2496	0.1300
$FeTPPF_{20}$	Neutral	1.9914	N/A	0.0116
	Anion	1.9889	N/A	0.0109
$FeTPPF_{20}Cl$	Neutral	1.9962	2.1675	0.1906
	Anion	1.9945	2.2400	0.1239

Distances for Spin Unrestricted C_{4v} Octaethyl Series

Molecule	Charge	Fe-N (Å)	Fe-Cl (Å)	Fe-N_4 plane (Å)
FeOEP	Neutral	1.9906	N/A	0.0008
	Anion	1.9898	N/A	0.0007
FeOEPCl	Neutral	1.9893	2.2271	0.1593
	Anion	1.9898	2.264	0.1241
$FeOEP(NO_2)_4Cl$	Neutral	2.0377	2.1695	0.2061
	Anion	2.0326	2.2403	0.1064

IR MPD spectra of anionic iron carbonyl clusters

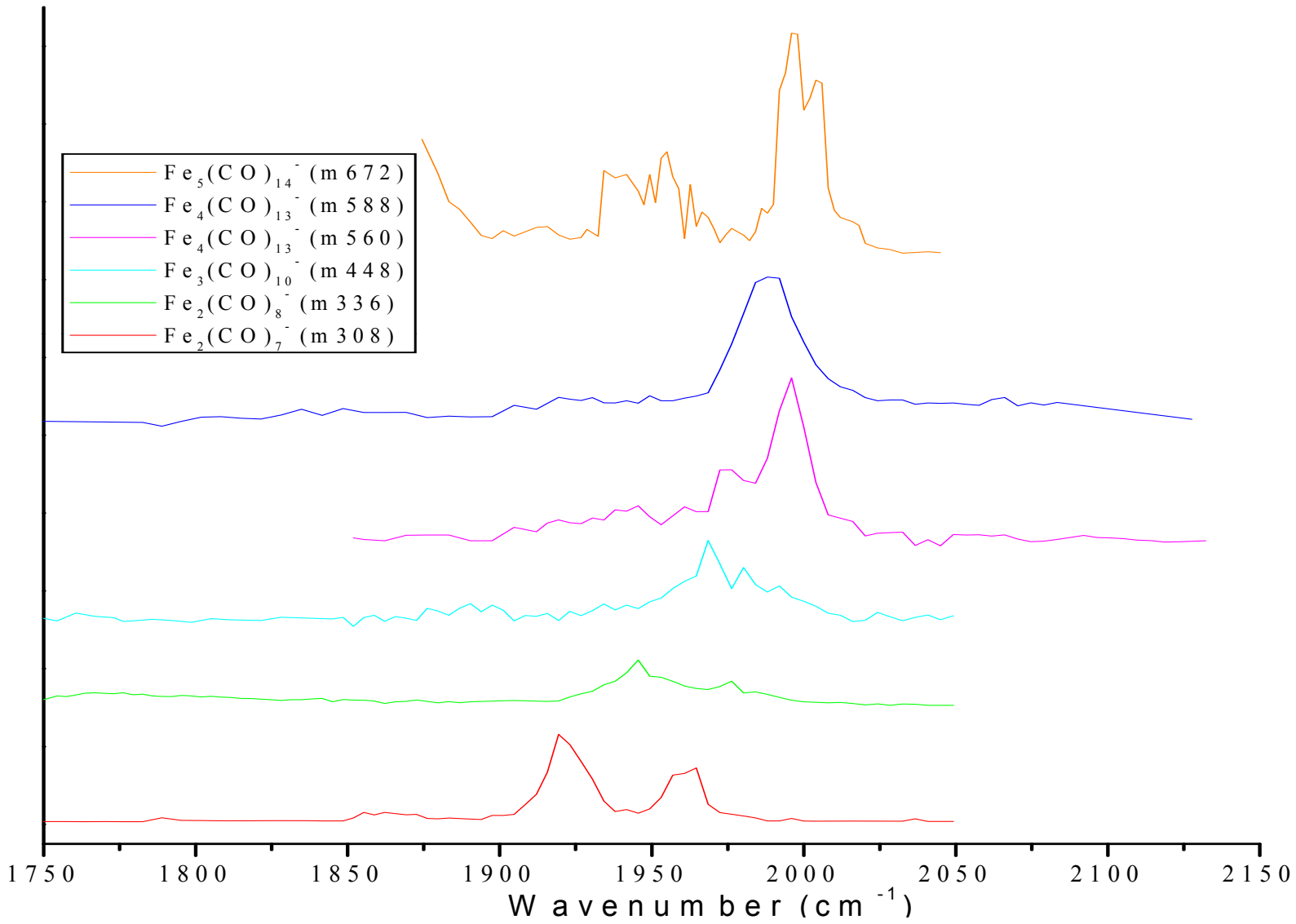

Theoretical spectrum from Schaefer's calculations for D2h unbridged structure. Frequencies lowered by 46 cm-1.

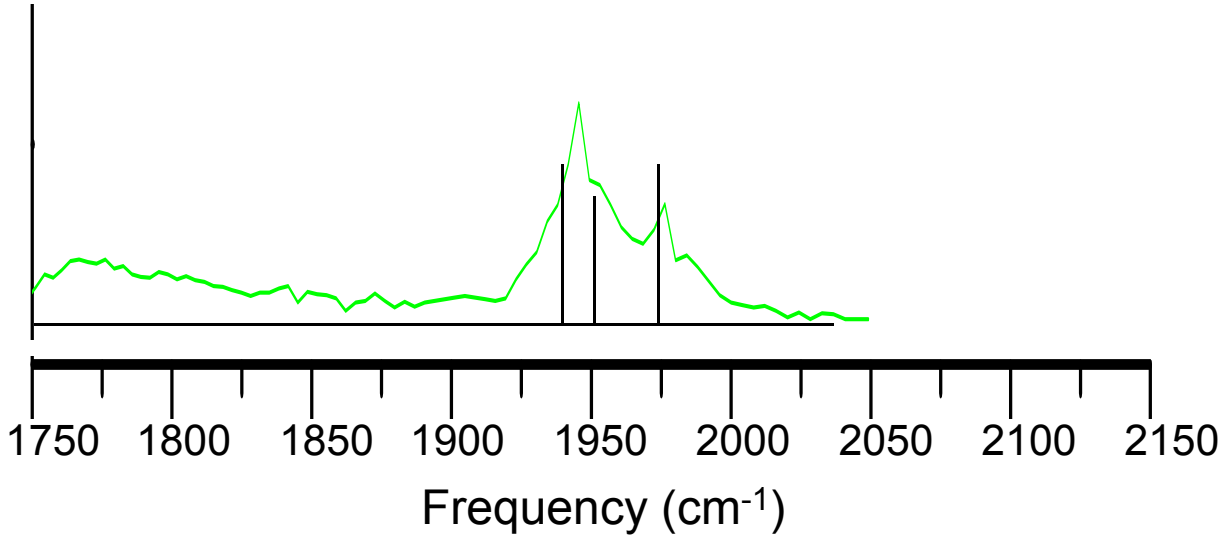

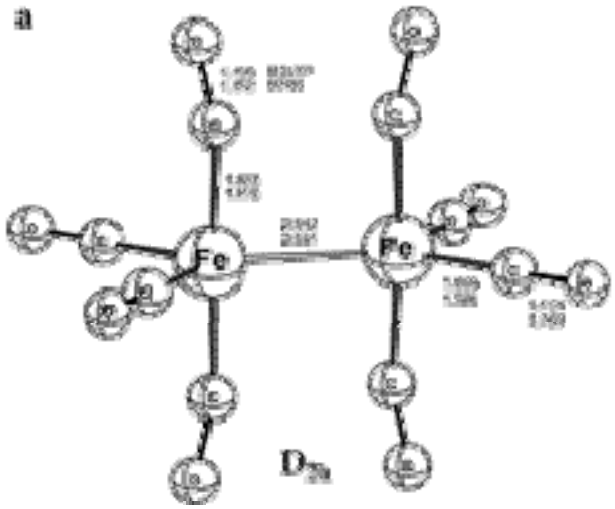

Theoretical spectrum from Schaefer's calculations for tetrabridged structure. Average lowered by 40 cm-1and range expanded 10% about average. Imported from Excel plot

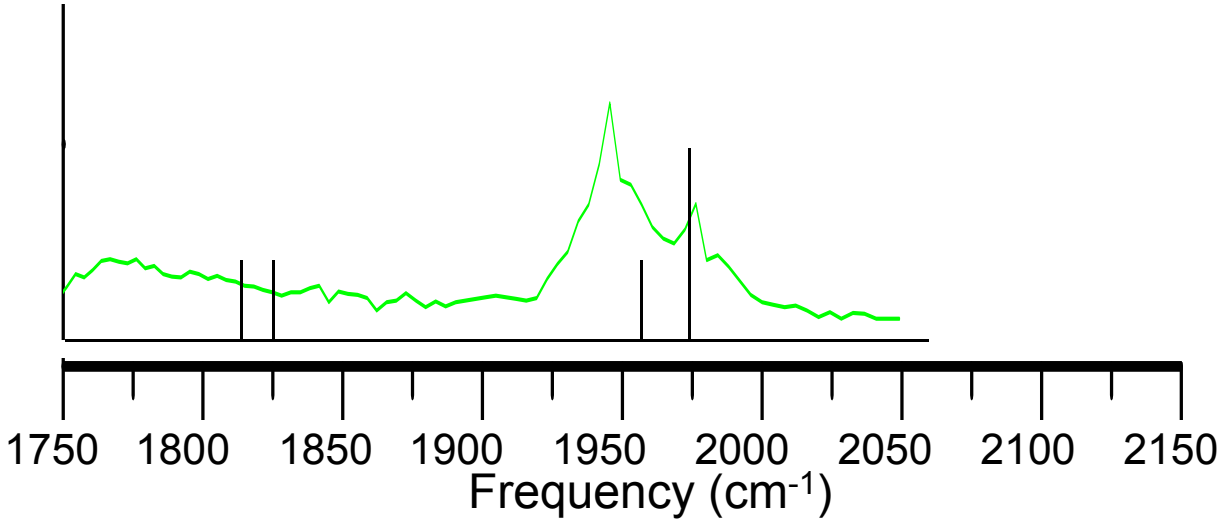

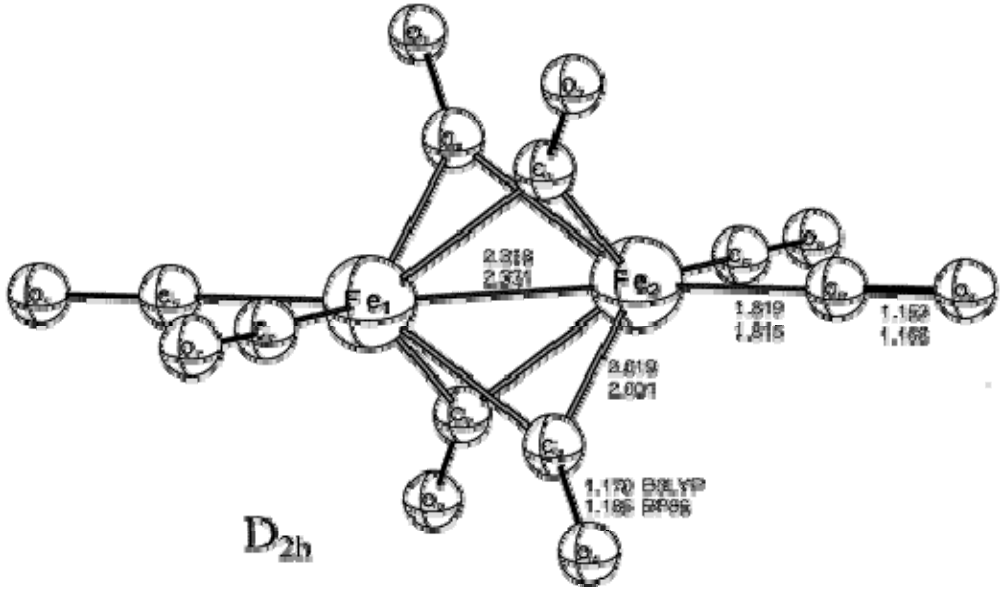

Theoretical spectrum from Schaefer's calculations for a dibridged C2h structure. Average lowered by 57 cm-1. Imported from Excel plot

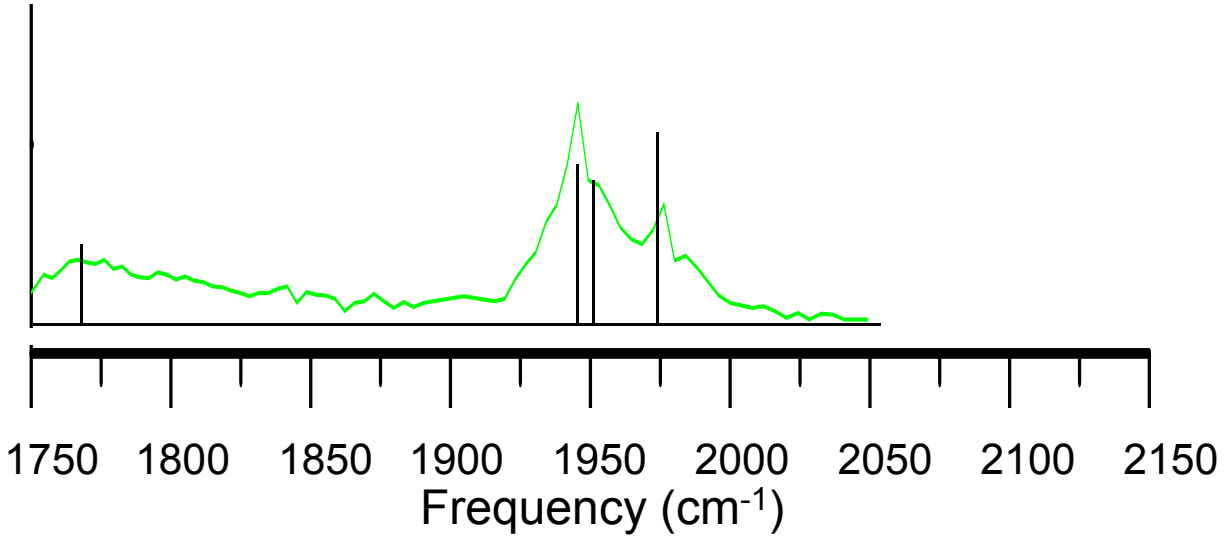

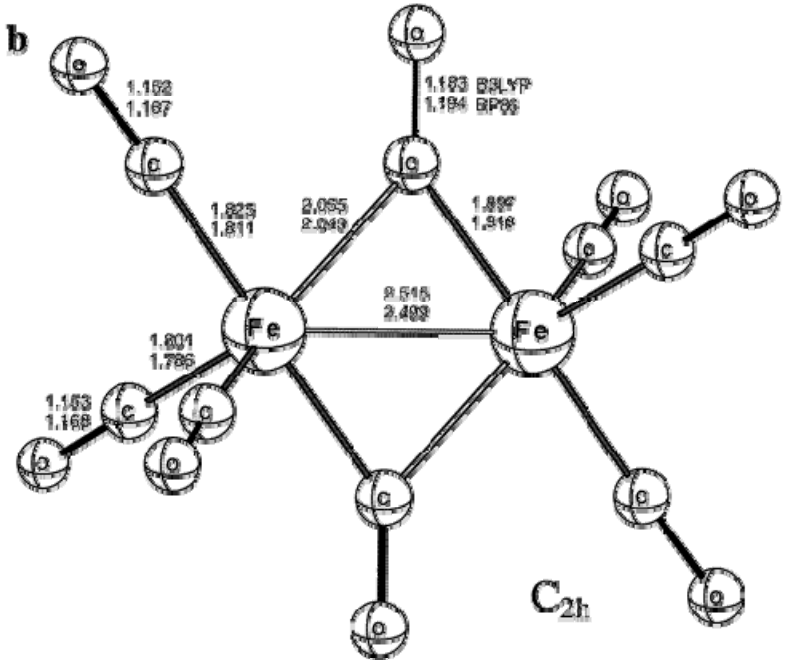

$Fe_2(CO)_8^-$ anion spectrum

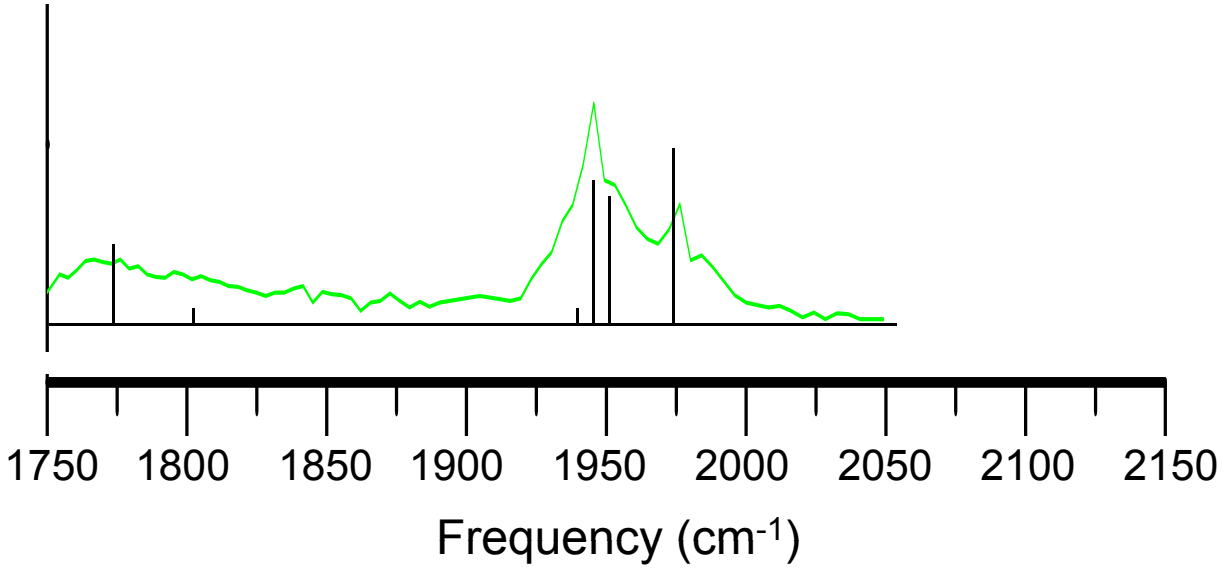

Theoretical spectrum from Schaefer's calculations for dibridged C2v structure. Average lowered by 60 cm-1 and range expanded by 10%. Imported from Excel plot

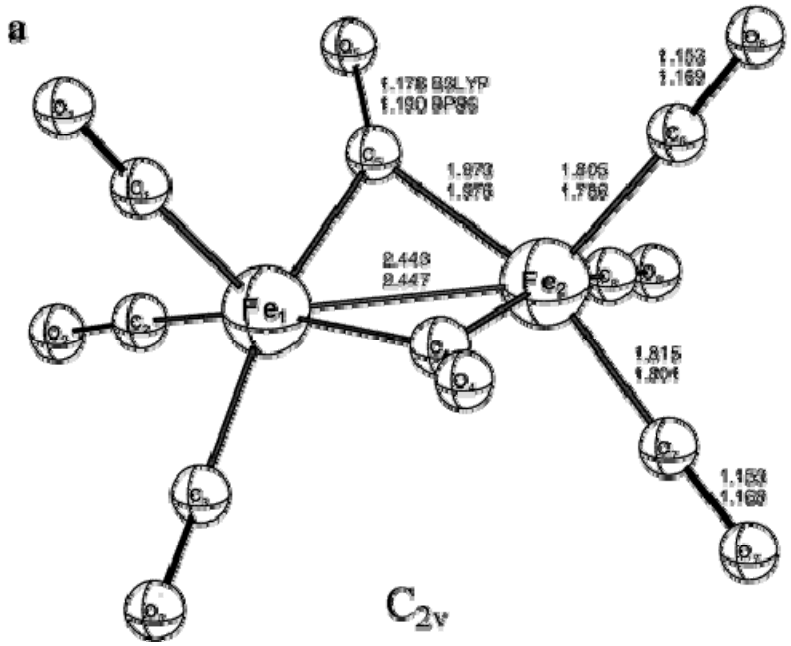

$Fe_2(CO)_7^-$ anion spectrum

$Fe_2(CO)_7$ neutral harmonic frequencies (lowered by 52 cm^{-1} and expanded by 10% about the average) and intensities from DFT calculations for triply bridged structure in ref. 1.

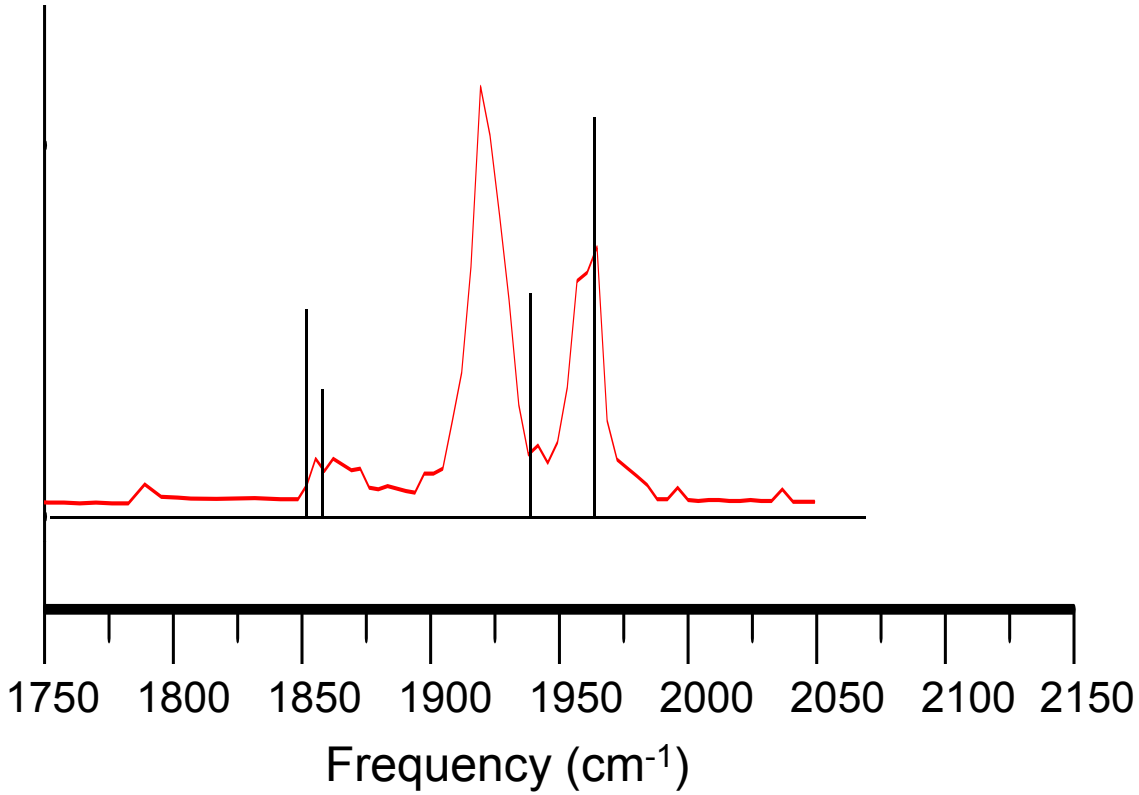

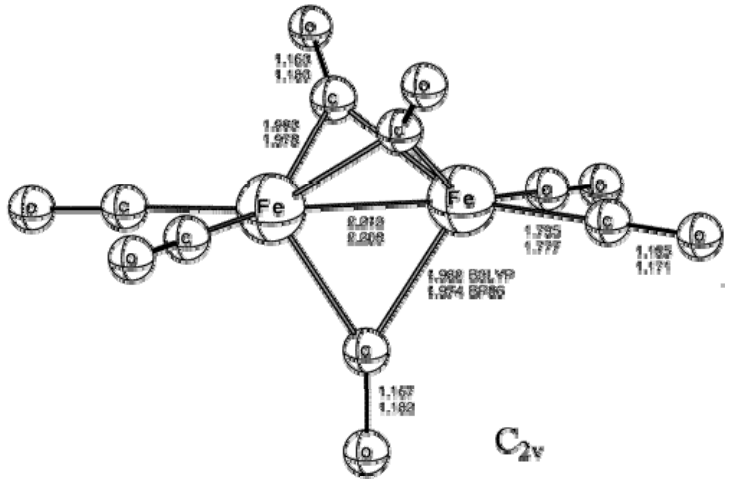

$Fe_2(CO)_7$ neutral tribridged C_{2v} structure optimized using DFT from ref. 1.

1. Xie, Schaefer and King, JACS, 122, 8746(2000)

$Fe_2(CO)_7^-$ anion spectrum

$Fe_2(CO)_7$ neutral harmonic frequencies (lowered by 52 cm^{-1} and expanded by 10% about the average) and intensities from DFT calculations for singly bridged structure in ref. 1.

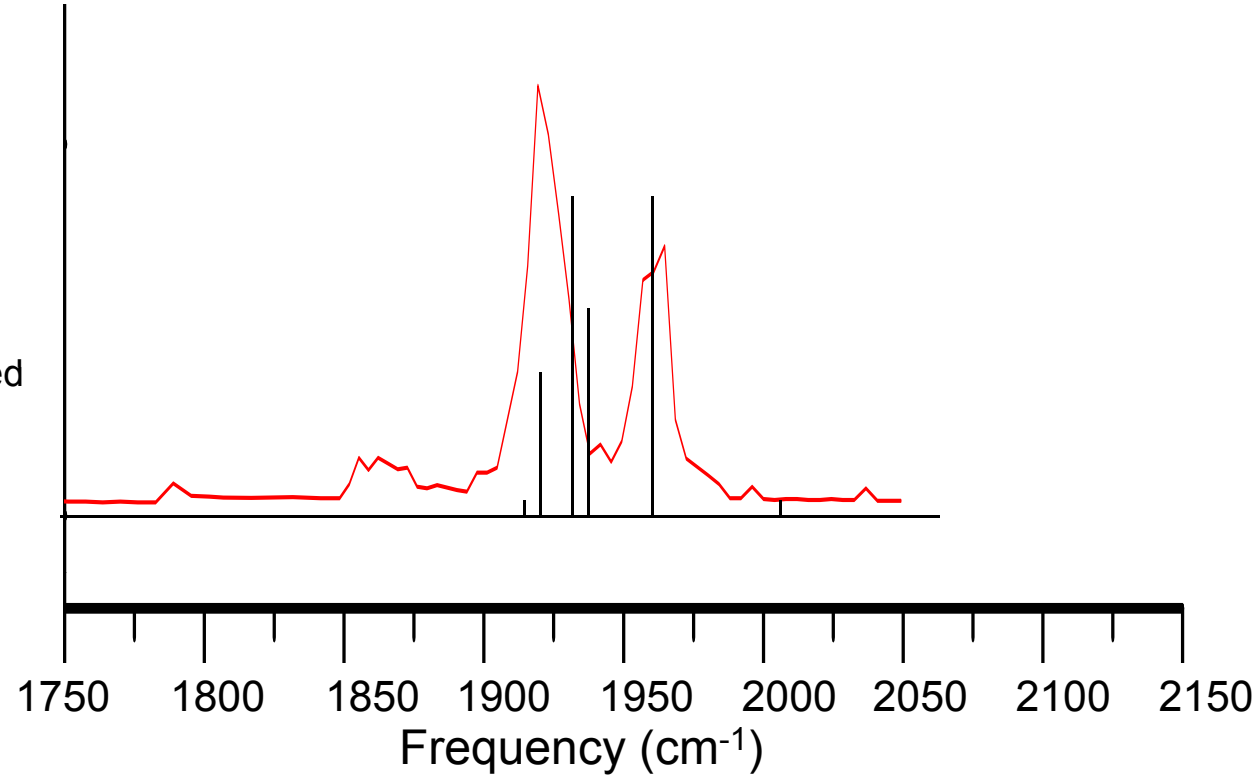

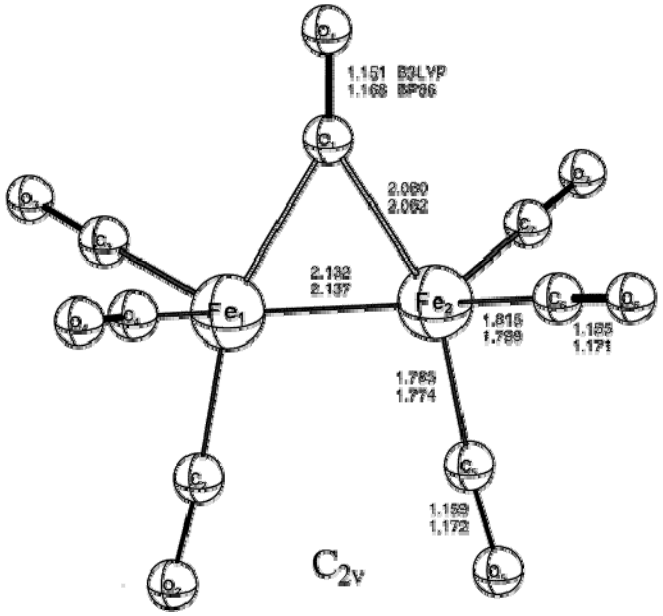

$Fe_2(CO)_7$ neutral monobridged C_{2v} structure optimized using DFT from ref. 1.

1. Xie, Schaefer and King, JACS, 122, 8746(2000)

$Fe_2(CO)_7^-$ anion spectrum

$Fe_2(CO)_7$ neutral harmonic frequencies (lowered by 62 cm^{-1} and expanded by 10% about the average) and intensities from DFT calculations for unsymmetrically doubly bridged structure in ref. 1.

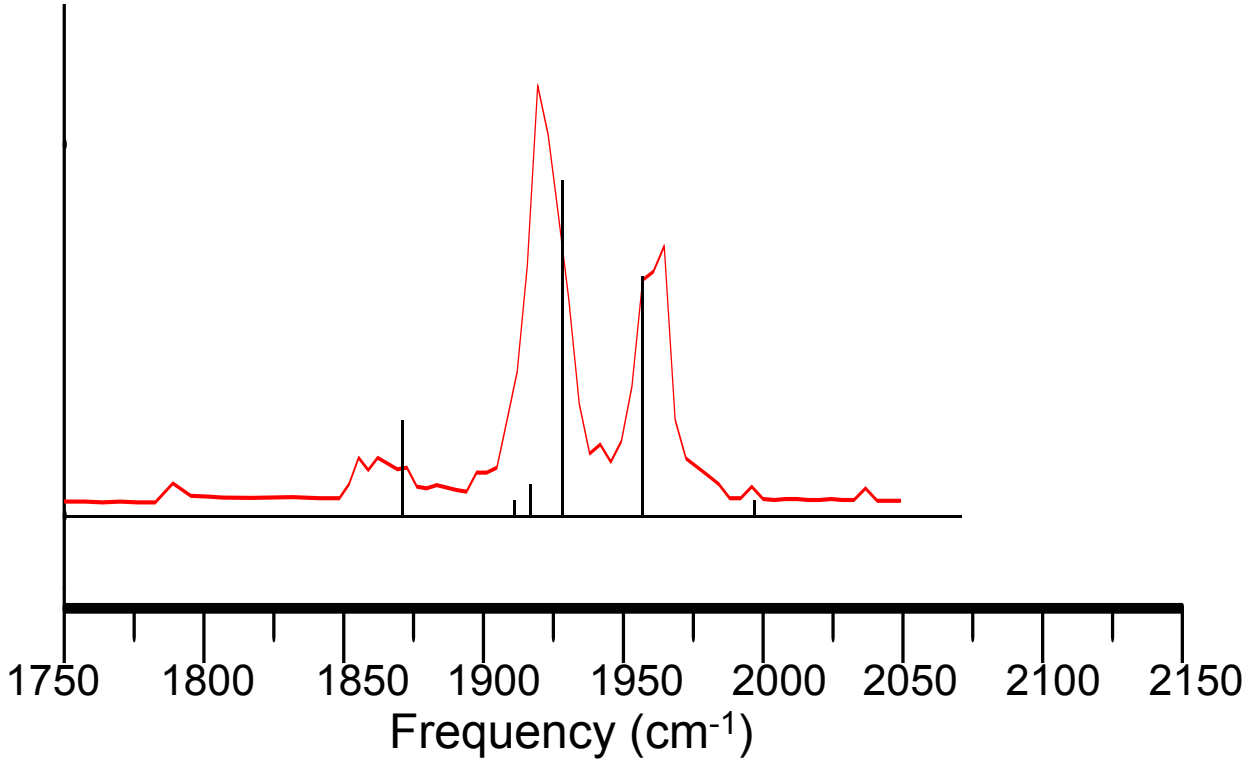

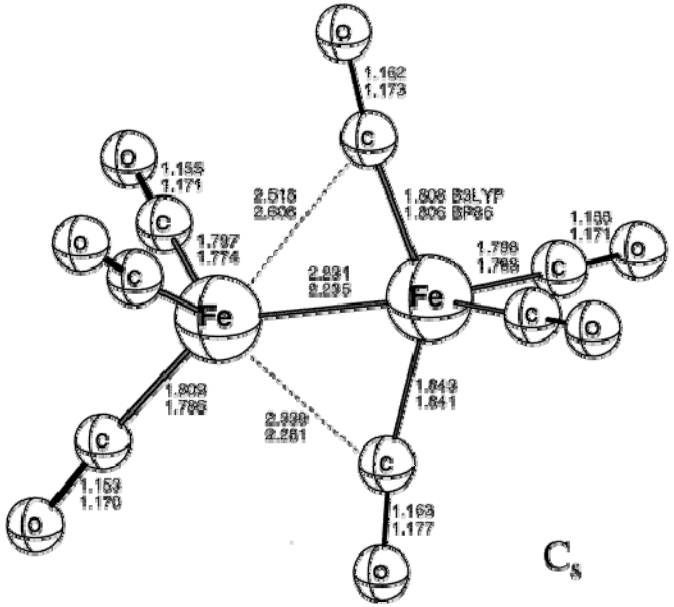

$Fe_2(CO)_7$ neutral asymmetrically dibridged C_s structure optimized using DFT from ref. 1.

1. Xie, Schaefer and King, JACS, 122, 8746(2000)

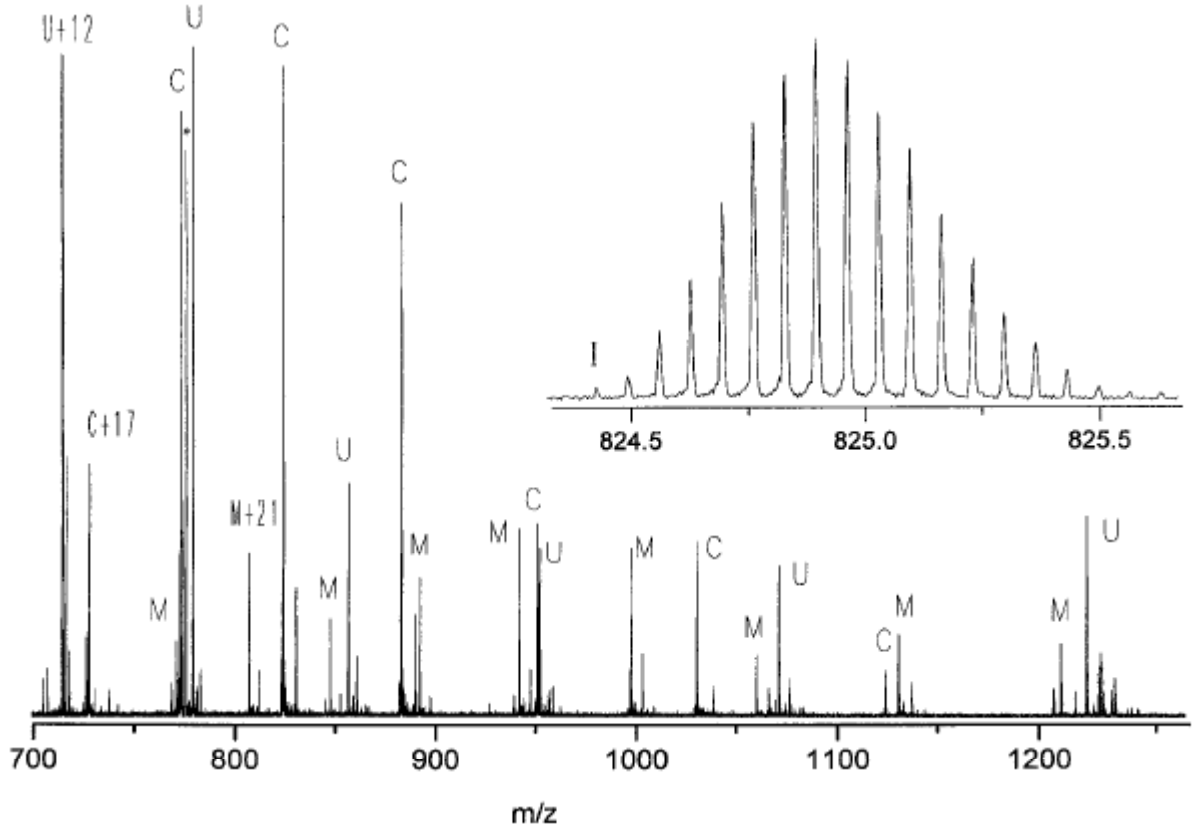

FIG. 3. ESI-FTICR spectrum of a mixture of ubiquitin, cytochrome *c* and myoglobin. U, ubiquitin peaks; C, cytochrome *c* peaks; M, apomyoglobin peaks; *, noise spike. Additional peaks due to sodium and phosphate adducts are present. Inset: Expansion of the +15 charge state region of cytochrome *c*. I, monoisotopic peak.

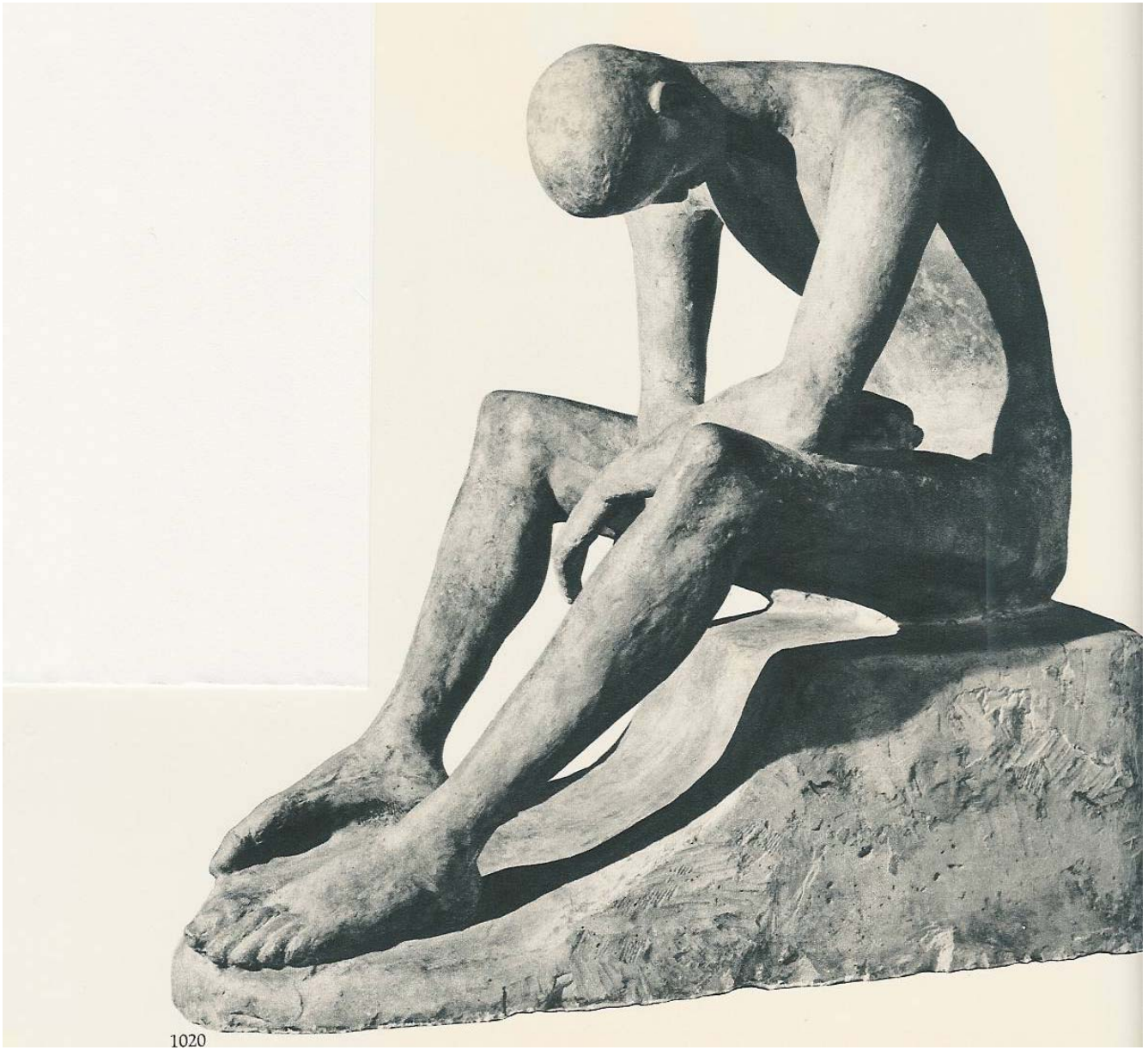

1020

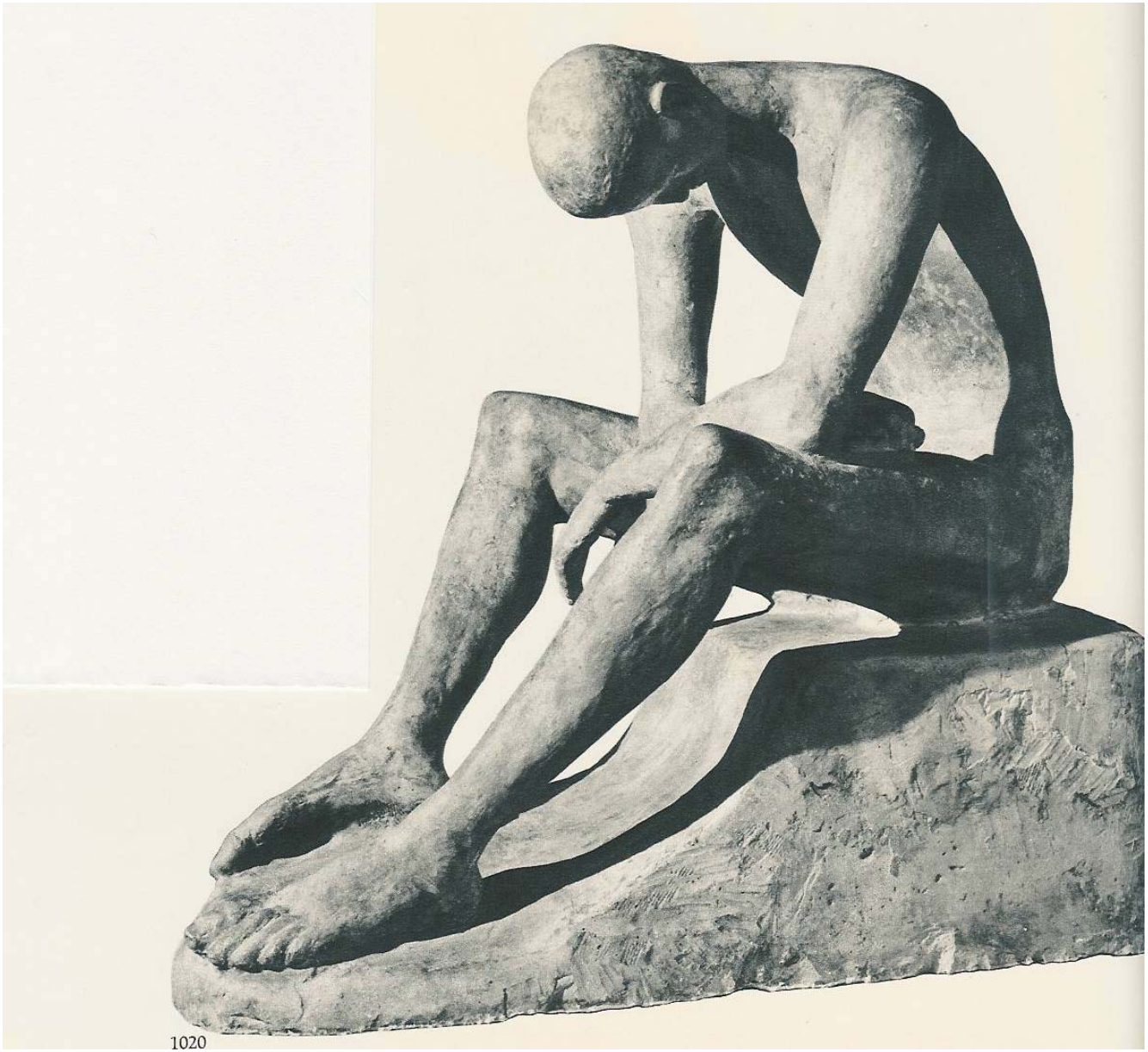

“The goddammed mass spectrometer is broken again!”
(title by Frank Field)

Electron Capture Dissociation of Human Parathyroid Hormone

A comparison with common fragmentation techniques and selective cleavage at histidine

Human Parathyroid Hormone (hPTH)

- 84 amino acid protein that regulates calcium levels in blood
- Mild to moderate hyperthyroidism results in increased bone density
- Treatment with the amino portion of hPTH (amino acids 1-34) promotes bone formation

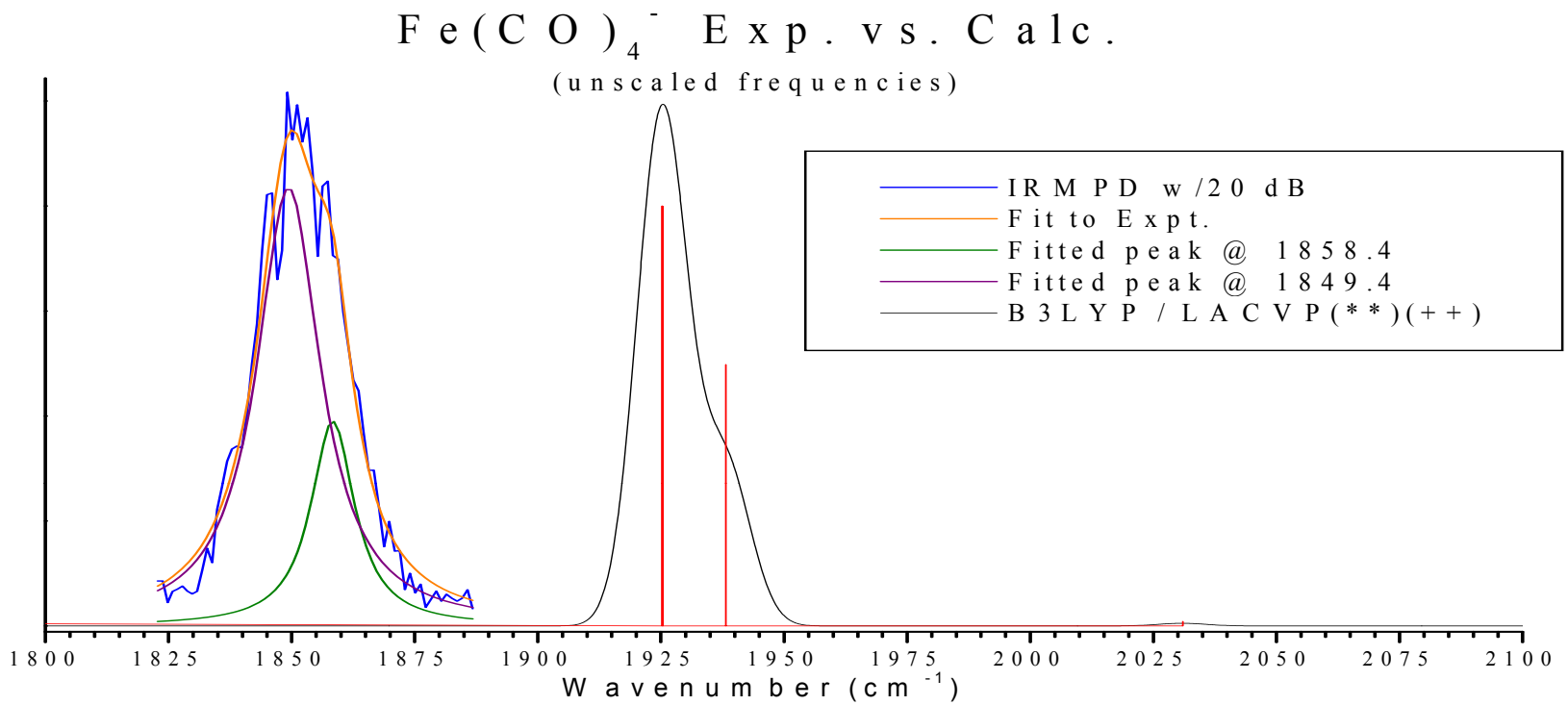

Notes:

The calculated curve was generated by convoluting the stick spectrum with a 12 cm^{-1} gaussian lineshape. The fitted widths for the two peaks in the experimental spectrum are ~15 and ~10 cm^{-1} . Forcing them to be 12 cm^{-1} does not significantly alter the fit, other than to make the areas of the peaks more similar.

The calculated frequencies are unscaled, but the "optimal" factor is ~0.97, which I find quite reasonable, particularly since the basis set used an ECP (effective core potential). Also, this scaling makes the splittings more similar (9 cm^{-1} and 12 cm^{-1} for the expt. and calc, repsectively.)

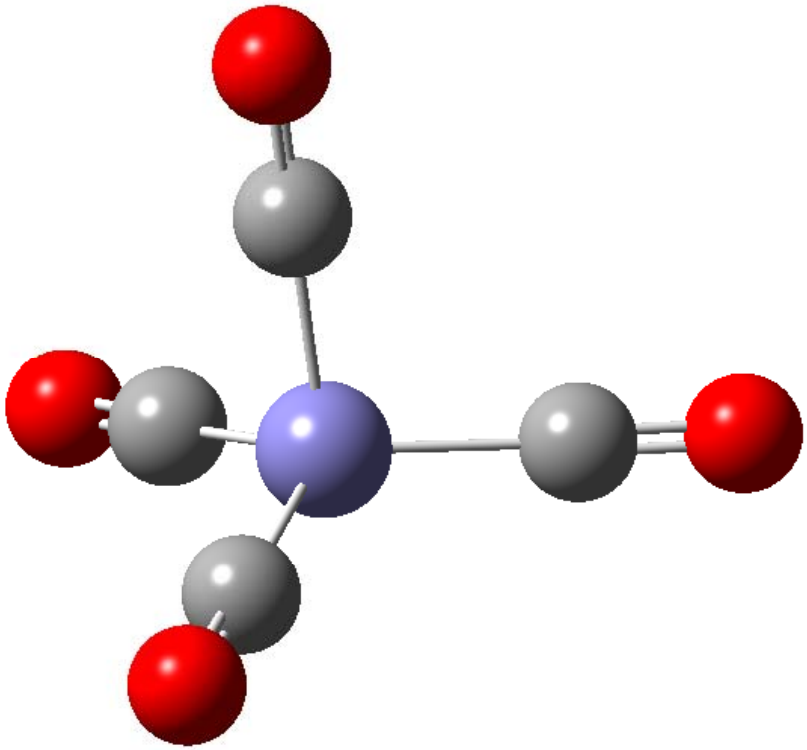

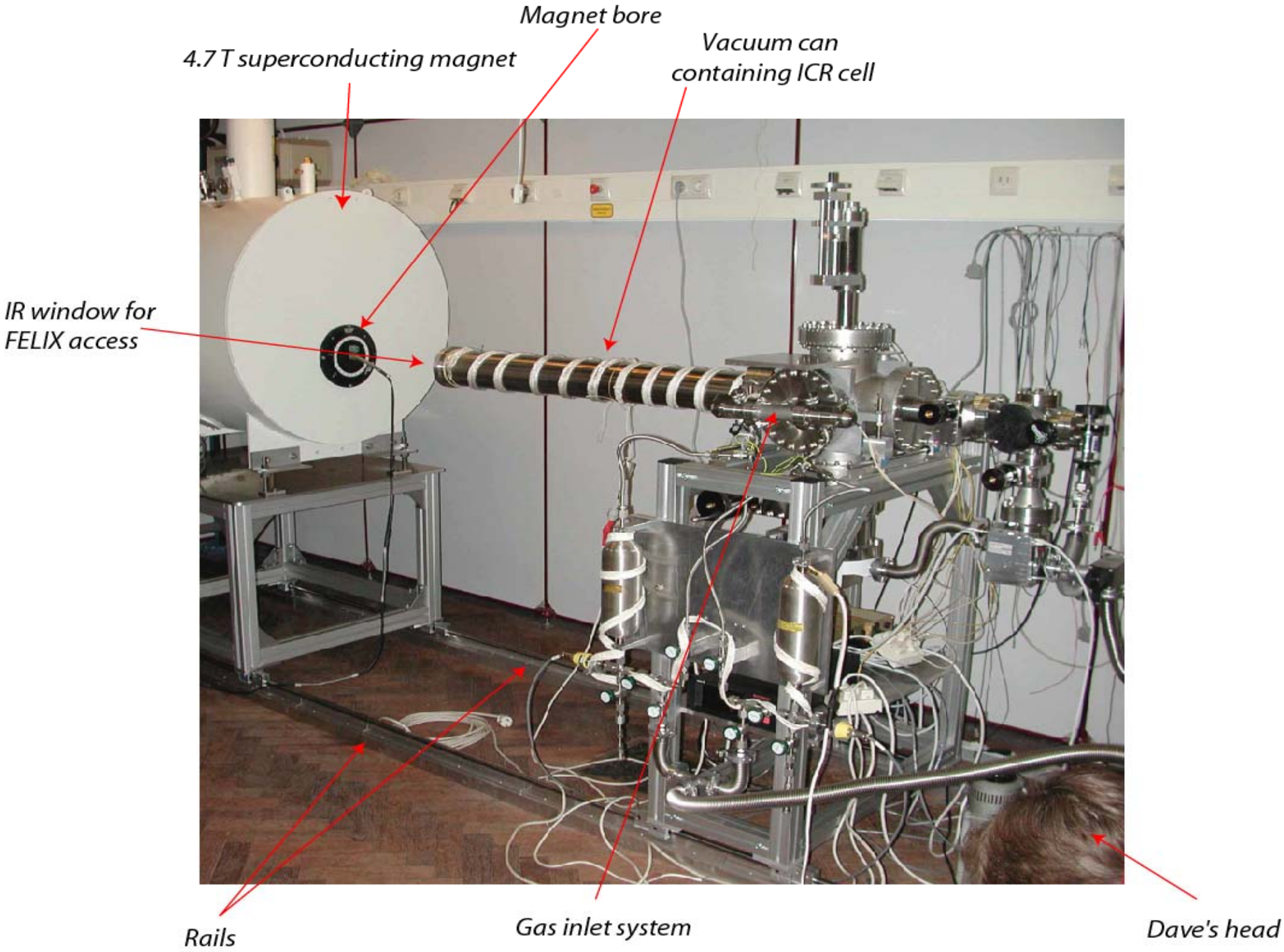
Magnet bore
4.7 T superconducting magnet
Vacuum can
containing ICR cell
IR window for
FELIX access
Rails
Gas inlet system
Dave's head